The Characteristics and Interactions of Mixed Pyrophyte and Mesophyte Litter Fuel Beds

by

Michael Austin Childree

A thesis submitted to the Graduate Faculty of
Auburn University
in partial fulfillment of the
requirements for the Degree of
Master of Science

Auburn, Alabama
August 3, 2024

Keywords: Mesophication, Burning Characteristics, Optical Diagnostics

Approved by

David Scarborough, Associate Professor of Aerospace Engineering
Heather Alexander, Associate Professor of Forest and Fire Ecology
Brian Thurow, Department Chair, W. Allen and Martha Reed Professor

Abstract

Oak trees are of great ecological and economic importance in the southeastern United States. These trees are being replaced through the mesophication process, presenting a major risk to regional ecosystems. This study applies an established method to measure the burning characteristics of longleaf pine ($Pinus\ palustris$), southern red oak ($Quercus\ falcata$) and sweetgum ($Liquidambar\ styraciflua$ L.). The combustion fraction, the mass loss rate, the temperature at multiple heights and the propagation rate were measured for each individual species and mixtures with 30% oak mass and variable pine and sweetgum mass. Pine was found to be the most consistently flammable species with the highest median measurements for all measured burning characteristics. Conversely, sweetgum had the lowest median values for all burning characteristics. The results for oak were bimodal. The low flammability mode had results similar to those of sweetgum, whereas the high flammability mode had lower temperatures than that of pine but higher mass loss and propagation rates. Burning characteristics generally decreased as the sweetgum content increased; however, using principal component and cluster analysis, five clusters were identified. In the first cluster, the test had higher mass loss and propagation rates than any of its constituent species. In the second cluster, the propagation rate and flame height decreased, but the temperature along the fuel bed was greater than that of its constituent species. In the third cluster, the temperature decreased to expected values. The fourth cluster contained tests with combustion fractions lower than that found for any of the individual species. However, in the fifth cluster the combustion fraction approached the values found for sweetgum. It was concluded that there exist distinct pine-oak and oak-sweetgum interactions, which lead to competing changes in the overall fuel-bed burning characteristics. These results contribute to the current discussion on how the progression of mesophication impacts the forest floor flammability; and can be used to improve prescribed burning to suppress mesophication.

Acknowledgments

First and foremost, I would like to thank my wife Elizabeth who has always been steadfast in her support, regardless of the curve balls the world may have thrown our way.

To my friends and family, thank you for encouraging me and reminding me to push forward one step, assignment, or day at a time.

To my advisor, Dr. David Scarborough, thank you for your direction and advice you have provided throughout graduate school. Without you, I would not have had the opportunity to engage in research opportunities or to complete the work presented here.

Lastly, I wish to thank the members of the Auburn University Combustion Physics Lab, especially Daniel Stubbs, who's work provided the foundation that this study builds on.

Table of Contents

List of Abbreviations

$\dot{L}_{CH*}$ Propagation rate calculated from CH* chemiluminescence measurements.

$\dot{L}_{est}$ Propagation rate estimated from steady-state burn time and propagation distance.

ν Fuel specific volume

σ Standard deviation

DSC Differential scanning calorimetry

L_{ss} Steady-state propagation distance.

$M(t)$ Mass as a function of time

m Linear fit slope

M_f Final mass

$M_n(t)$ Normalized mass a function of time

M_o Initial mass

M_{nf} Combustion fraction

p The p-value from two-sample t-tests.

p_{stat} p-value

PCA Principal component Analysis

r Correlation coefficient between a given variable and principal component.

$T_{14.45}$ Maximum temperature along the middle row

$T_{24.45}$ Maximum temperature along the top row

$T_{4.45}$ Maximum temperature along the bottom row

t_{ss} Steady-state burn time.

t_{stat} t-statistic

TGA Thermogravimetric analysis

Chapter 1

Introduction

The forests of the Central and Eastern United States have historically consisted of pyrophytic oak and longleaf pine trees [1]. Pyrophytic species are resistant to fire and often depend on periodic fires to aid proliferation and remove competing species. However, the presence of these pyrophytic species has declined in favor of mesophytic species such as maple and sweetgum through the mesophication process [2–5]. These mesophytic species are characterized by an increased tolerance to shade and fire sensitivity and often produce closed canopies, compared to the open canopies found in oak-pine forests. Without the presence of periodic fires, forests begin to go through mesophication, the positive feedback loop in which mesophytes suppress forest fires and outcompete local pyrophytic species. Oak trees provide a stable food source for several species of mammals and birds through acorns [6, 7]. Low-to-moderate intensity forest fires promoted by oak serve to kill tree seedlings and saplings, maintain an open canopy, and increase light access to understory species. Low intensity fires have also been shown to often increase soil nutrients through ash [8]. These contributions lead to a greater diversity of understory species, which in turn supports a wide range of herbivorous insects [1, 9, 10]. In contrast, mesophytes reduce biodiversity by creating low-light conditions and redirecting rainfall and nutrients to a smaller region around them [11, 12]. Therefore, mesophication raises concerns about the loss of ecological functions provided by oak and the ensuing consequences for the regional ecosystem. Furthermore, oak serves as a high-value source of timber, leading to mesophication that threatens both the regional ecosystem and the economy [13].

Small-scale laboratory and intermediate-scale field tests have been conducted to explore the mechanics of mesophication. Small-scale laboratory tests serve to reveal the upper limits

of combustion characteristics for multiple fuel compositions within a controlled environment. However, these tests typically rely on external sources of heat applied to the entire fuel bed for ignition, thus reducing the impact of fuel heating and excluding flame propagation measurements. In contrast, intermediate-scale field tests closely emulate naturally occurring forest fires and provide direct insight on how mesophication alters flame development and propagation. Although field tests offer the most accurate representation of naturally occurring forest fires, they are limited by reduced control over the test environment. To bridge the gap between these methods, intermediate-scale laboratory tests can serve to explore flame development and propagation while operating within a controlled setting.

For this reason, the present study employed the Wildland Fire Integrated Research Experiment (WildFIRE) facility; an intermediate facility capable of direct fuel bed mass and temperature measurements, as well as optical measurements of flame front propagation and geometry. Originally developed by Stubbs et al. [14] at the Auburn University Combustion Physics Laboratory (AUCPLab) and has been shown to produce accurate results within similar experiments.

This study explored the burning characteristics of three species involved in mesophication, specifically longleaf pine ($Pinus\ palustris$), southern red oak ($Quercus\ falcata$) and sweetgum ($Liquidambar\ styraciflua$ L.). The tests were carried out in single species fuel beds and mixed species fuel beds, where oak litter was kept constant, while pine litter was incrementally replaced with sweetgum litter. These mixtures were chosen because pine litter has been shown to vary more than oak litter as the species composition of the forest midstory changes [15]. The progression of mesophication threatens both the ecological and economic benefits of oak, and as such understanding the mechanism of mesophication is critically important.

Chapter 2

Previous Work

Much work has been done to study the behavior of wildland fires over the course of several decades; however, only recently has there been a focus on the relationship between mesophication and the behavior of wildland fires. This chapter will review a selection of studies that focus on this relationship, as well as studies that are foundational to this topic. Previous studies have focused on a variety of topics and diagnostic methods. Several tests have been conducted that focus on the underlying chemical kinetics of forests using differential scanning calorimetry (DSC), thermogravimetric analysis (TGA), and mass spectrometry. Other tests explored the resulting burning characteristics of different fuel bed compositions over a wide range of test scales. The diagnostic methods used for these studies often included heat flux sensors, load cells, thermocouples, and various optical measurements. Small-scale tests, typically of the magnitude of centimeters and occurring within a laboratory setting, included recordings of the mass loss rate, temperature, burn time, and flame height. Intermediate-scale tests recorded flame propagation in addition to the burning characteristics recorded in small-scale tests. These tests were carried out on a meters scale and occurred in both laboratory and field settings. Large-scale tests measured similar burning characteristics, were exclusive to field settings, and on the magnitude of tens of meters to kilometers. In this section, an overview of several of these studies will be presented.

2.1   Chemical Kinetic Studies

Multiple studies have focused on the chemical kinetic properties that govern the combustion of forest fuels. These tests used TGA and DSC to isolate lignocellulosic components within fuel

samples and to determine how they affect the overall chemical kinetic properties. The three primary lignocellulosic components present in biomasses are hemicellulose, cellulose, and lignin, which exhibit different combustion characteristics and are crucial to develop accurate combustion models. In TGA, the mass of the sample is measured as a function of temperature and time to determine the activation energy and reaction rate as a function of temperature. For DSC, the heat required to increase the temperature is recorded so that the heat release profile can be determined for the sample.

Diez et al. used TGA to develop a method to determine the content of the lignocellulosic components of a biomass [16]. This study used five fuel samples - wheat straw, spruce bark, pine bark, poplar wood, and willow wood - which were ground into particles no larger than 100 μm. TGA was carried out using 10 mg samples in a nitrogen atmosphere and heated by 5 °C per minute to a maximum temperature of 1000 °C. The results were then used to develop a pseudocomponent kinetic model that can be used to estimate the contents of the lignocellulosic components of other biomasses. Elder et al. studied the chemical kinetic properties of the North American Longleaf Pine ecosystem using TGA in nitrogen and air to find the degradation rates of different understory grasses [17].

Yang et al. investigated the characteristics of the three lignocellulosic components using TGA and DSC in a pure nitrogen environment [18] . In this study, cellulose and lignin samples were used, while xylan was used as a substitute for hemicellulose due to limited availability. Yang et al. found that hemicellulose readily decomposed at lower temperatures with moderate solid residue remaining. Cellulose decomposed at a higher temperature than hemicellulose but did so rapidly once it occurred and left very little solid residue. Lignin decomposed the slowest of the three components, with significantly more solid residue remaining. All three components were initially endothermic, although less so for cellulose, which was attributed to the removal of moisture. With the onset of pyrolysis, lignin and hemicellulose quickly became exothermic, while cellulose decomposition became significantly endothermic and occurred later than that of the other components. During char combustion, lignin and hemicellulose became increasingly endothermic, while cellulose became increasingly exothermic.

4

Pasangulapati et al. used TGA to study how the content of lignocellulosic components affected the thermal decomposition of four biomass materials; switchgrass, wheat straw, eastern redcedar and dry distilled grains with solubles [19]. Switchgrass and wheat straw had cellulose as the most prevalent component, with similar mass fractions for hemicellulose and lignin. Eastern redceder had a cellulose content similar to that of switchgrass and wheat straw, but significantly less hemicellulose. The dry distilled grains were mainly composed of proteins that were not associated with any of the three lignocellulosic components. Three stages of mass loss were found. The first corresponded to moisture evaporation, the second corresponded to the primary decomposition of cellulose and hemicellulose, and the remaining mass loss occurs in the final stage. In switchgrass and wheat straw, a significant portion of the lignin mass remained; however, the overall remaining mass of eastern redceder was close to that of switchgrass and wheat straw despite its increased lignin content. Pasangulapati et al. suggested that char and ash produced by cellulose and hemicellulose may act as catalysts for the combustion of lignin.

TGA and DSC have also been used to investigate how fuel chemical kinetic properties change under various conditions. Amini et al. conducted two studies that focused on the differences between live and air-dried dead samples for various species found in the southern United States [20, 21]. Amini et al. found that the initial activation energy was lower for live samples because of the moisture content; however, dead samples typically had higher activation energies for pyrolysis. Despite changes in the activation energies, the overall pyrolysis profile was found to be mostly unchanged. Rovira et al. used TGA and DSC to study changes in the chemical kinetic properties of the fuel due to decomposition [22]. The results showed that pyrolysis occurred at lower temperatures and released more energy per fuel mass as the decomposition progressed. The impacts of wet torrefaction on fuel properties were studied by Bach et al., using TGA and kinetic modeling to describe the devolatilization of each of the lignocellulosic components [23]. Each study found a two-peak pattern in the mass loss rate for each species and condition tested; where the peaks were associated with the decomposition of different lignocellulosic components.

Cone calorimetry has also been used to find the heat of combustion by burning samples in an oxygen environment and measuring the heat released by combustion. Studies by Polka and While et al. employed cone calorimetry to study the heat release of several species found in the United States [24, 25]. Dickinson et al. used cone calorimetry to measure the heat of combustion and peak heat release for multiple species groups and from multiple topographic regions within the southeastern United States [26]. During cone calorimetry measurements, samples are supplied with a constant radiant heat flux to cause ignition. Combustion products are evacuated through a fume hood and sampled by a gas analyzer to measure oxygen consumption. Heat release is calculated from measurements of oxygen consumption and mass loss. The results indicated that fuel beds dominated by oak litter are more capable of sustaining fires than fuel beds dominated by maple litter. However, Dickinson et al. also states that, regardless of composition, fuel beds within moderately moist mesic environments are less likely to sustain a fire and generally produce lower intensity flames than fuel beds within dry xeric environments.

2.2   Small-Scale Laboratory Studies

While wildland fires are driven by chemical kinetics, burning characteristics cannot be derived from these alone. In addition to chemical kinetics, the physical conditions of wildland fuels are required for the generation of accurate wildland fire and mesophication models. Studies that have focused on these macroscopic fuel properties have directly measured the flame temperature, height, and mass loss rate of stationary flames in a laboratory setting with variations in fuel mass, bulk density, and fuel composition.

Small-scale laboratory studies have predominantly followed the method developed by Fonda et al. [27]. This study investigated the burning characteristics of western conifer needles with additional species tested in Fonda [28]. The tested species were divided between species of "fire resistors", which can survive the direct effects of wildfires, and "fire evaders", which are killed by wildfires, but return through seed germination. Fonda et al. measured flame height, flame time, ember time, burn time, percentage of fuel consumed, and mean weight loss rate for each of the eight species. The tests were burned in a test chamber of 1 m x 1 m x 3 m, with a chimney to direct the exhaust and induce an air velocity of 9.9 cm/s over the test bed. 18 g of

6

pine needle samples were placed on a 35 cm x 35 cm grid of xylene-soaked strings and ignited. Timers were used to measure the time from ignition to flames extinguishing as the flame time and the time from ignition to embers extinguishing as the burn time. The difference between the flame time and the burn time was recorded as the ember time. The flame height was measured by two observers comparing the flame height to a 2 m ruler within the test chamber. The results showed that fire resisters had a higher flame height, percent fuel consumed, and mean weight loss rate, while fire evaders had higher flame and burn times. Although the study conducted by Fonda predates the formation of the mesophication hypothesis, the traits of both fire resistors and evaders can be attributed to pyrophytes.

The study by Kane et al. (2008) used the method developed by Fonda et al. to study the burning characteristics of eight oak species found in the southeastern United States [29]. Kane et al. found that each species could be classified as a "fire facilitator" or "fire impeder". Fire-facilitating species were characterized by higher flame, mass loss rates, and fuel consumption with shorted flame and smolder times, with impeding species having mirrored results.

Kreye et al. (2008) applied the method of Fonda et al. directly to the study of mesophication [30]. Kreye et al. collected litter from a site in north-central Mississippi and separated the samples into sets consisting of 0%, 33%, 66%, and 100% mesophytes by weight and assigned as wet, moderate, or dry tests. The wet and moderate fuel beds were soaked in water for 24 hours and allowed to dry for 12 and 24 hours, respectively. It was found that mesophytic tree litter can absorb and retain more moisture; however, only substantial increases in mesophytic litter were required to cause significant impacts on flammability.

Varner et al. conducted tests on tree litter found in the southeastern United States, as well as consolidated data from previously published studies using the method developed by Fonda et al. [31]. In total, Varner et al. included results for 50 species from four forest ecosystems. Using principal components analysis (PCA), Varner et al. identified multiple clusters in each ecosystem that grouped species with similar burning characteristics. In all four ecosystems, the species associated with mesophication resulted in reduced flammability, while the pyrophytic species showed increased flammability. Studies by Kane et al. (2021) and Kreye et al. investigated the flammability of additional species using the method developed

by Fonda et al. and incorporating measurements of the physical characteristics of leaf litter and moisture retention [32, 33]. For each species, the litter mass, length, thickness, surface area, volume, and curl were measured. Litter dry mass was measured using a digital scale, the thickness of the leaf was measured using electronic calipers and the curl was measured as the maximum height of a horizontally oriented dry leaf on a flat surface. The length and surface area were found using image processing software. Fuel volume, density, and surface area-to-volume ratio were calculated as measurements. Other variables considered included fuel bed bulk density, packing ratio, saturated moisture mass, and "lag time", which was indicative of the time required for a saturated sample to reach equilibrium moisture levels. The results of both studies found rapid drying, reduced moisture retention, and increased flammability in oak species, while mesophytic species displayed increased moisture retention and reduced flammability.

Grootemaat et al. (2015) studied how leaf litter traits impact flammability and decomposability [34]. Grootemaat et al. conducted tests on 32 plant species to measure and compare their trait–flammability relationships to trait–decomposability relationships. The traits measured in this study included leaf length, width, thickness, and mass. The surface area was estimated and used to calculate the volume and specific leaf area (SLA). Nitrogen, phosphorus, lignins, and soluble polyphenols were the chemical traits measured. The decomposability measurements included litter weight after 11 and 22 months of decomposition. The flammability measurements included the time to ignition, flaming duration, and smoldering duration. The time to ignition was found to depend primarily on the SLA, while flaming duration and smoldering duration depended mostly on litter mass. The decomposition traits were found to be independent of the flammability.

2.3   Intermediate-Scale Laboratory Studies

Small-scale laboratory tests provide valuable data on the burning characteristics of wildland fuels, but exclude information on the sustainability and propagation of the flame front. Intermediate-scale laboratory studies use test beds on the scale of meters and ignite fuel samples along one end so that flame sustainability and propagation results can be measured. These studies have

focused on a range of conditions that affect flame propagation, such as fuel loading, slope, wind conditions, and moisture content, using a variety of fuel species.

Stubbs et al. investigated the burning characteristics of loblolly pine needles ($Pinus$ $taeda$) at different fuel loadings and developed the WildFIRE facility used in the present study [14]. Stubbs et al. measured the mass loss rate, the flame temperature, the propagation rate, the flame geometry, and OH^* chemiluminescent flame intensity. The tests were burned on a fuel bed suspended by two load cells to measure the mass loss rate. The flame temperature was measured with a fine-wire thermocouple probe. The propagation rate, flame geometry, and OH^* chemiluminescent flame intensity were captured with a scientific camera with a band-pass filter corresponding to the CH^* radical chemiluminescence wavelength and filtered out the light produced by soot and solid fuel species to isolate heat release. The mass loss rate was found to increase linearly with fuel loading. Flame propagation slightly increased with mass loading, while flame height and surface area increased significantly. Flame intensity and temperature did not change significantly.

Santoni et al. incorporated oxygen consumption calorimetry to determine fireline intensity and compared their findings with previously accepted methods [35]. The tests were carried out on a 2 x 2 m table supported by a load cell to record the mass measurements; however, the fuel beds ranged from 0.9 x 1.1 m to 1 x 2 m. Santoni et al. found that oxygen consumption calorimetry produced a more accurate estimation of fireline intensity than previous methods and was applicable to a wider range of conditions. Barboni et al. expanded on the study by Santoni et al., using the same facility and a similar method [36]. In this study, flame length measurements were included, which were found to further improve fireline intensity estimation.

Morandini et al. studied the effects of the wind and the slope of the fuel bed on flame propagation [37]. Morandini et al. incorporated mass balances, thermocouples, heat flux sensors, and infrared imaging to record measurements during each test. The results indicated that flame propagation increased with wind speed and fuel bed slope and that radiative heating has a greater impact on propagation than convective heating. Tihay et al. also studied the impacts of slope and fuel load on forest litter combustion, using the same facility and method as Santoni

et al. and Barboni et al. [38]. In contrast to Morandini et al., Tihay et al. found that convection accounts for a majority of fuel heating, although to a lesser extent as the fuel bed slope increases.

Awad et al. conducted laboratory tests with different fuel loadings and moisture [39]. The tests were carried out on a 1 x 2 m burn table beneath a fume hood. Fuel loadings consisted of kg/m^2, 0.20 kg/m^2, and 0.40 kg/m^2 with the moisture content varying from 0 to 114% of the fuel mass. The results showed that fire extinction is primarily affected by fuel moisture content and fuel load; however, this threshold tends to become independent of the load as fuel loads increase. These studies provided additional data on the impact of moisture content on wildland fuel burning characteristics.

Magalhaes et al. investigated the combustion characteristics of mixed litter fuel beds [40]. The tests were carried out in a 15 x 150 cm channel with flame height, temperature, propagation rate, time to ignition, mass consumption, and temperature integration. Eight species were tested, both single fuel tests and fuel beds consisting of three species, each comprising a third of the fuel mass. Magalhaes et al. found that mixed fuel beds often showed results that differed from the results of their constituents, indicating additional interactions between each fuel species.

Grootemaat et al. (2017) measured several physical and chemical leaf litter traits to several flammability traits [41]. Physical traits measured included leaf size, curliness, thickness, and tissue density. From these measurements, the packing ratio, bulk density, and specific surface area (SLA) were calculated. The chemical traits measured included concentrations of nitrogen, phosphorus, lignin, and tannin. The measured flammability traits included maximum temperature, spread rate, burning time, and fuel consumption. The packing ratio was found to increase the rate of spread and decrease the burning times of the samples. SLA was found to decrease the maximum temperature and increase the rate of spread. Tannin concentration was shown to decrease the rate of spread of fuel consumption, and lignin concentration was shown to increase fuel consumption.

2.4 Field Tests

Laboratory tests benefit from controlled conditions and repeatable methods, allowing the measurement of specific characteristics of flammability. Although these results are crucial, laboratory settings cannot ideally recreate the conditions under which wildland fires occur. To address this need, field tests have been conducted to investigate the flammability characteristics of forest fuels in environments similar to those of naturally occurring fires.

Davies et al. investigated the role that moisture content plays in the development of self-sustained fires in the lower canopy of UK heathlands [42]. Experiments were carried out at two locations in the UK, where 2 m by 2 m sections of the canopy were burned. Fuel beds were ignited in a single spot with a drip torch filled with a 3:1 diesel / petrol mixture, unless this failed three times, in which case a line ignition was used. Burn time was recorded with a stopwatch and fires that took more than 5 minutes were considered sub-sustaining. Davies et al. found that tests with moisture content greater than 70% failed to ignite, but tests below 60% moisture content ignited consistently. The spread rate after ignition decreased as the moisture content increased.

Arthur et al. studied the impact of repeated prescribed burns on forest composition and tree vigor [43]. Tests were carried out on 10-m x 40-m plots that were randomly assigned one of the three treatments. The plots assigned as "frequent burn", had four prescribed fires over an eight-year period, those assigned to "less frequent burn" had two prescribed fires over the same time span, and "fire-exlcuded" areas were not burned. The species present in each plot were classified as xerophytic, mesophytic, or ubiquitous according to established knowledge on whether the species was more prevalent in dry, moist, or either condition, respectively. Each plot was then classified as occurring in a sub-xeric, sub-mesic, or intermediate landscape based on the prevalence of the species within the plot. During burns, fire temperature was recorded using temperature-sensitive paints placed 0 cm, 20 cm, and 40 cm above the forest floor. After the tests, the highest point of char on each tree was recorded. Each year, several traits were measured for each tree, including the diameter at breast height, crown dieback class, and number of basil sprouts. Crown dieback class were on the percent of crown death and was

used to represent loss in tree vigor. Char height was found to correlate with increased crown dieback, more so in maples than in oaks. The results also showed that maples were more prevalent than oaks at the sapling and midstory levels; however, frequent fire had a greater impact on tree mortality at these levels. The presence of maples decreased significantly after prescribed fires, but remained the most prevalent species along the sapling level in intermediate and sub-mesic landscapes. In general, the results indicated that repeated prescribed fires may be effective for preventing mesophication, but they are not effective for reversing it.

McDaniel et al. investigated how changes in the composition of forest species impacted the structure, moisture, and flammability of leaf litter [44]. Two oak species, southern red oak ($Quercus\ falcata$) and post oak ($Quercus\ stellata$) and three non-oak species, sweetgum ($Liquidambar\ styraciflua$), winged elm ($Ulmus\ alata$) and hickory ($Carya\ spp$) were selected as test species. For each species, the mean curl, leaf perimeter, surface area, dry mass, and thickness were measured. The 15 g litter beds of single species and mixed species were soaked in water and then dried until the mass remained constant. The mixed litter beds used consisted of 0% to 100% non-oak litter, increasing in increments of 33%. Burn tests were carried out on a 1.75 m x 1.75 m plot using 937 g samples of single species and mixed species. The tests were ignited along a single edge and the percent burned area, temperature, flame height, flame spread rate, and flaming duration were recorded. The flame temperature was measured using temperature-sensitive paint attached to pin flags on top of the fuel bed, and the remaining characteristics were visually measured. Oak litter was found to have thicker and larger leaves, absorbed moisture slower and dried faster than non-oak litter. Mixed fuel beds were found to retain more moisture with increased non-oak litter content, which reflected the increased moisture retention found for those species. Non-oak litter was shown to increase the duration of flaming and decrease the remaining measurements in mixed fuel beds.

Cabrera et al. studied how the removal of mesophytic in addition to prescribed burns affected the behavior of the fire [15]. Tests were assigned to one of two treatments; thinned tests in which all midstory non-pyrophytic species were removed and non-thinned tests. Each test experienced one prescribed burn in one of three seasons: early dormant (January), late dormant (April), and growing season (September). The initial condition of each plot was recorded,

including canopy cover, litter bed composition, and total fuel load, including understory plants, leaf litter and other organic matter. The plots were monitored for 14 months to access the impacts of the thinning treatment before the experimental burns were carried out. The fire temperature was measured using a 3 x 3 grid of pin flags with temperature-sensitive paint along the forest floor. The height of the flame, the spread rate, the ignition time, the total duration of the flame, and the perfect fuel consumed were visually recorded. The midstory thinning was to significantly increase the pine litter content, while the pine litter content decreased in the control tests between initial and pre-burn measurements as the mesophytic litter increased. Early and late dormant season burns resulted in fairly similar results, while growing season burns were typically subdued. The results showed that midstory thinning had relatively minimal impact on canopy cover and overall fire behavior.

Several previous intermediate-scale laboratory studies have employed methods similar to those used in the present study. These common traits include the use of burn plates in environments of controlled air flow using load cells, thermocouples, and optical diagnostics to record burn behavior. In contrast, several small-scale laboratory and field studies have focused, similarly to the present study, on the mechanics of mesophication. While several studies have used similar methods and others that have focused on the topic of mesophication, there exists a need for research that bridges the gap between these. This work contributes to the existing literature by contributing this need and can be used to inform and direct future studies to additional knowledge gaps in this topic.

Willis et al. conducted field tests using tree litter that included fruits and cones [45]. The quantity of litter to fruits and cones was varied between tests, with litter only tests being used as a control. When present, fruits and cones consisted of 10%, 30%, or 50% of the surface area of the fuel bed. Seven species were used during the testing, with single species tests and mixed species tests. During testing, the height of the flame, the spread rate, the percent of area consumption, the duration of the flame, and the smolder time were recorded. The composition of each litter was measured, including the mass, moisture, lignin, nitrogen, and carbon content. Lignin and carbon were shown to increase fuel consumption and flame height, while nitrogen had the opposite effect, despite only varying by fractions of a percent.

13

Chapter 3

Experimental Methods

3.1 Test Species

This study measured the burning characteristics of three individual tree species associated with mesophication and mixtures of these species, with the objective of determining the impact that mesophyte litter has on aggregate fuel beds. Each test was comprised of 0.4 kg of fuel, consisting of longleaf pine ($Pinus\ palustris$), southern red oak ($Quercus\ falcata$) and sweetgum ($Liquidambar\ styraciflua$) litter. The oak and sweetgum litter used was freshly senesced and collected in the winter of 2022 and 2023 from local sources. The longleaf pine straw used was purchased locally. These species were selected for this study because they are prevalent within the ecosystem of the southeastern United States and are relevant to the mesophication process.The experiment included trials with fuel beds of single and mixed species. In mixed tests, the mass fraction of oak was kept constant at 0.3, while the mass fractions of pine and sweetgum ranged from 0 to 0.7 in increments of 0.1. During mesophytic encroachment, the presence of pine litter on the forest floor has been shown to decrease more significantly than oak, as such the pine mass fraction was varied and the oak content remained constant [15]. In addition to mixed fuel tests, high moisture tests were performed. In these tests, the fuel samples were submerged in water for 24 hours to fully saturate, then suspended on a drying rack for 24 or 48 hours to air dry before testing. In previous small-scale laboratory studies, moisture tests were dried for 12 to 24 hours; however, unlike the present study, these previous experiments did not investigate the propagation rate. In the present study, preliminary tests were consistently unable to sustain combustion when dried for 12 hours. At 24 and 48 hours, only the unmixed

pine tests were able to propagate successfully, as such, only a limited number of moisture tests were conducted to conserve the remaining fuel litter. The availability of litter from each species was a determining factor in the number of trials for each fuel group. The number of trials for each fuel group is shown in Table 3.1, and the average fuel specific volume (ν) is shown in Table 3.2.

Table 3.1: Fuel bed compositions tested

Fuel Bed Composition	Number of Tests
Pine	47
Wet Pine	8
Sweetgum	10
Oak	17
70% Pine, 30% Oak	15
60% Pine, 30% Oak, 10% Sweetgum	17
50% Pine, 30% Oak, 20% Sweetgum	5
40% Pine, 30% Oak, 30% Sweetgum	9
30% Pine, 30% Oak, 40% Sweetgum	15
20% Pine, 30% Oak, 50% Sweetgum	6
10% Pine, 30% Oak, 60% Sweetgum	15
30% Oak, 70% Sweetgum	5

Table 3.2: Fuel specific volume

Fuel	Bulk Density (m^3/kg)
Pine Needle	0.166
Oak Leaves	0.133
Sweetgum Leaves	0.122

3.2 Experimental Facility

This study was carried out at the Auburn University Combustion and Propulsion Laboratory using the Wildland Fire Integrated Research Experiment (WildFIRE) facility, shown in Figure 3.1, originally developed by Stubbs et al. [14]. Tests were carried out within the WildFIRE facility, which facilitated simultaneous measurements of fuel mass, combustion temperature, and flame temperature, and it was visually accessible for optical diagnostics.
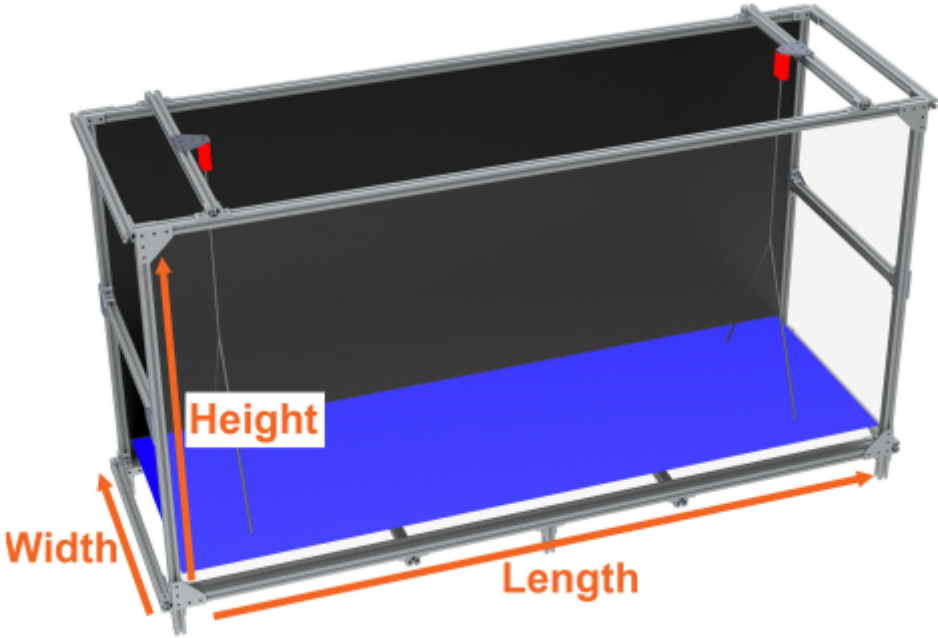
Figure 3.1: Computer graphics rendering of the WildFIRE Facility. The load cells and the weight plate are highlighted in red and blue, respectively [14].

3.3 Burn Tests

The procedure used in this study is derived from the method developed by Stubbs et al. [14]. For each trial, 0.4 kg fuel samples were placed on the test bed. Once the fuel samples were placed on the test bed, they were leveled by hand so that the fuel was evenly distributed across the table. In addition, mixed fuel samples were mixed by hand so that each species was evenly distributed within the fuel bed. The samples were not compressed to a specific volume or height and, therefore, the volume was allowed to vary. This was done to better reflect the natural conditions as the litter fell to the forest floor. Before burning the sample, fuel height was measured as well as ambient temperature and humidity in later trials. A string soaked in denatured alcohol was placed along the width of one side of the fuel bed and lit using a blow torch to achieve simultaneous ignition across one width of the fuel bed. Measurement recordings were initiated directly before fuel ignition, and the burn index was initiated once fuel combustion was self-sustaining. Test measurements were completed once the fuel mass remained constant, while the burn index was concluded once active combustion ended. The

burn index was used during data processing to isolate the time of visible combustion during each test. After each test, any solid residue was removed and the test bed was allowed to cool to avoid warping that would cause inaccurate mass measurements.

3.3.1 Fuel Mass Measurements

During testing, the fuel mass was recorded using two Omega LCCA-50 load cells that supported the floor plate. The load cells had a maximum load of 50 lb (22.68 kg), which exceeded the weight of the floor plate, and had a sensitivity of $\pm$ 8.391 g, which was equivalent to 2.1% of the initial fuel load of 0.4 kg. The temperature of the load cells was tracked using surface mount thermocouples to verify that they did not exceed their maximum operating temperature of 150 °F (65 °C).

Mass measurements were used to calculate the combustion fraction (M_{nf}), the mass loss rate ($\dot{M}$), and record the mass fraction over time for each test. To account for slight deviations in the initial mass load, the normalized mass load was used for these calculations rather than the true mass measurements. The normalized mass (M_n) was found as the fuel mass at a given time divided by the initial mass reading and is shown in Equation 3.1.

$$M_n(t) = \frac{M(t)}{M_o} \tag{3.1}$$

For each fuel group, the mean and 95% confidence interval of the normalized masses were found at each time point. To account for variations in burn time, only measurements up to the final time of the shortest test in a given fuel group were averaged. The combustion fraction was found as the fraction of the mass removed from combustion and is shown in Equation 3.2.

$$M_{nf} = \frac{1 - M_f}{M_o} \tag{3.2}$$

The normalized mass loss rate was found using a linear fit of the normalized mass using data between flame ignition and 25 seconds before flame extinction to isolate the region with a nearly linear normalized mass time history and minimize the impacts of flame development and extinction.

17

3.3.2 Combustion and Flame Temperature Measurements

Nine Omega model number KMQSS-062E-12, 0.0625 inch (1.6 mm) diameter, exposed junction, 12 inch (30.5 cm) long K-type thermocouple probes in a 3 x 3 grid were used to measure the temperature at several locations along the fuel bed. The bottom row of the thermocouples was located 4.45 cm above the test bed, which resulted in the thermocouples being within the fuel bed. The second row of thermocouples was 14.45 cm above the test bed. Thermocouples along this row were typically 4 to 6 cm above the fuel bed, but occasionally within the top layer of the fuel sample. The upper row of the thermocouple was 24.45 cm above the test bed; at this height, the flames did not reach the thermocouple consistently. Figure 3.2 illustrates the arrangement of the thermocouples [14].
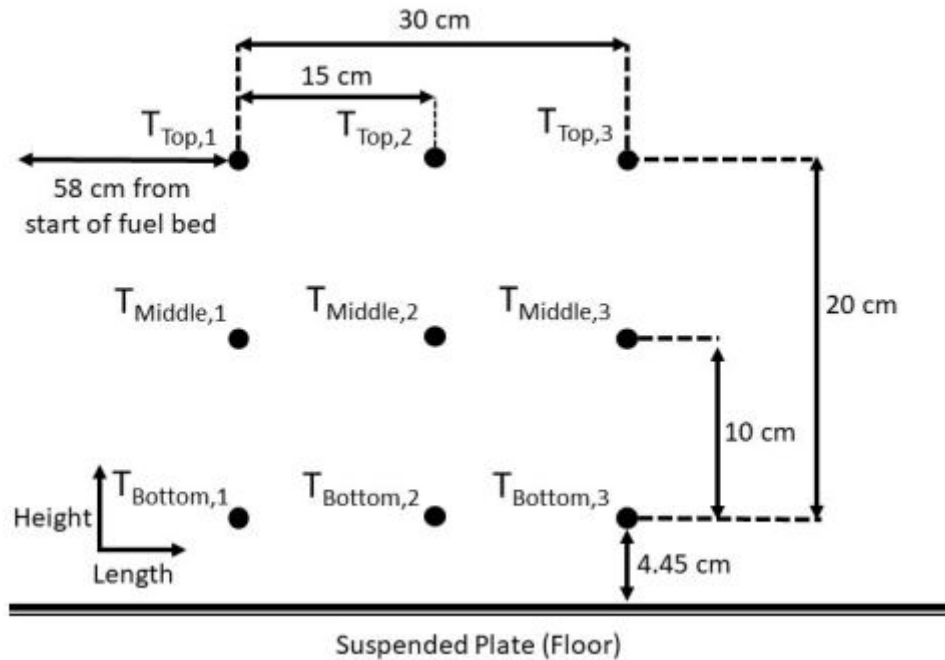
Figure 3.2: Diagram showing the locations of each thermocouple within the WildFIRE facility [14].

Temperature measurements were used to calculate the maximum temperature ($T_{4.45}$, $T_{14.45}$ $T_{24.45}$) and time-averaged temperature along each row for each test. The thermocouple would occasionally fail mid-test and produced impossibly high measurements. To account for this, readings greater than 1200 °C were discarded. To find the maximum temperature in each row,

18

a moving mean of 10 samples was taken for the measurements of each thermocouple, and the maximum value was used to represent the maximum temperature reading for that thermocouple. For each row, the median value of the three thermocouples in that row was found to be the maximum temperature along that row. The time-averaged temperatures and the 95% confidence interval were found using the same method used for mass measurements.

3.3.3 Flame Front Propagation Measurements

The flame front was tracked using a Ximea xiD MD061MU-SY CCD scientific camera with a 10 nm band-pass filter. This isolated CH* radical chemiluminescence wavelength so that only the light produced by the flame was measured. An example of Ximea measurements can be seen in Figure 3.3. From the location of the flame front, the propagation rate ($\dot{L}$) was calculated. The experimental design originally included the measurement of flame front intensity and geometry; however, these were neglected due to technical limitations. This was due to the wide range of flame intensities between each species exceeding the range that could be accurately measured at a given exposure. The measurements from the Ximea camera each pixel was found to have a value from 0 to 1 representing the CH* radical chemiluminescence emission relative to the exposure range of the camera. Values above 0.05 were considered to be regions of active combustion. This threshold was selected to minimize false positive reading caused by reflections off of the support structure.

To account for the reduced flame detection of low intensity tests, the flame front was considered for each point in time as the forward most point detected in each image, up to the current time. This prevented brief drops in flame intensity that produced false reports of significant flame front regression. To further reduce the effect of false positives, all points found to be greater than three standard deviations from the median location of all points were discarded. The forward most point was then recorded as the median of the ten most forward points of the flame along each row, excluding outliers, and then smoothed with a rolling average of ten points. The same method used to find the time-averaged mass and temperature was also used to find the time-average flame front location and the 95% confidence interval. From the results of the flame front location, the mean propagation rate ($\bar{\dot{L}}$) for individual tests was found
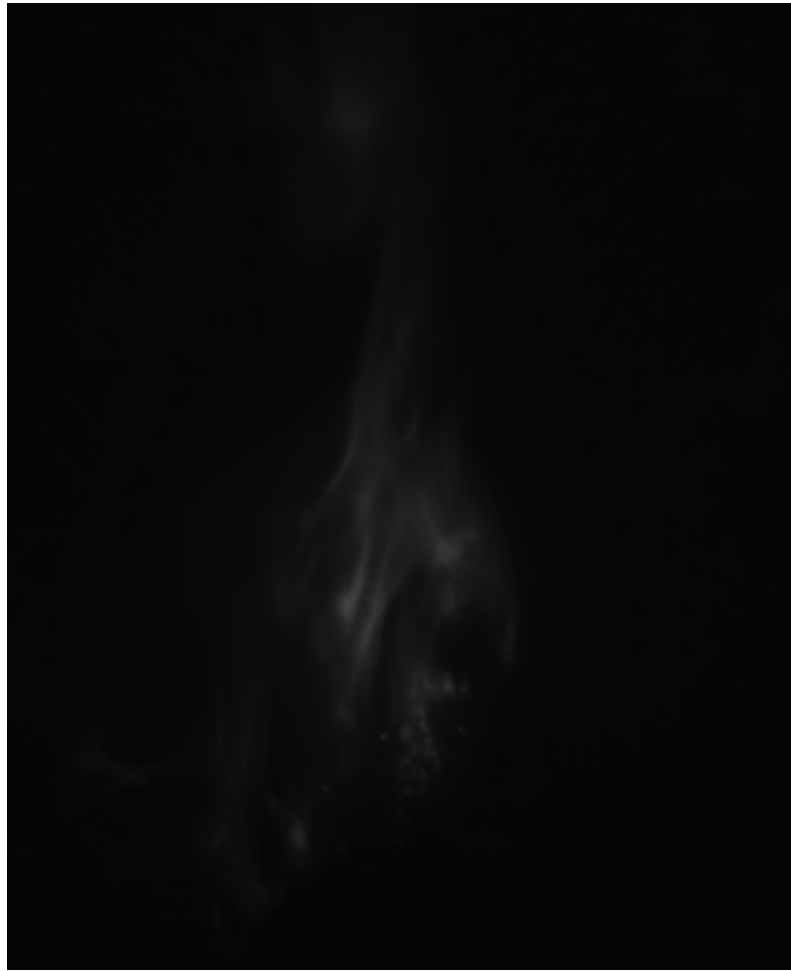
Figure 3.3: Example of the measurements recorded using the Ximea scientific camera with the 10 nm band-pass filter [14].

using a linear fit to the flame front location as a function of time during the non-optical steady-state regime of each test using least squares regression.

$$\dot{L}_{est} = \frac{L_{ss}}{t_{ss}} \tag{3.3}$$

Despite efforts to reduce error in the propagation rate calculated from CH*, low intensity tests produced measurements below reasonable expectations. To correct for this and include tests without CH* chemiluminescence measurements, the propagation rate was estimated from the steady-state burn time, (t_{ss}), and propagation distance, (L_{ss}), using Equation 3.3. The steady-state burn time is the time that each trial was within its non-optical steady-state regime. The steady-state propagation distance was the distance that each test traveled during its optical

steady-state regime. However, since this was found using CH* chemiluminescence measurements, the average propagation distance was used for tests without CH* chemiluminescence measurements and for tests with propagation distances below 50 cm. The 50 cm cutoff was used to correct tests with inaccurate propagation distances due to low intensities. This was done to account for the slight differences between the optical steady-state and non-optical steady-state regions. Pine was selected as the reference because it showed consistent results and had an increased number of tests.

$$Error_{Rel} = \frac{|\dot{L}_{CH*} - \dot{L}_{est}|}{\dot{L}_{CH*}} \qquad (3.4)$$

3.3.4 Fuel Bed Temperature Measurements

In a select number of tests, the mean fuel bed temperature was measured instead of the flame front location and propagation rate. The mean fuel bed temperature was measured using a FLIR A500 infrared camera positioned above and behind the fuel bed, so that the flame front propagated away from the camera to clearly observe the flame region and the smoldering fuel. The FLIR camera automatically focused on the center of the fuel bed and maintained a constant focus throughout the test. The images were sampled at 30 Hz and reported fuel temperatures between 273 K and 923 K. Using FLIR Research Studio software, the time-averaged temperature of the fuel bed was found for each instance in time throughout the duration of the test. An example of the measurements collected by the FLIR infrared camera can be seen in Figure 3.4.
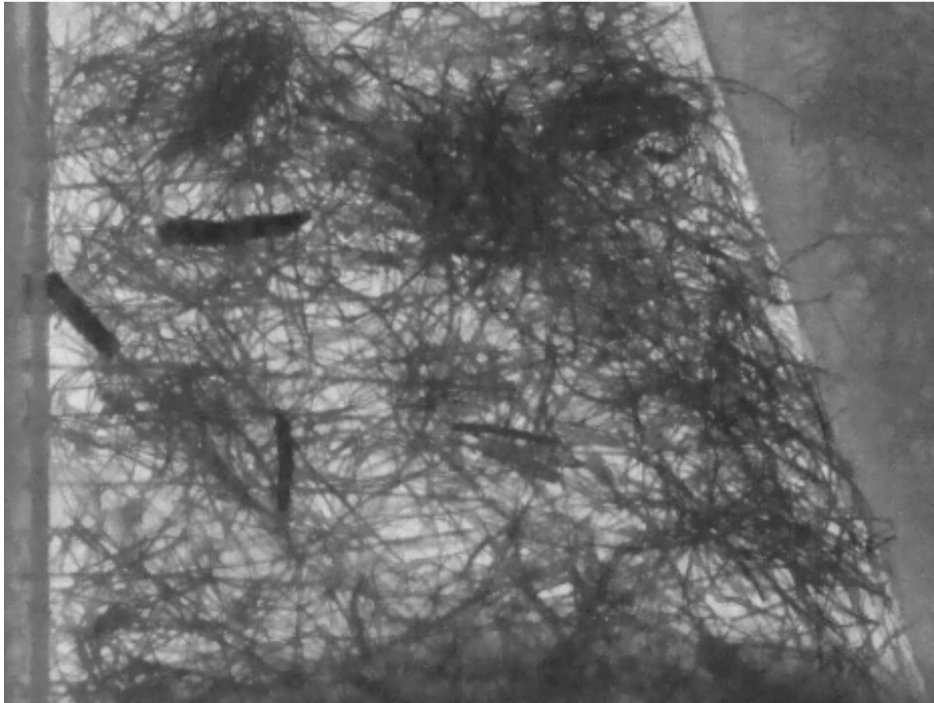
Figure 3.4: Example of the measurements recorded using the FLIR infrared camera.

3.4   Principal Components Analysis

To account for the intrinsic correlation between the flammability characteristics measured, principal components analysis (PCA) was used to better compare the results of each fuel group. Because the flammability characteristics measured are not independent of each other, it is difficult to determine how much variation in the data is directly caused by changes in the fuel composition versus changes in other variables. PCA can be used to reduce the number of variables to a smaller group of interpretable linear combinations of the original variables. The inbuilt MATLAB PCA function was used to complete the PCA calculations.

PCA generates a number of new variables, termed principal components, equal to the number of original variables. However, each principal component also describes a known percentage of the variation in the data, and the principal components with the least significance can be discarded to decrease the number of variables. Once the significant principal components have been selected, their linear combinations with each directly measured variable can be used to describe what each principal component physically represents.

22

Using PCA, tests were separated into a number of clusters. Each cluster included tests with similar principal components that were distinct from the principal component values of the tests in the other clusters. The number of clusters was determined by the MATLAB evalclusters function. Each test was assigned to a cluster using the MATLAB kmedoids function, which finds a central point for each cluster in a n-dimensional scatter plot where n is the number of principal components, in this case 6. The tests are then assigned to the cluster with the closest central location to the test.

3.5 Results Presentation

The time plots and scatter plots presented in chapter 4 are color-coded to quickly distinguish the fuel composition of each data set. Each fuel group was colored with an RGB value corresponding to the mass fraction of each fuel species, where red, green, and blue corresponded to the content of pine, sweetgum, and oak, respectively. For example, oak tests were displayed with a RGB value of [0,0,1], while a mixture with 20% pine, 50% sweetgum and 30% oak content was presented using a RGB value of [0.2,0.5,0.3]. To distinguish wet pine from dry pine, wet pine tests were presented in black. The colors used for the single fuel groups are shown in Table 3.3, and the colors used for the mixed fuel groups are shown in Table 3.4.

Some figures in chapter 4 used "clumped" fuel groups rather than the mixed fuel groups. These clumped fuel groups are groups that include tests with similar fuel mixtures, rather than delineating the each discrete fuel combination. This was done to condense the mixed fuel group results to provide an additional, less cluttered perspective for certain figures. Three clumped fuel groups were defined, with low (0% - 20%), moderate (30% - 40%) and high (50% - 70%) sweetgum content . The RGB values used for these groups are the mean values of their constituent fuel groups and are shown in Table 3.5.

Table 3.3: Single Fuel Group Colors

Fuel species	RBG Value & Color
Pine	[1,0,0]
Oak	[0,0,1]
Sweetgum	[0,1,0]
Wet Pine	[0,0,0]

Table 3.4: Mix Fuel Group Colors

Fuel Sweetgum Content	RBG Value & Color
0% Sweetgum	[0.7,0,0.3]
10% Sweetgum	[0.6,0.1,0.3]
20% Sweetgum	[0.5,0.2,0.3]
30% Sweetgum	[0.4,0.3,0.3]
40% Sweetgum	[0.3,0.4,0.3]
50% Sweetgum	[0.2,0.5,0.3]
60% Sweetgum	[0.1,0.6,0.3]
70% Sweetgum	[0,0.7,0.3]

Table 3.5: Clumped Fuel Group Colors

Fuel species	RBG Value & Color
Low Sweetgum Content	[1,0,0]
Moderate Sweetgum Content	[0.35,0.35,1]
High Sweetgum Content	[0,1,0]

Chapter 4

Results

Measurements of mass loss rate, combustion fraction, temperature, and propagation rate are valuable data on the burning characteristics of mixed wildland litter as they relate to the exploration of possible mechanisms of mesophication and the general interactions of mesophyte and pyrophyte litter in wildland fires. This study explores these factors related to possible mechanisms of mesophication, as well as several secondary factors on the characteristics of burning, which will help guide future studies. This chapter presents the results of this study and some discussion of the interactions between the aforementioned parameters.

Results of the experiments on the effects of fuel mixture on moisture retention and of moisture content on the burning characteristics were inconclusive. Preliminary tests resulted in no mixed fuel beds capable of sustaining combustion, providing little information on the effect of moisture on the combustion of the mixed fuel bed. In contrast, most of the pine tests were able to sustain a burn; the results of which are included below.

Initial experiments highlighted vulnerabilities in the testing environment. Although the facility was climate controlled, certain environmental conditions were found to complicate the ability to meet climate demands. The significant disparity between the humidity and temperature of the outdoor and indoor environment of the facility made it difficult to maintain the desired conditions in the testing area. During multiple tests, the rate at which the fume hood displaced air exceeded the ability of climate control to correct temperature and humidity, causing indoor conditions to converge with outdoor conditions. For this reason, the ambient temperature and humidity were recorded to track their effect on the burning characteristics. Although

both ambient temperature and humidity were recorded, only measurements with notable observations or statistically significant relationships are presented in the results and discussion. The climate control issue was not observed during the initial tests and, as such, ambient conditions were not measured for the initial mixture tests. These tests were unable to be repeated due to the limited availability of oak and sweetgum litter. Further tests will be needed to correct for this data gap.

4.1 Mass Measurements

The results for the mass-time history are presented here, including the normalized mass loss rate and the combustion fraction. In the present study, the normalized mass loss rate was found to be the fraction of the initial fuel mass lost per second, and the combustion fraction was found to be the ratio of the initial and final fuel load. The fuel bed was formed with various mixtures of longleaf pine ($P.\ palustris$), southern red oak ($Q.\ falcata$) and sweetgum ($L.\ styraciflua$) litters. For mixed fuel tests, oak leaves made up 30% of the fuel bed mass and the fraction of the pine and sweetgum mass ranged from 0% to 70% in increments of 10%. Furthermore, several tests with a single fuel species and pine tests with an increased moisture content were performed. For the moisture tests, each test was soaked in water for 24 hours and allowed to dry for 24 or 48 hours, resulting in different moisture levels in the tests. It should be noted that the moisture results presented here provide a general comparison with the dry test results and do not consider the variation in moisture content, only the presence of moisture content. An alcohol soaked string was used to ignite the fuel at one end of the test bed for simultaneous ignition along the width of the test bed. Measurement recording started immediately before ignition and the ignition time was recorded immediately after. The time of flame extinction was recorded and the measurements were concluded once the fuel mass was constant. The ignition and extinction times were used to determine the steady-state range of each test so that the effects of flame ignition and extinction could be minimized when determining the mass loss rate.

Figure 4.1 shows the average mass fraction of each fuel group plotted against time. The mass fraction was found to be the ratio between the fuel mass at a given time and the initial fuel load. The mass fractions at a given time and within the same fuel group were averaged to produce the results shown in Figure 4.1. Because the burn time durations were not the same for all tests, the average mass fraction of each fuel group was only found for the shortest test duration in that group.
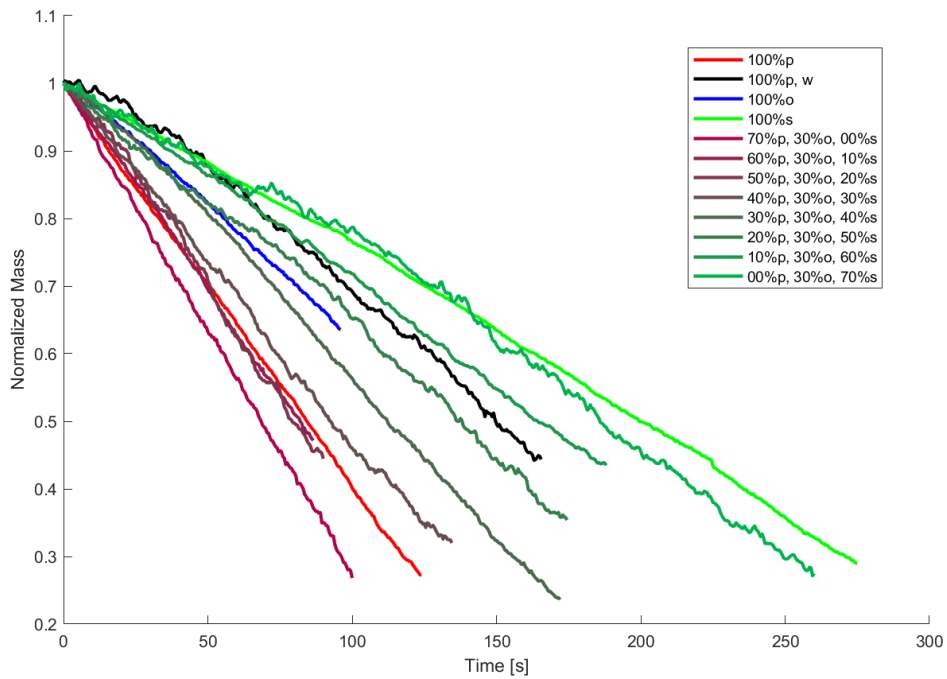
Figure 4.1: Average mass fraction of each fuel group.

The average mass fraction was recorded to explore how the mass loss changed during the test duration for each fuel group. As the tests progressed, the mass fraction decreased with varying rates between each fuel group. The slope of the average mass fraction reflects the mass loss rate of the fuel samples, with steeper slopes corresponding to higher mass loss rates. As a mesophyte, sweetgum is expected to burn slower than pyrophytes such as pine and oak. The slopes of the average mass fraction of the single fuel groups agree with the expectation, as dry pine showed the steepest average mass fraction slope, followed by oak and sweetgum in that order. This establishes the range of mass loss rates that mixed fuel groups are expected to produce. Notably, the results of the oak are significantly truncated as a result of large variations

in test duration. This suggests that additional factors have a greater impact on the slope of the average mass fraction and therefore on the mass loss rate of oak. The slope of the wet pine was between that of the oak and the sweetgum, reflecting that the moisture content decreased the mass loss rate of the fuel. The mixed fuel groups with high sweetgum content had an average mass fraction slope slightly steeper than that of the unmixed sweetgum. This is in agreement with initial expectations, as the introduction of pine and oak litter increases the mass loss rate of the fuel sample. As the sweetgum content decreases and the pine content increases, the average mass fraction slope becomes steeper; which again, aligns with initial expectations. However, mixtures with a sweetgum content of 20% or less resulted in steeper slopes of the average mass fraction than those of dry pine. This suggests the presence of an interaction between pine and oak that increases the mass loss rate.

All fuel groups initially had non-linear average mass fraction slopes; however, the duration of the non-linear profile and the magnitude of the change in slope differed for each fuel group. As the tests progressed, the average mass fractions transitioned into linear or near-linear profiles. The way in which the average slopes of the mass fraction initially changed over time reflects the distribution of the mass loss within and directly behind the flame front. Fuel groups that quickly transitioned to linear slopes likely had the majority of their mass loss occurring within a thin region of their flame front. This happens because the flame front is required to propagate a shorter distance before the flame front is fully established. This was especially present in dry pine tests that were found to have quasi-steady mass loss, which is consistent with the findings of previous work by Stubbs et al. [14]. Longer durations of a non-linear slope likely corresponded to a broader flame front, as a broader flame front would require more time to propagate before it was fully developed. Both the oak and especially sweetgum displayed large regions of initially non-linear mass loss, suggesting that both fuel groups had broader flame fronts. Wet pine also displayed a large region of initially non-linear mass loss, indicating that moisture content broadens the flame front. The region of mass loss near the flame front may have been widened due to an extended region of drying ahead of the flame front. In mixed fuel groups, groups with 0% to 30% sweetgum had short non-linear regions. This suggests that when the content of pine is greater than that of sweetgum, the region of mass loss near the flame

front remains thin. Once the sweetgum constituted 40% or more, the duration of the initial non-linear region increased, with 70% sweetgum tests having similar results to the sweetgum fuel group. This indicates that once the sweetgum content surpasses the pine content, the flame front begins to broaden.

The average mass fraction profile after the initial non-linear region reflected the mass loss due to smoldering combustion behind the flame front, with non-linearity corresponding to smoldering. This relationship is due to the region of mass loss increasing after the flame front has fully developed. Both dry and wet pine tests displayed linear mass loss after their initial non-linear region, suggesting that minimal mass was lost due to smoldering. Sweetgum tests became increasingly non-linear as they progressed, suggesting that there was significant mass loss due to smoldering. The results for oak are unclear because they were truncated earlier than those for the other fuel groups. Mixtures with more pine than sweetgum mirror the results of pine. Once the quantity sweetgum surpasses pine, the results begin to more closely resemble those of sweetgum.

Figure 4.2 presents the average mass fraction for the single fuel groups, with the addition of the 95% confidence interval denoted by the shaded region. This figure was included to provide a more streamlined perspective of the results of the single fuel groups presented in Figure 4.1. For all single fuel groups, the 95% confidence interval increased as the tests progressed, although the degree varied for each group. A continued increase in the confidence interval should be expected, as the impact of the variation in the mass loss rate would compound over the duration of the test. Pine had a relatively narrow 95% confidence interval, indicating consistent results; however, an increase in the number of pine tests likely contributed to shrinking the 95% confidence interval. The oak tests had the broadest 95% confidence interval, which is consistent with the expected variations indicated by their early truncation. Sweetgum and wet pine both had moderately broad 95% confidence intervals, indicating moderate deviations in mass loss rate.
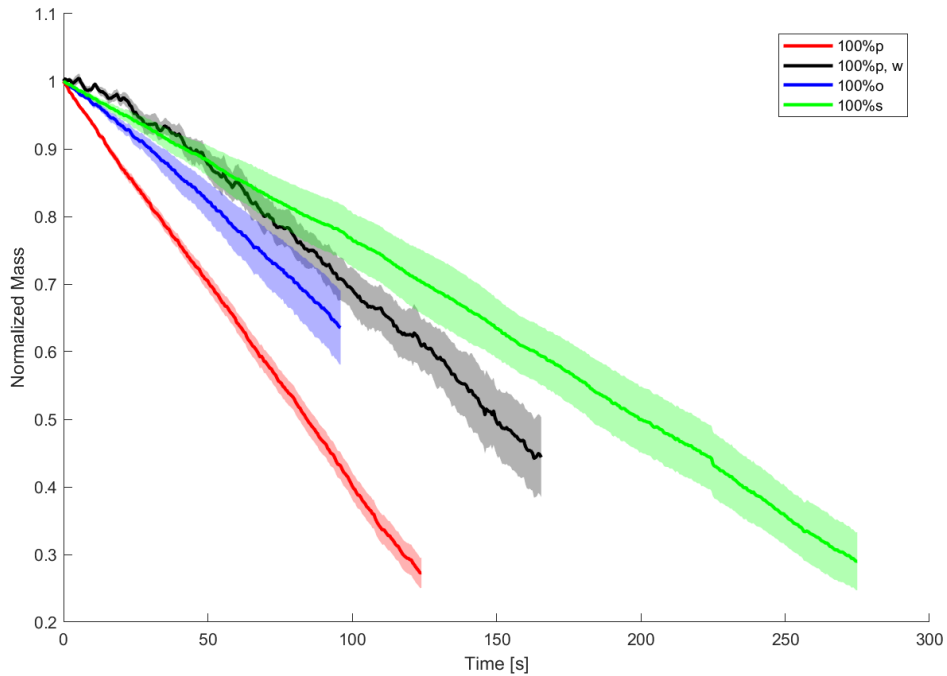
Figure 4.2: Average mass fraction of each single fuel group.

Figure 4.3 presents the average mass fraction for the "clumped" fuel groups, with the addition of the 95% confidence interval denoted by the shaded region. The clumped fuel groups are a combination of mixed fuel groups with similar fuel compositions, and the methods used to define them are also explained in Section 3.5. The mixed groups were clumped into one of three groups, low, moderate, and high sweetgum groups. The low sweetgum group consisted of tests with 0% to 20% sweetgum, the moderate sweetgum group consisted of tests with 30% to 40%, and the high sweetgum group consisted of tests with 50% to 70% sweetgum. This was done to reduce clutter and provide a clearer perspective of the mixed fuel groups. The 95% confidence interval for the moderate sweetgum group is slightly lower than that of the other clumped groups, which can be attributed to the reduced variation in fuel composition. Otherwise, the results mirror those seen in Figure 4.1, where the mass loss rate decreases with additional sweetgum content.
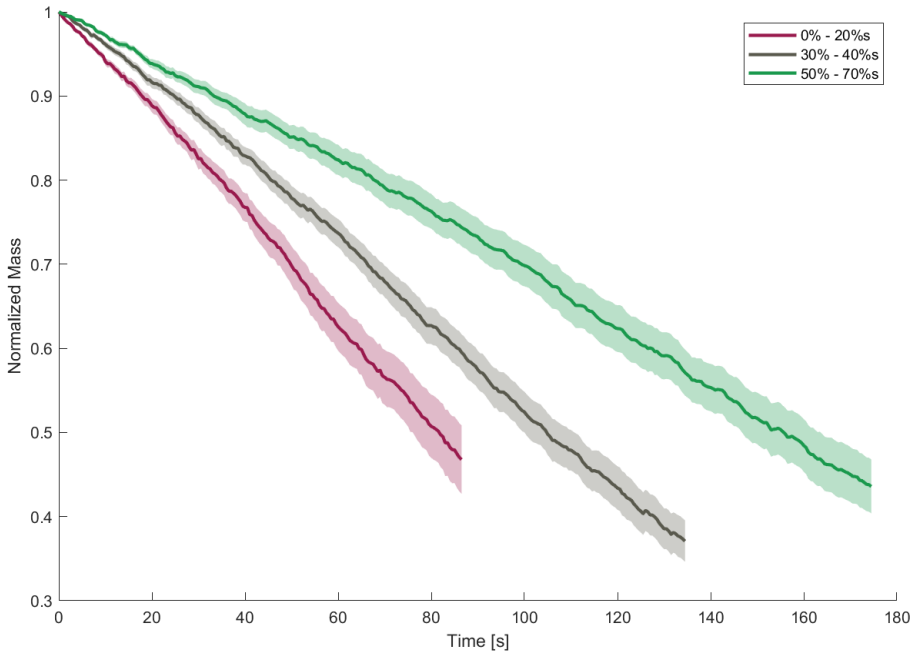
Figure 4.3: Average mass fraction of each clumped fuel group.

4.1.1 Mass Loss Rate

The mass loss rate is directly proportional to the rate of heat release, which is potentially the most significant factor in determining the flammability of a substance [46]. From the average mass fraction measurements, the normalized mass loss rate was calculated as the slope of a linear best fit from the mass loss data through the steady-state region of each test. Figure 4.4 presents the box plots of the normalized mass loss rate of each fuel group.

Figure 4.4 shows the inner and outer quartiles, the median value, and the outliers for the normalized mass loss rate of each fuel group. The inner quartile is denoted by blue boxes, and the outer quartile by the dashed lines that extend from the inner quartile. The median values occurred at the red line found within the inner quartile, and the outlying values were distinguished by a red "+". The results shown in Figure 4.4 reflected those found from the measurements of the average mass fraction shown in Figures 4.1, 4.2 and 4.3. When discussing box plot figures, the median measurements of pine will be used as a reference point. The median values of the other fuel groups will be displayed as a percentage of the pine values in parentheses after the fuel group is discussed.

31
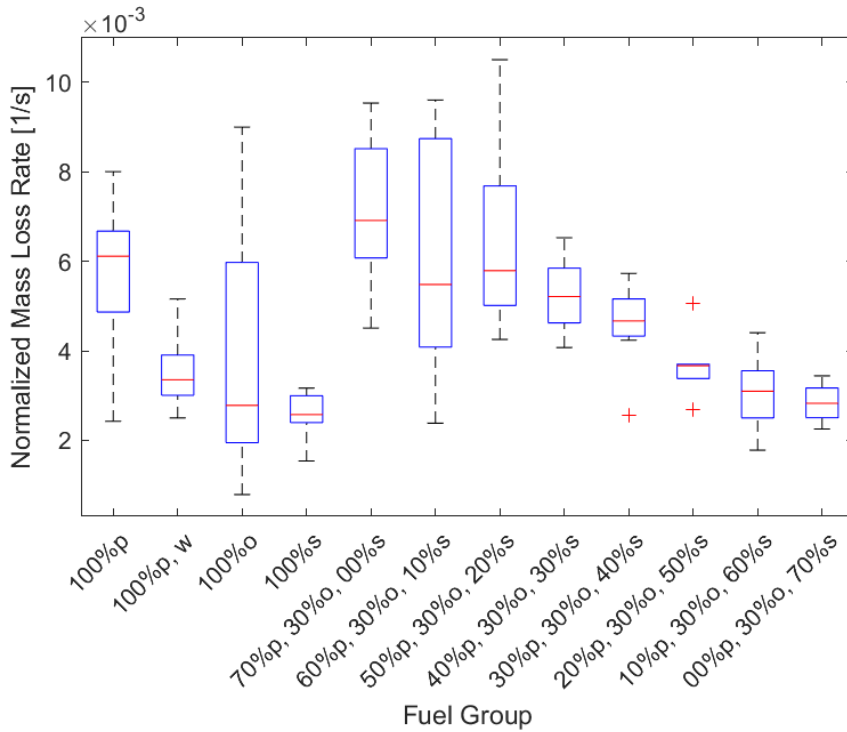
Figure 4.4: Normalized mass loss rate for each fuel group.

Of the dry single fuel groups, pine had the highest median normalized mass loss rate, followed by oak (45%) and then sweetgum (42%). The normalized mass loss rate of the oak had a significant positive skew, reflecting the early truncation seen in the oak results in Figures 4.1 and 4.2. Oak tests within the upper quartile had normalized mass loss rates similar to those of the upper quartile of pine, while the lower two quartiles of oak had results similar to the median sweetgum value. In the following Figure 4.5 the normalized mass loss rates of oak will be shown to be bimodal. This suggests that oak combustion is more dependent on additional factors than that of pine or sweetgum. The increase in moisture significantly decreased the median normalized mass loss rate of pine (55%); however, the median values were still similar to the lower quartile values of dry pine. Furthermore, the lowest normalized mass loss rates for wet pine were similar to the minimum values for dry pine. This suggests that wet pine may have a normalized mass loss "floor" where mass loss rates below this value correspond to inconsistent combustion. Most likely, the normalized mass loss rate within the flame front remains consistent, and moisture primarily impacts the propagation rate of the flame front.

Below the normalized mass loss rate "floor", there is not sufficient total heat release along the leading edge of the flame front to dry the fuel ahead of it.

The results shown in Figure 4.4 for mixed fuel groups reflect those found for the measurements of the average mass fraction, with the normalized mass loss rate decreasing with increasing sweetgum content. These results correspond to expectations of how pyrophytic and mesophytic litter promotes and suppresses wildland fires, respectively [30]. In addition to the expected general decrease in the normalized mass loss rate, distinct changes in the normalized mass loss rate occur once the sweetgum content reaches certain thresholds.

For mixtures with a sweetgum content of 0% (113%), normalized mass loss rates exceed the pine values for each quartile and the median value. Like in Figure 4.1, this indicates an interaction between pine and oak that accelerates the combustion of both fuels. Once the sweetgum content increased to 10% (90%), the median and low quartile values of the normalized mass loss rate decreased substantially; however, the upper quartile values were similar to that of 0% sweetgum mixtures. This indicates that the presence of sweetgum may disrupt the interaction between pine and oak, leading to a sharp drop in the normalized mass loss rate. There was little change once the sweetgum content reaches 20% (95%), indicating that the impact of sweetgum is still inconsistent. Although it may appear that the normalize mass loss rate increases at 20% sweetgum content, this is likely due to the reduced number of tests carried out for this mixture. At 30% (85%) the normalized mass loss rate begins to decrease more consistently. The lower quartile values for this mixture are similar to those found for the 20% tests; however, the upper quartile decreases significantly. This suggests that once sweetgum reaches 30%, the interaction between pine and oak is consistently disrupted. As sweetgum increases further to 70% (46%), the normalized mass loss rate approaches the values found for sweetgum at a roughly consistent rate. Given that the median value for the 70% sweetgum tests is not increased by the presence of oak, it is likely that sweetgum can serve to limit the rate of mass loss of oak to its lower mode.

Figure 4.5 compares the normalized mass loss rate with the fuel specific volume for each test. Similarly to Figures 4.1, 4.2, and 4.3, the tests are color-coded according to their fuel composition, as described in Section 3.5. To avoid compressing the fuel beds and to closely emulate an undisturbed forest floor, the depth of the fuel bed was not kept constant. The depth of the fuel bed was recorded before each test to allow the effects of the fuel specific volume to be examined. The fuel specific volume was used in this figure instead of fuel bulk density because it showed a stronger linear relationship to the mass loss rate.
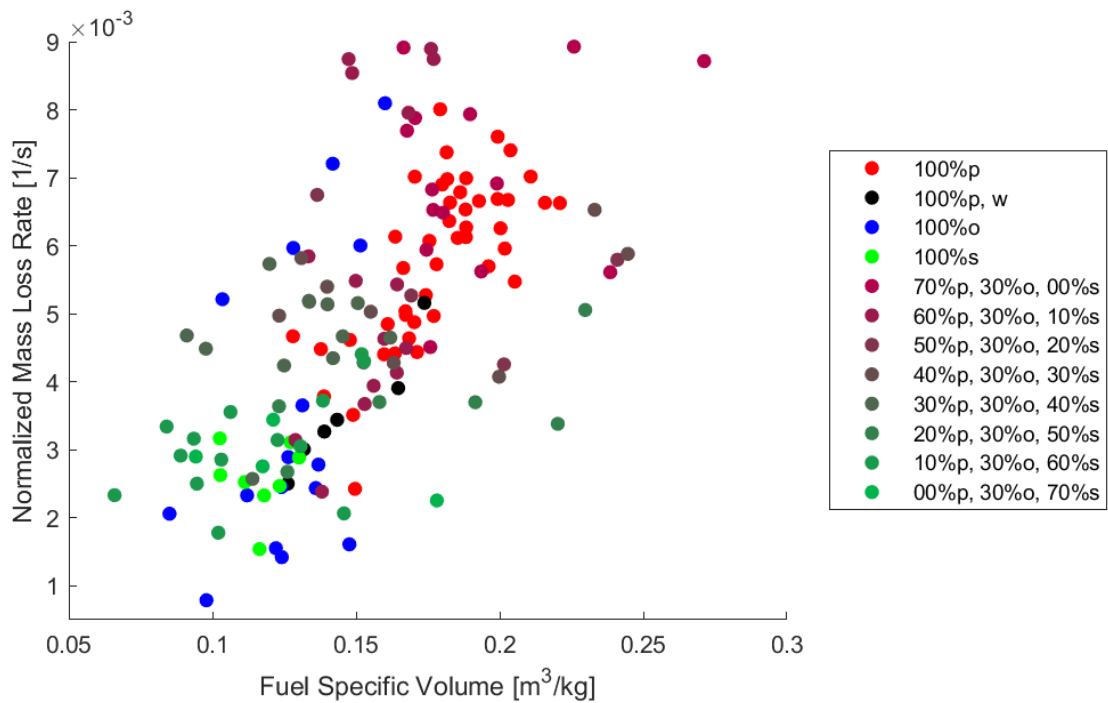
Figure 4.5: Normalized mass loss rate compared to fuel specific volume for each test.

Figure 4.5 shows that the relationship between fuel specific volume and normalized mass loss rate was statistically significant ($m = 0.033\ m^3/kgs$, $\sigma = 0.0035$, $t_{stat} = 9.43$, $p_{val} = 5.60\text{e-}17$). This relationship is expected for fuel-rich combustion, as an increase in the amount of oxygen available moves the reaction closer to stoichiometric conditions. In particular, two groups of oak tests can be observed in Figure 4.5 that have significantly different normalized mass loss rates, despite having similar fuel specific volumes. This indicates that oxygen availability is not responsible for the variance in the normalized mass loss rate observed in oak.

Figure 4.6 compares the normalized mass loss rate and the ambient humidity of each test. Ambient humidity did not have a statistically significant impact on the normalized mass loss

rate. However, in Figure 4.6 it is shown that all oak tests with increased rates of normalized mass loss occurred when the ambient humidity was noticeably lower. Combined with the results that no mixed moisture tests were able to achieve sustainable combustion, this suggests that the moisture content may have a greater impact on the combustion of oak. The dependence on ambient humidity would suggest that the heat required to remove moisture represents a much larger proportion of the total heat required to propagate oak combustion. When considering the increased mass loss rates found in tests with low sweetgum content, it is possible that this is caused by pine, which produces enough excess heat to decrease moisture ahead of the flame front sufficiently so that the oak can burn more easily. In this study, pine has been shown to sustain combustion in high moisture conditions, further supporting this interaction.
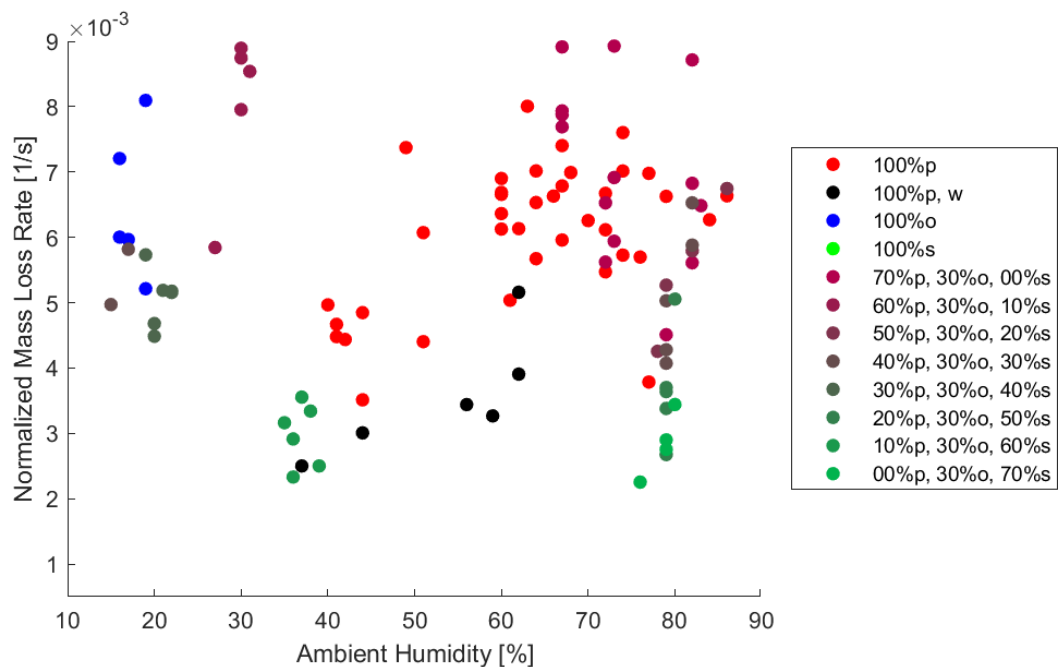

Figure 4.6: Normalized mass loss rate compared to ambient humidity for each test.

In contrast, mesophytes have been shown to have increased moisture retention [30], presenting the possibility that this moisture content within the sweetgum slows oak combustion. For these reasons, as the sweetgum mass fraction increases and the pine mass fraction decreases, the effect of moisture on the combustion of oak becomes more pronounced. In particular, Figure 4.5 shows that low sweetgum content mixtures often have higher mass loss rates than pine tests with similar fuel specific volumes. In addition to this, low humidity oak tests produced higher mass loss rates than pine with similar fuel specific volumes. Together, these findings suggest that once the oak has been dried out by the pine, it ignites before the surrounding pine and then accelerates the pine combustion.

4.1.2 Combustion Fraction

While mass loss rate is related to the heat release rate, the combustion fraction (η) was used to approximate the consumption efficiency of each fuel group. The combustion fraction is correlated with the efficiency of fuel consumption and was calculated using the fraction of the mass that remains after the test with the initial loading mass. The combustion fractions of each fuel group are presented in Figure 4.7, which uses the same method to present the results as the previous normalized mass loss box plot, Figure 4.4.

Like the mass loss rate, dry pine was found to have the highest combustion fraction among individual species. Furthermore, the combustion fraction of pine (98%) only marginally decreased with high moisture content. The combustion fraction of oak (95%) was not found to be bimodal and was the lowest of the single fuel groups. As the combustion fraction of the oak was not bimodal and the moisture had only a mild impact on the combustion fraction of the pine, this suggests that the moisture only increases the heat required for initial combustion. The combustion fraction for sweetgum (97%) was comparable to that of wet pine. The combustion fraction generally decreased with an increase in sweetgum. The mixtures with sweetgum content of 0% (101%), 10% (95%), 20% (97%), 30% (91%) and 40% (98%) had similar results to those found for the single fuel groups. However, once the sweetgum content reached 50% (80%), the combustion fraction dropped dramatically and produced much lower combustion fractions than its constituent species. Once the sweetgum content increased further
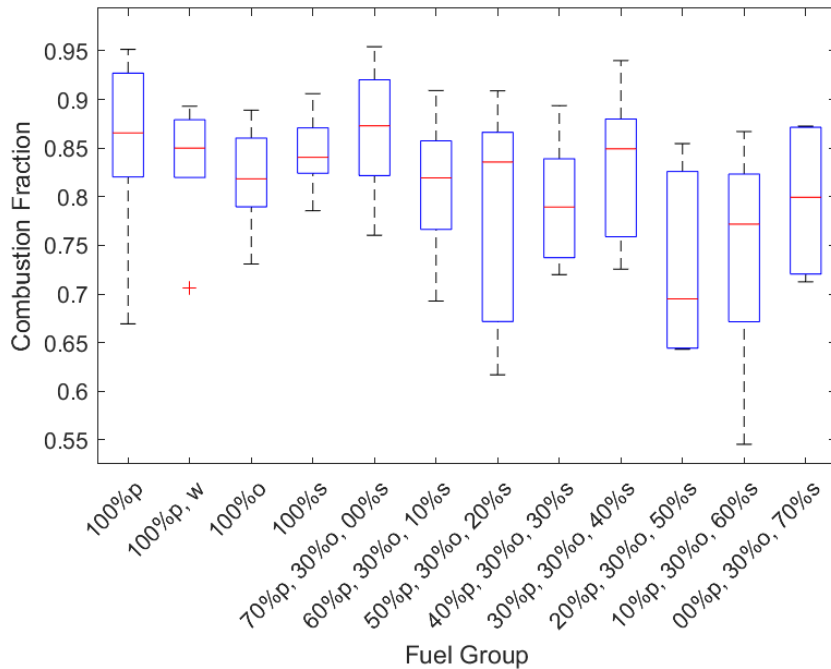
Figure 4.7: Combustion fraction for each fuel group.

to 60% (89%) and 70% (92%) the combustion fraction began to increase. This implies that the decrease in the combustion fraction is not due to the combustion fractions of the constituent species but to an interaction between the species that disrupts combustion.

Figure 4.8 displays the combustion fraction and the fuel specific volume for each test. Fuel specific volume has a significant impact on the oxygen available to the fuel and is therefore expected to have a significant impact on the combustion efficiency. In Figure 4.8 it is shown that the fuel specific volume has a positive relationship ($m = 0.606$ kg/m^3, $\sigma = 0.164$, t_{stat} = 3.70, p_{val} = 8.01e-04), with the combustion fraction. This would be expected for fuel-rich combustion; as oxygen availability increases and the combustion approaches its stoichiometric condition.
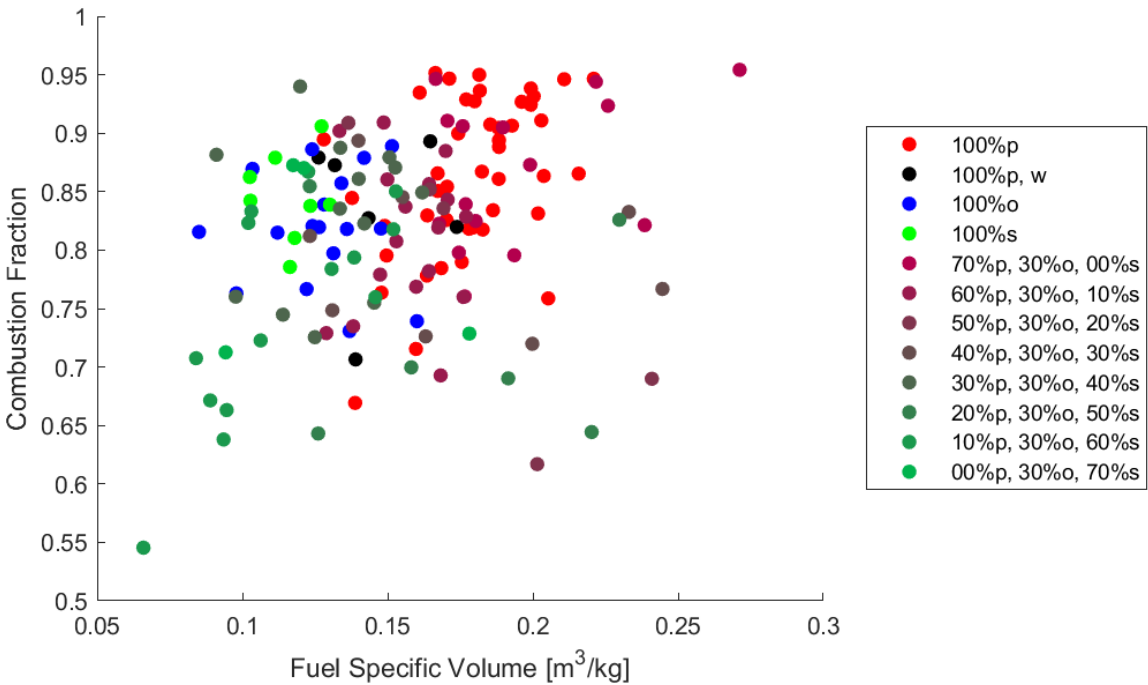
Figure 4.8: Combustion fraction compared to fuel specific volume for each test.

The results of the mass measurements show that the fuel composition significantly affected the normalized mass loss rate of the fuel. Pine was found to consistently overcome the increase in moisture content, while oak showed an increased sensitivity to it. The results indicate that this reflects pine combustion having a greater heat release near the flame front, which provides enough heat to consistently dry and ignite the fuel ahead of the flame front. In contrast, oak may have low heat requirements for combustion, thus allowing for rapid propagation with small changes in the heat requirement having larger impacts proportionally. Tests with a 0% sweetgum content showed normalized mass loss rates that were higher than those of any of the single fuel groups. The results indicate that this may be due to the combustion of pine drying the oak ahead of the flame front and then oak igniting surrounding pine before it would otherwise ignite. The combustion fraction decreased for mixtures that included 50% to 70% sweetgum. This was most prevalent with 50% sweetgum mixtures, indicating an additional interaction between fuel species that interrupts combustion. The next section displays the results of the temperature measurements to provide further insight into these observations.

4.2 Combustion Temperature Measurements

The temperature of the flame has been shown to have a significant impact on combustion efficiency [47]. To understand how sweetgum can suppress the combustion efficiency of oak, the flame temperature was investigated using the method described in Section 3.3.2. During testing, an array of nine thermocouples was used to measure the flame temperature at multiple heights. The time of each thermocouple was offset so that each thermocouple recorded its first measurement of 350 K at $t = 0$ for the middle and top rows. In the bottom row, the first 400 K measurement was used for $t = 0$, as some fuel compositions would inconsistently heat the fuel ahead of the flame front. Then, for each test, the thermocouple measurements along each row were averaged at each point in time using the same method as the average mass fraction measurements. The results for the temperature profile of the bottom row are shown in Figure 4.9.
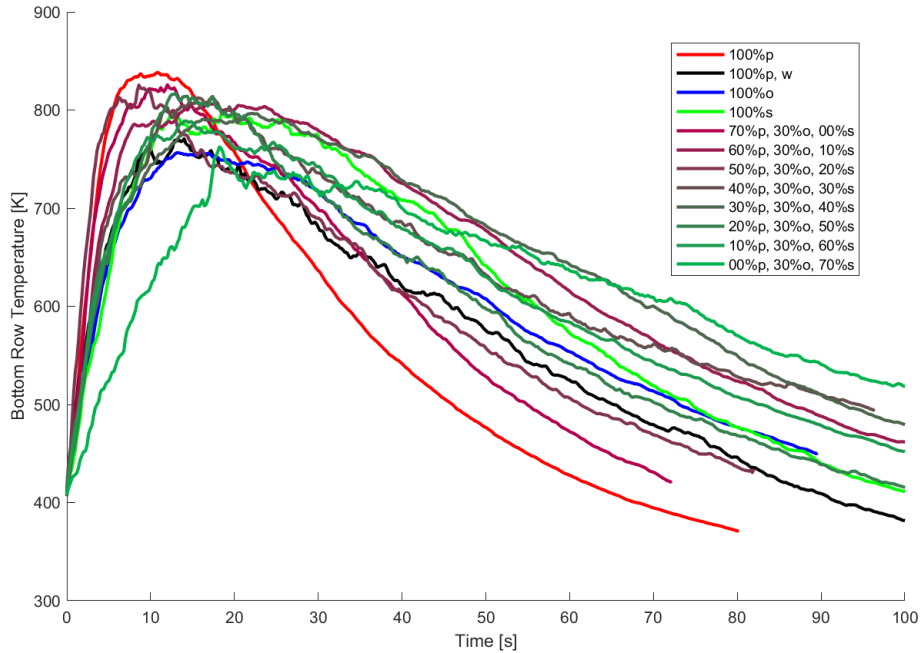

Figure 4.9: Temperature profile across the bottom row.

Figure 4.9 displays the temperature profile along the bottom row of the thermocouples. The temperature distribution ahead, within, and behind the flame front can be observed as the flame front propagates across the test bed. Specifically, along the bottom row, the temperature profile allows insight into the distribution of heat release within the flame front. The pine temperature profile along the bottom row showed a narrow, rounded temperature peak and a rapid decrease behind the peak. This suggests a thin flame front, where combustion is concentrated with reduced smoldering behind it. The increase in moisture content decreased the temperature peak and slowed the rate at which the temperature decreased. This indicates that a sufficiently high moisture content broadens the flame front. The temperature profile for oak was similar to that of wet pine, except with a more rounded peak and higher residual temperatures. Again, this reflects increased combustion behind the flame front and a potential increase in smoldering combustion. The temperature profile for sweetgum produced a peak that was lower than that of dry pine but above that of oak and wet pine's peak. The peak was much flatter than that of the other species. Furthermore, while the trailing edge of the temperature peak was greater than that of oak, the temperature then decreased rapidly to a lower residual temperature. This may reflect a broad flame front with evenly distributed combustion and moderate smoldering behind the flame front.

Like the average mass fraction Figure 4.1, Figure 4.9 was split into two additional figures that focus on the single fuel and the clumped fuel groups with the addition of the 95% confidence interval. Figure 4.10 displays the temperature profile across the bottom row of the thermocouples for the single fuel groups. This figure provides a more streamlined perspective by reducing the number of data sets. The pine had a narrower 95% confidence interval than the other fuel groups. Oak and sweetgum had similar moderate 95% confidence intervals, while wet pine had the largest 95% confidence interval. This is expected, as the wet pine tests included a wide range of moisture levels, which would result in less consistent results between each test. Although oak exhibits bimodal normalized mass loss rates, its 95% confidence interval is fairly moderate, indicating little difference in the heat release profile.

40
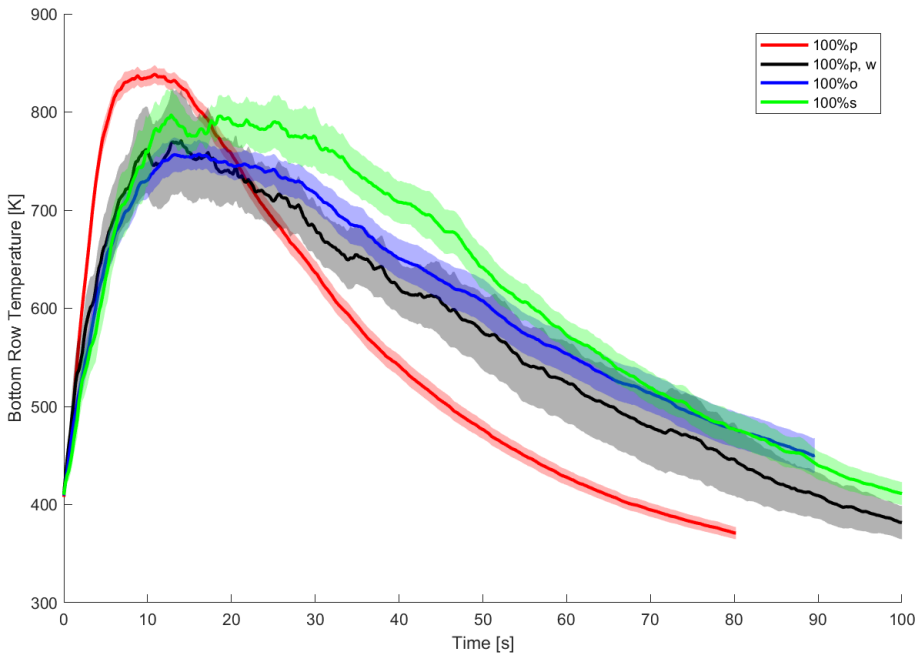
Figure 4.10: Temperature profile across the bottom row for single fuel groups.

Figure 4.11 displays the temperature profile across the bottom row of the thermocouples for the clumped fuel groups. Again, this was done to reduce the number of data sets presented and provide a clearer view of the data. All three mixture clumps produced similar peak temperatures, which was likely caused by pine combustion. Since each mixture clump included multiple fuel compositions, there was likely greater variance within them. The low sweetgum content tests resulted in rapid increases in temperature, probably as a result of increased propagation rates. These mixtures also had broad, flat temperature peaks. However, as shown in Figure 4.4, the mass loss rate typically varied more as the sweetgum content decreased. These variances are likely the cause of the temperature peak profile rather than the actual temperature profile. The temperature decreased rapidly compared to the other the other clumped fuel groups, reflecting the previously observed temperature decrease trends found in the pine tests.
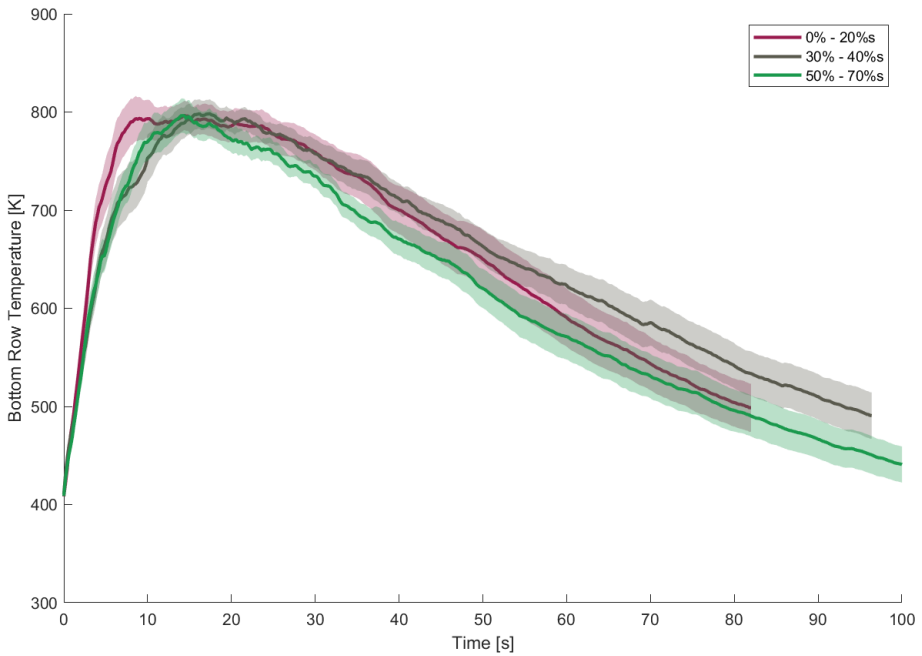
Figure 4.11: Temperature profile across the bottom row for clumped fuel groups.

The moderate sweetgum content mixtures increased in temperature more gradually, reflecting slower propagation. The temperature peak was also found to be broad and rounded as a result of less variation given the smaller sweetgum content range. The temperature gradually decreases with a higher residual temperature than that found in tests with a low sweetgum content. This suggests greater smoldering behind the flame front, given the reduced impact of the pine. High sweetgum content tests also had gradual increases in temperature, again reflecting slower propagation. Here, the temperature peak was also rounded but much narrower. In addition, the temperature gradually decreased, but had the lowest residual temperature. These indicate moderately reduced smoldering, which is also reflected in the sweetgum temperature profile. Additionally, reduced smoldering in the high sweetgum content tests may have caused the reduced combustion fractions in these mixtures.

Figure 4.12 shows the temperature profile across the middle row of the thermocouples. Along the middle row, the impact of the mass loss rate distribution across the flame front begins to have an increased impact on the temperature profile. The distribution of mass loss and heat release is not necessarily synchronized, and the concentration of mass loss has a greater impact on flame height. Additionally, as the height of the temperature measurements increases, the affects of smoldering combustion on the measurements are reduced.
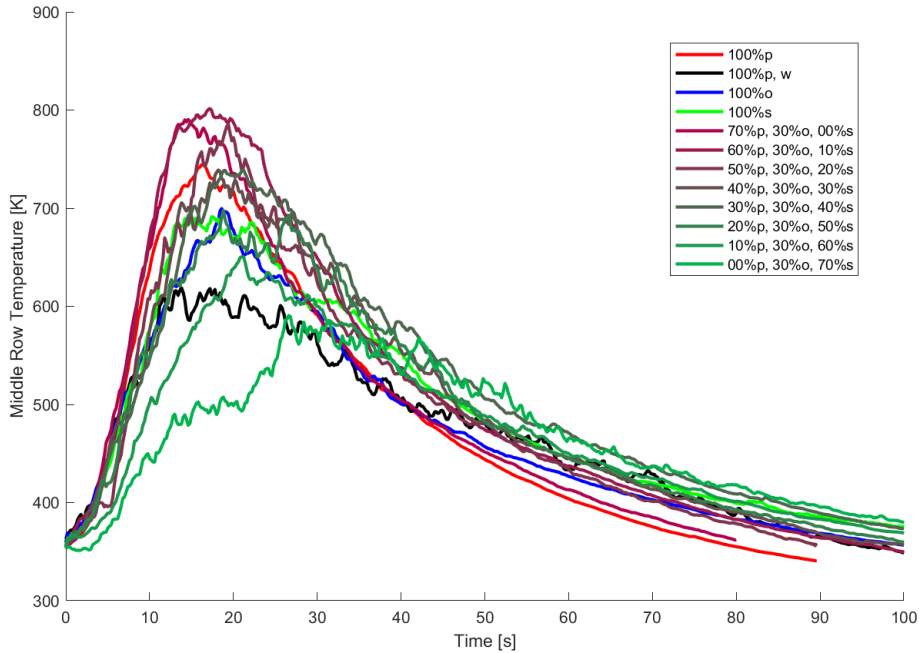
Figure 4.12: Temperature profile across the middle row.

The peak of the pine temperature was again the highest among the individual species, but lower than its peak along the bottom row. Because the distance from the flame bed has increased, a decrease in temperature is expected; this is also observed in the other fuel groups. The temperature profile of the pine had a much sharper peak than along the bottom row, and a short flat region, or shoulder, appeared as the temperature decreased. The temperature profile suggests a small region of increased mass loss within the flame front, followed by a second region of slightly reduced mass loss. The increased concentration of mass loss within these regions would then directly increase the height of the flame at that point. The increase in moisture content reduced and flattened the temperature peak along the middle row. Since dry pine showed a smaller region of increased flame height and the moisture content varied between

43

tests, this profile may not provide an accurate description of the true results. Like pine, the temperature peak of the oak became sharper along the middle row, possibly because of a thin region of rapid combustion. Along the bottom row, oak's temperature decrease was much more gradual than pine's but is now similarly steep. This reflects the reduced impact of smoldering combustion farther away from the fuel bed. Sweetgum's temperature profile was flatter than those found in the other species and again reflects a broader flame front with evenly distributed combustion. The temperature decrease remained gradual, also suggesting a broader flame front.

Figure 4.13 shows the temperature profile across the middle row of the thermocouples for the single fuel groups, with the inclusion of the 95% confidence interval. The size of the 95% confidence intervals for pine, wet pine and oak was similar to that seen along the bottom row in Figure 4.10. Sweetgum, however, displayed a much broader 95% confidence interval along its peak region. This may suggest intermittent combustion within the sweetgum flame front. This would cause the flame height to reach the thermocouples at this height inconsistently, producing significant variation in the measurements above the flame front.
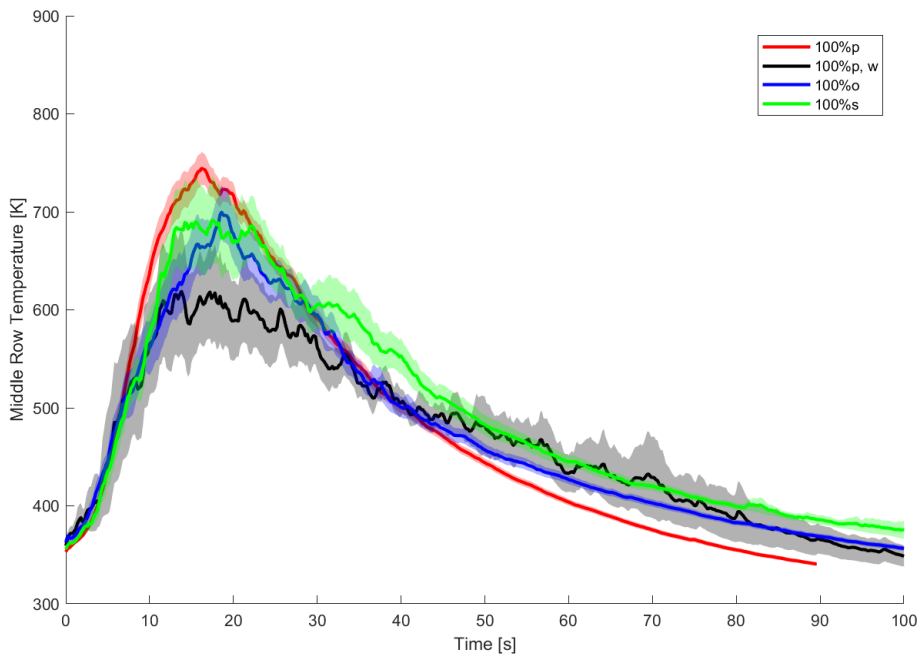
Figure 4.13: Temperature profile across the middle row for single fuel groups.

Figure 4.14 displays the temperature profile across the middle row of the thermocouples for the clumped fuel groups. In the middle row, the differences between the clumped fuel

44

groups were more distinct. The sweetgum content significantly decreased both the rate at which the temperature increased and the temperature peak. Fuel mixtures with a low sweetgum content had a higher temperature peak than pine; however, as the sweetgum content increased, the temperature decreased below that of the sweetgum. The low sweetgum content mixtures likely produced flame fronts with greater height, as their temperature peaks are still below that found for pine along the bottom row, which is supported by the increased mass loss rate found in low sweetgum content mixtures. Conversely, high sweetgum mixtures probably resulted in lower flame heights, as the small region of peak combustion for each fuel may have occurred at different locations within the flame front.
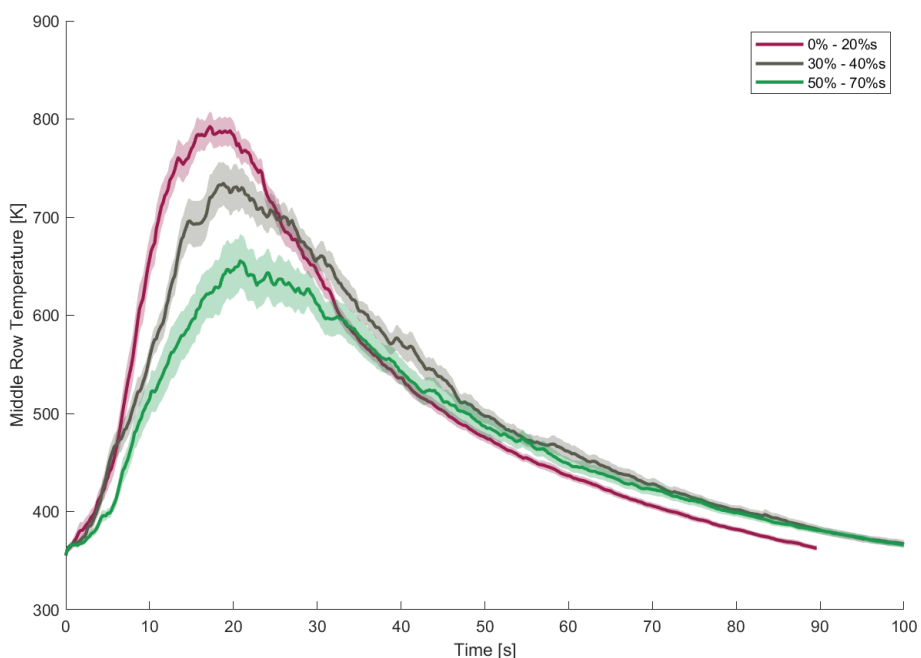

Figure 4.14: Temperature profile across the middle row for clumped fuel groups.

Figure 4.15 shows the temperature profile across the top row of thermocouples. As the distance from the fuel bed increases, the temperature measurements become increasingly dependent on flame height and therefore the mass loss instead of the heat release rate distribution, combustion temperature, and smoldering combustion.
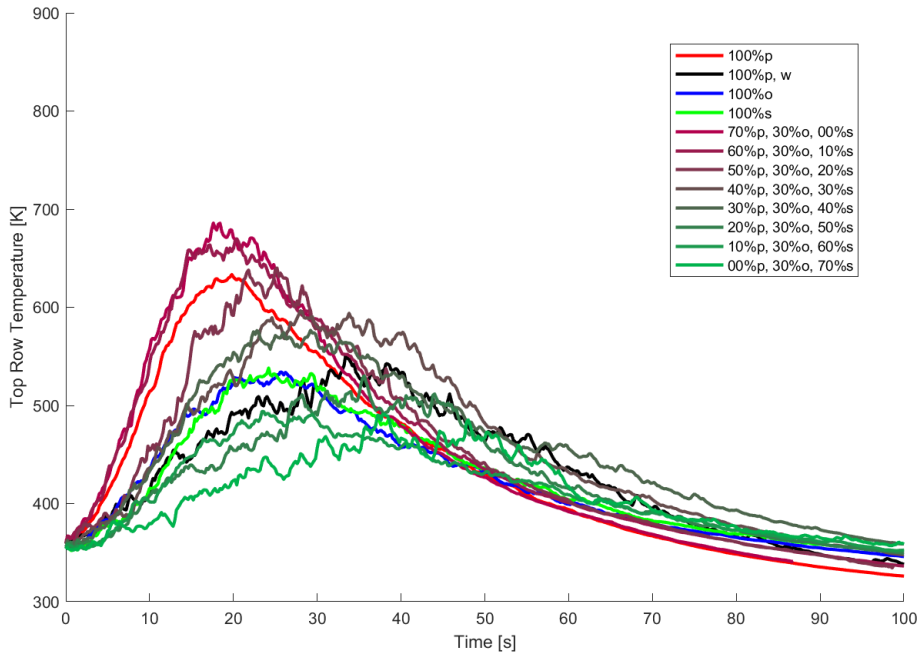
Figure 4.15: Temperature profile across the top row.

Temperature peaks are reduced again as distance from the fuel bed is increased, which is to be expected. At this height, the temperature profile for the pine was similar to that found along the middle row. This reflects the possibility that the pine produces flame heights sufficient to reach the top row of thermocouples. The temperature peak for wet pine was significantly delayed, but higher than that for the other species. This reflects a relatively high heat release and a low propagation rate because the temperature would reach its threshold farther away from the thermocouples but would take longer to reach them. The temperature profile of the oak became rounded, and the peak temperature dropped significantly, indicating that the flame height no longer reached the thermocouples. Sweetgum was similarly rounded with a drop in peak temperature; however, oak had slightly higher temperatures along the leading edge of the flame front. In contrast, the sweetgum had a slightly higher temperature along the trailing edge of the flame front. This indicates that the regions of the peak concentration of mass loss and,

46

therefore, the height of the flame for oak and sweetgum occurred at different points within their respective flame fronts. The peak mass loss concentration for oak probably occurred toward the leading edge of its flame front, while sweetgum had its peak mass loss concentration toward the trailing edge of its flame front.

Figure 4.16 shows the temperature profile across the top row of thermocouples for the single fuel groups, with the inclusion of the 95% confidence interval. The 95% confidence interval for pine was wider than it was at other thermocouple placements, indicating more variation in peak temperature. This can probably be attributed to the slight flickering of the flame, which would cause small dips in temperature near the highest point of the flame. Oak and sweetgum also had wider 95% confidence intervals near their peaks, and to a greater extent than pine. Although pine flames may occasionally have dropped below the thermocouples, it was likely the reverse for oak and sweetgum, which only occasionally reached the thermocouples. Wet pine had the widest 95% confidence interval for its entire duration, although this is likely caused by variations in propagation rate due to different moisture contents.
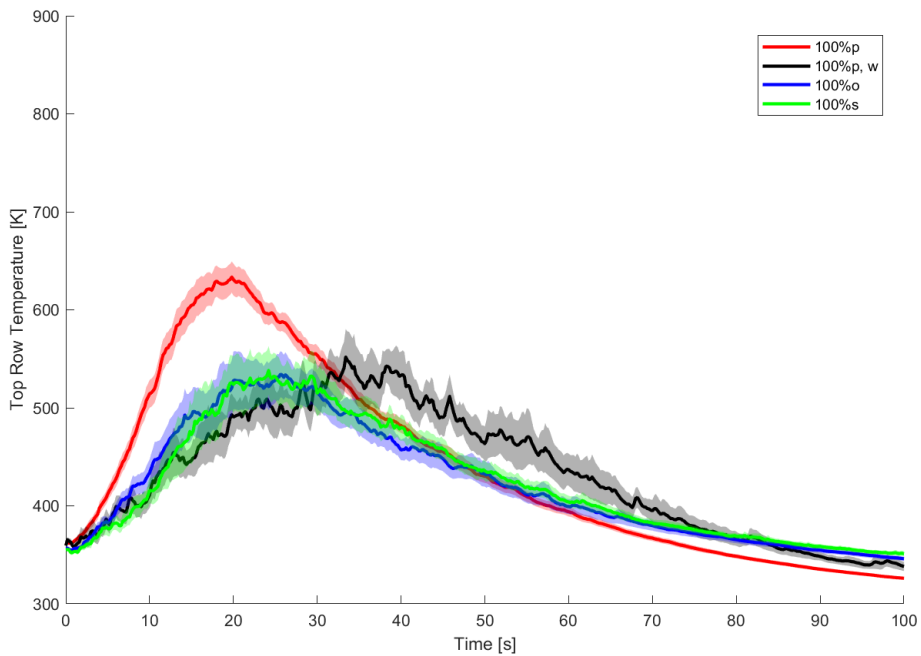

Figure 4.16: Temperature profile across the top row for single fuel groups.

Figure 4.17 displays the temperature profile across the top row of the thermocouples for the clumped fuel groups. The differences between the clumped fuel groups were more pronounced

at this height. Like in the middle row, the sweetgum content significantly decreased both the rate at which the temperature increased and the temperature peak. Fuel mixtures with a low sweetgum content had a higher temperature peak than pine; however, as the sweetgum content increased, the temperature decreased below that of sweetgum. The low sweetgum mixtures likely produced flame fronts with greater height as their temperature peaks are still below that found for pine along the bottom row, which is supported by the increased mass loss rate found in low sweetgum mixtures. Conversely, high sweetgum mixtures probably resulted in lower flame heights, as the small region of peak combustion for each fuel may have occurred at different locations within the flame front. In addition, the temperature peak for the moderate sweetgum mixtures occurs after both the low and high sweetgum mixtures. This supports the possibility that the three species experience a peak mass loss at different points in the flame front. Since moderate sweetgum mixtures had similar concentrations for all three species, it is expected that this would be most pronounced in moderate sweetgum mixtures.
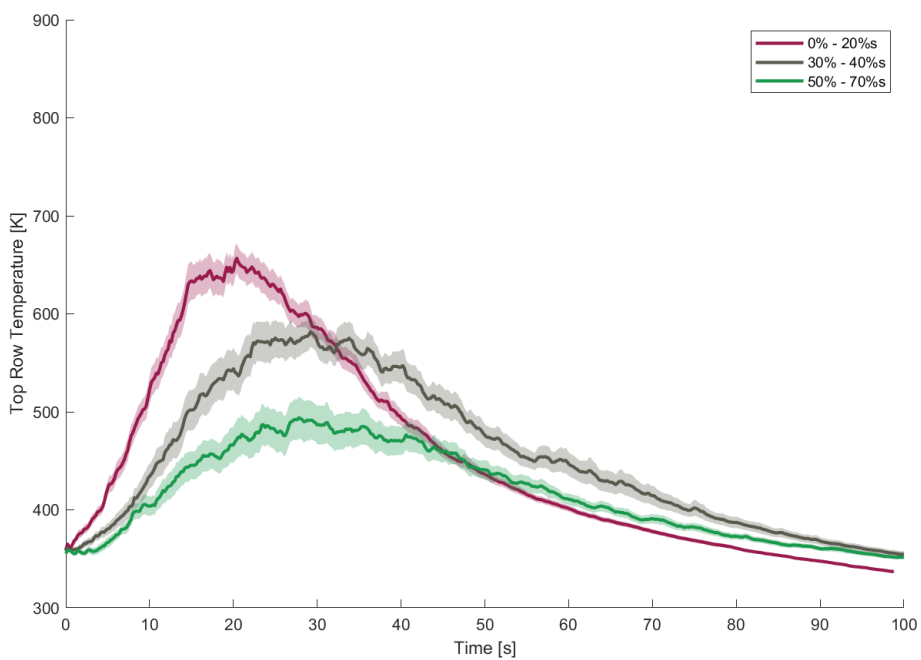
Figure 4.17: Temperature profile across the top row for clumped fuel groups.

4.2.1 Maximum Temperatures

In addition to the temperature-time measurements, the median maximum flame temperature was recorded for each fuel group. The maximum flame temperature was found as the median of the maximum temperature recorded along each row of thermocouples for each test. Figure 4.18 shows the maximum temperature for each fuel group in the bottom row. It should be noted that the maximum temperatures measured and presented in Figures 4.18 through 4.20 are higher than the temperature profile peaks shown in Figures 4.9 through 4.17. This is because the peak temperatures did not occur at the same point and time in each test, so the peak temperature values shown in Figures 4.9 through 4.17 do not reflect the maximum temperature achieved.
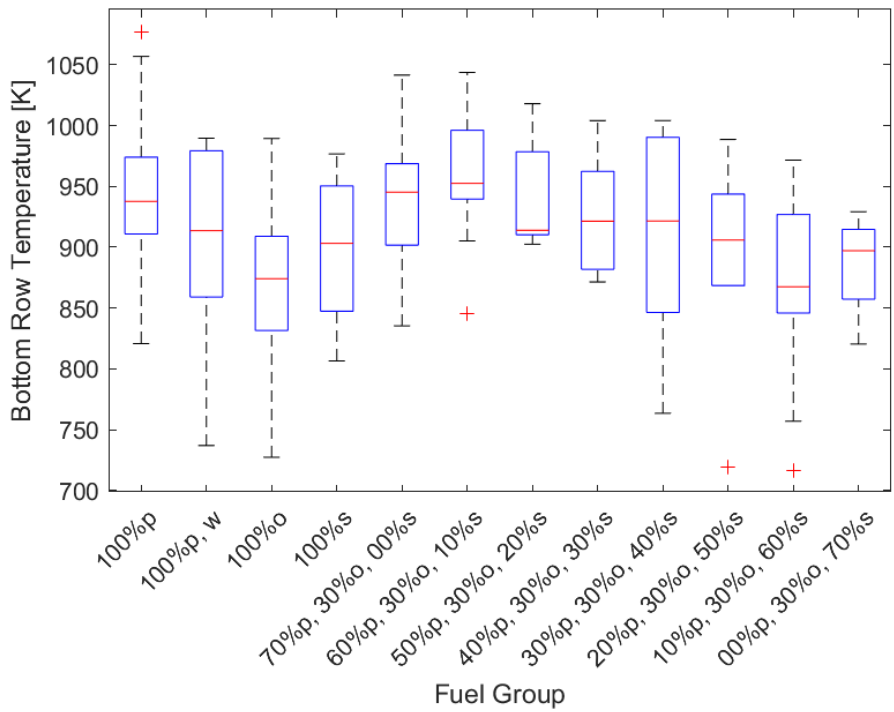
Figure 4.18: Max temperature measurements along the bottom row for each fuel group.

Among the single fuel groups, pine produced the highest maximum temperature, and wet pine (97%) only had a moderate drop in maximum temperature. Oak (93%) had the lowest maximum temperature of the three fuel species and did not have a bimodal distribution. The maximum temperature of sweetgum (96%) was between those of oak and wet pine. The maximum values for pine, oak, and sweetgum set the expectations for maximum temperature and,

by extension, the peak heat release for the mixed fuel groups. The moderate decrease in maximum temperature for wet pine suggests that the flame front and region of peak heat release were slightly broadened. Given that additional heat is required to propagate the flame front, the reduced heat available for combustion completion likely causes the flame front to progress through combustion slower. Since the bimodal distribution of the normalized mass loss rate found for oak did not translate into a bimodal distribution maximum temperature, oak may have had a thin region of high heat release. This is because oak tests with low normalized mass loss rates still resulted in maximum temperatures comparable to tests with high normalized mass loss rates.

In the mixed fuel groups, the mixtures with a sweetgum content of 0% (101%) and 10% (102%) had values slightly higher than pine and probably had higher rates of heat release within the flame front. Although the 10% sweetgum mixture tests produced only slightly higher maximum temperatures than the 0% sweetgum mixture tests, it is still notable given that the 10% sweetgum mixture tests had lower normalized mass loss rates and combustion fractions. This would suggest that the introduction of sweetgum litter caused the region of peak heat release to become narrower and therefore more concentrated, leading to higher maximum temperatures. This is also reflected in the lower quartile of the maximum temperatures of the 0% sweetgum mixture tests being much lower than those of the 10% sweetgum mixture tests. Although the tests for the 0% sweetgum mixture had high maximum temperatures, their peaks of the temperature profile were lower and flatter, as seen in Figure 4.9, indicating greater variability in the location of the peak heat release region. This was likely caused by an increase in propagation rate variability, which would also cause the larger spread of normalized mass loss shown in Figure 4.4.

For mixtures between 20% (97%) to 40% (98%) sweetgum content, the median value of the maximum temperature remained nearly constant, although the average values decreased. As the sweetgum content increased further to 50% (97%) and 60% (93%), the median values for the maximum temperature decreased, although it increased slightly for the 70% (96%) sweetgum mixtures. Since the median values approached the value found for sweetgum (96%),

it is likely that the decrease in temperature is a direct result of the temperatures produced by sweetgum.

The maximum temperatures found along the middle row of the thermocouples were also found and presented in Figure 4.19. Both the methods used to calculate and present the results are the same as those used for the bottom row maximum temperatures. At this height, the maximum temperatures found are again higher than the peak temperatures found along the middle row row temperature profile, shown in Figure 4.12. Observing the maximum temperatures along the middle row of thermocouples provides a better understanding of the flame temperatures, as the thermocouples are removed from the fuel bed at this height. The temperatures found along the bottom row are expected to be primarily influenced by the magnitude and distribution of heat release. Although heat release is still expected to influence the temperature measurements along the middle row, the magnitude and distribution of mass loss should also influence the temperature measurements. The reason for this is that changes in mass loss at a given point influence the amount of particulates released, and therefore the flame height.
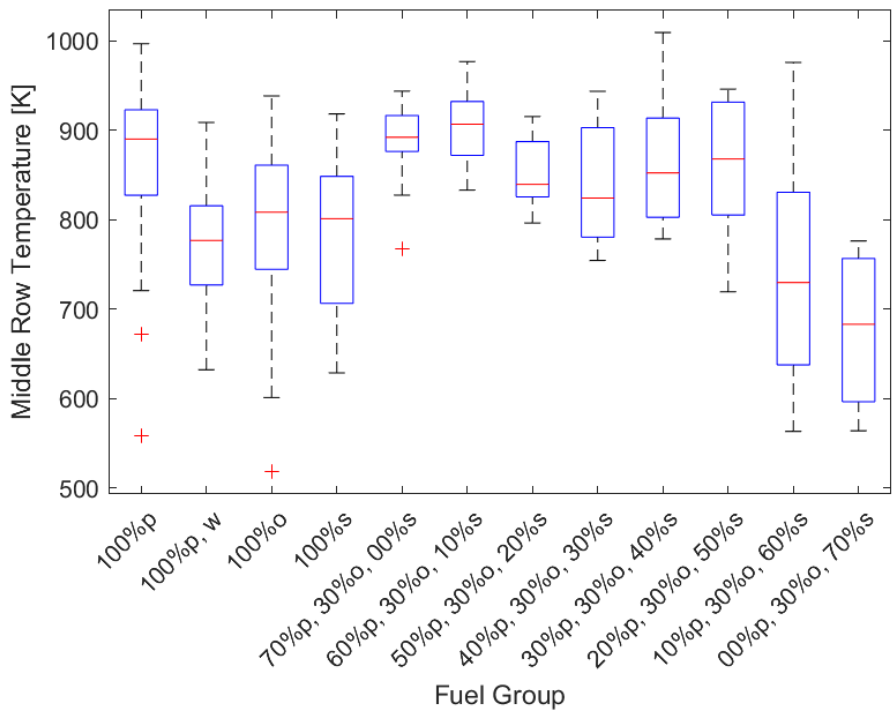

Figure 4.19: Max temperature measurements along the middle row for each fuel group.

Pine again had the highest maximum temperature of the single fuel groups, with a median value only 3% lower than that found for the bottom row. The median values for oak (91%) and sweetgum (90%) were slightly lower than their relative values in the bottom row, but are within reasonable expectations. Wet pine (87%) had a much lower relative maximum temperature along the middle row than that found in the bottom row. This is in agreement with the temperature profile for the bottom row, shown in Figure 4.15, which suggested that the increase in moisture broadened the flame front. Given that the moisture content directly increases the heat requirement for propagation, the reduction in excess heat likely slows the rate at which combustion can be completed within the flame front.

In the bottom row, the maximum temperature increased slightly from 0% to 10% sweetgum, then generally decreased with increasing sweetgum content, approaching values similar to sweetgum. In contrast, along the middle row the maximum temperature fluctuates between increasing and decreasing with sweetgum content. The mixtures with 10% (102%) sweetgum again had the highest median values, followed by 0% (100%) sweetgum mixtures. The temperature decrease between the 10% (102%) and 20% (94%) sweetgum mixtures was much greater than the 5% decrease found along the bottom row. The maximum temperature decreases slightly as the sweetgum increases to 30% (93%), but the temperature increased for 40% (96%) and 50% (98%) sweetgum mixtures. Then at 60% (82%) the maximum temperature suddenly decreases and continues to decrease at 70% (77%) sweetgum.

From the bottom row temperatures for 0% (100%) and 10% (102%) sweetgum, the results suggest that the region of peak heat release became thinner with the introduction of sweetgum. This probably also caused the increase in temperature found in the middle row. Similarly, the temperature decrease from 10% (102%) to 30% (93%) sweetgum is caused by the same changes in the heat release distribution responsible for the temperatures seen for these mixtures along the bottom row. In contrast, the increase in temperature from 30% (93%) to 50% (98%) likely resulted from changes in the distribution of mass loss. Pine probably has its highest concentration of mass loss toward the leading edge of its flame front, while sweetgum probably has a higher concentration toward the rear of its flame front. This is in agreement with observations from the temperature profile results in each row, shown in Figures 4.10, 4.13, and 4.16. In

these figures, the peak temperatures for sweetgum were found to occur later than the other single fuel groups and to have temperatures relatively higher behind its peak. Since the sweetgum content exceeds the pine content for 40% (96%) and 50% (98%) sweetgum mixtures, the mass loss concentration probably converges to the region of peak sweetgum mass loss. While the location of the maximum temperature is expected to shift from pine's to sweetgum's peak mass loss region, the total temperatures are still notably higher than that of sweetgum. This is mainly due to the increased mass loss rate, and therefore the heat release rate due to the presence of pine in these mixtures leading to thinner flame fronts. The maximum temperature found for wet pine mirrors this, as the decreased mass loss rate was expected to have caused the drop in temperature found along the middle row.

Once the sweetgum becomes 60% (82%) of the mixture, the temperature drops precipitously, and again at 70% (77%) sweetgum. This temperature drop was not seen along the bottom row, and as such this indicates that the flame height decreases below the height of the middle row thermocouples. Since these temperatures are lower than those of oak (91%) and sweetgum (90%), an interaction likely occurs between these two species that broadens the flame front and therefore decreases the concentration of mass loss at any given point. In addition, sweetgum probably disrupts the combustion completion of the other species, which may affect the height of the flame. Although the combustion fraction likely affected the flame height, it is probably not the primary cause of the decrease in flame height. This is because some mixtures with lower combustion fractions still reached the middle row. In Figure 4.14, which shows the temperature profile of the clumped fuel groups, the high sweetgum mixtures were shown to have a much more gradual temperature increase than the low or moderate sweetgum fuel groups. This also suggests broadened flame fronts, as the time between the initial temperature measurement and peak temperature would increase with the width of the flame front.

The maximum temperatures found along the top row are shown in Figure 4.20. Along the top row, the maximum temperature is expected to be mostly dependent on flame height and therefore on the distribution of mass loss, rather than that of heat release. Other than changing the location of temperature measurements, the methods used to find and present the maximum temperature are the same as those used for the bottom and middle rows.
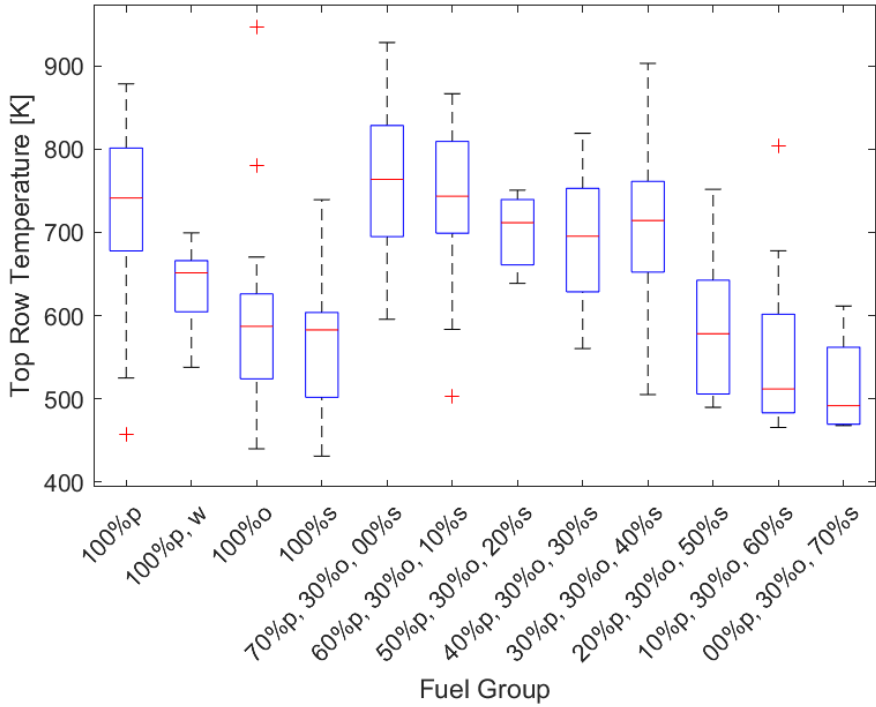
Figure 4.20: Max temperature measurements along the top row for each fuel group.

Again, pine had the highest maximum temperatures of the single fuel group tests at this height. The temperatures decreased again as height increased and to a greater extent than seen along the middle row. Pine's middle row temperature was 97% that of its bottom row temperature, whereas the top row temperature was only 82%. Likewise, oak (79%) and sweetgum (79%) probably did not reach the top row and as a result had much lower temperatures relative to pine. This reflects the increased importance of mass loss and the decreased importance of heat release. The relative temperature for wet pine (88%) remained roughly the same as that of dry pine along the middle row, indicating that the decrease in its maximum temperature was comparable to that of dry pine. Although moisture likely broadened the pine flame front, the

54

relative distribution of mass loss was likely unchanged, resulting in a decrease in the wet pine temperature mirroring that of dry pine.

The highest maximum temperature was produced by the 0% (103%) sweetgum tests while 10% (100%) sweetgum tests had the second highest value. This is in contrast to the temperature measurements in the bottom and middle rows, where 10% sweetgum tests had higher values. This further supports the claim that the 0% sweetgum tests had higher concentrations of mass loss while the 10% sweetgum tests had higher concentrations of heat release. Like in the bottom and middle rows, the temperature decreased at 20% (96%) sweetgum. The temperatures remained relatively consistent for 30% (94%) and 40% (96%) sweetgum. Like in the results in the middle row, the temperature drops precipitously; however, along the top row, this occurred earlier, at 50% (78%) sweetgum. The temperature continued to decrease as the sweetgum content reached 60% (69%), but only decreased slightly for 70% (66%) sweetgum. Given that the temperature drop occurred with a lower sweetgum content, the flame height is likely to decrease as the sweetgum content increases, rather than dropping once sweetgum content reaches 60%. The distribution of mass loss and heat release in sweetgum is likely to differ from pine and oak more than those species differ from each other. Potentially, these differences cause the flame front to broaden as each fuel progresses through its combustion separately at different points in the flame front.

Similarly to the mass loss rate, the effects of fuel specific volume on temperature were explored. The fuel specific volume directly impacts the oxygen available to the fuel bed and is expected to affect the combustion temperature as a result. The maximum temperature compared to the specific fuel volume is shown in Figure 4.21. The fuel specific volume is shown to have a statistically significant relationship with the maximum temperature ($m = 734$ Kkg/m^3, $\sigma = 146$ K, $t_{stat} = 5.40$, $p_{val} = 2.39$e-08). This aligns with expectations, as increased oxygen availability should increase the temperature in fuel-rich combustion.
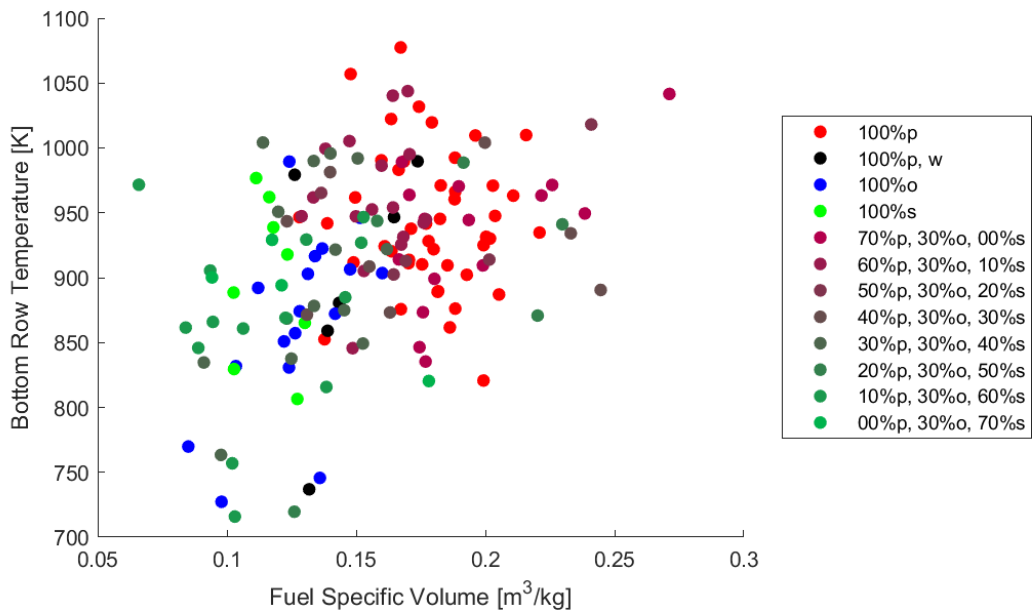
Figure 4.21: Maximum temperature along the bottom row compared with fuel specific volume.

Figure 4.22 shows the maximum temperature along the middle row compared to the fuel specific volume. The relationship between temperature and fuel specific volume is statistically significant ($m = 1.15$e+3 Kkg/m^3, $\sigma = 199$ K, $t_{stat} = 5.77$, $p_{val} = 4.13$e-08) and more pronounced than along the bottom row of thermocouples. This is reasonable, given that the mass loss had a strong positive relationship to the fuel specific volume and is expected to have an increasing impact on the temperature as the height increases.
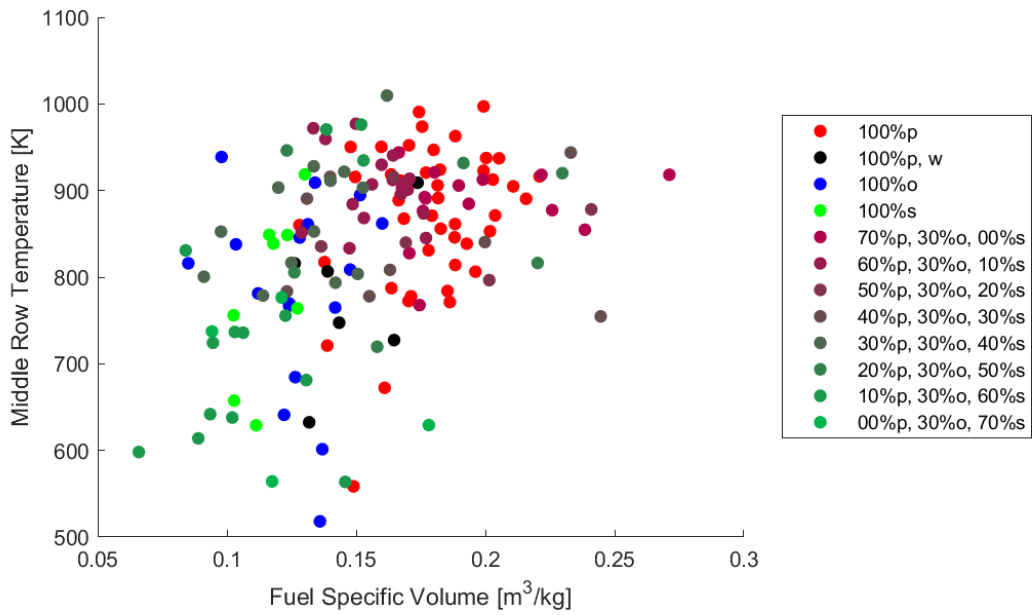
Figure 4.22: Maximum temperature along the middle row compared with fuel specific volume.

Figure 4.23 shows the maximum temperature along the top row compared to the fuel specific volume. Again, the relationship between temperature and fuel specific volume is statistically significant (m = 1.76e+3 Kkg/m^3, σ = 217 K, t_{stat} = 8.16, p_{val} = 1.04e-13). The relationship between temperature and fuel specific volume is the strongest at this height and aligns with the expectations from the previous figure.
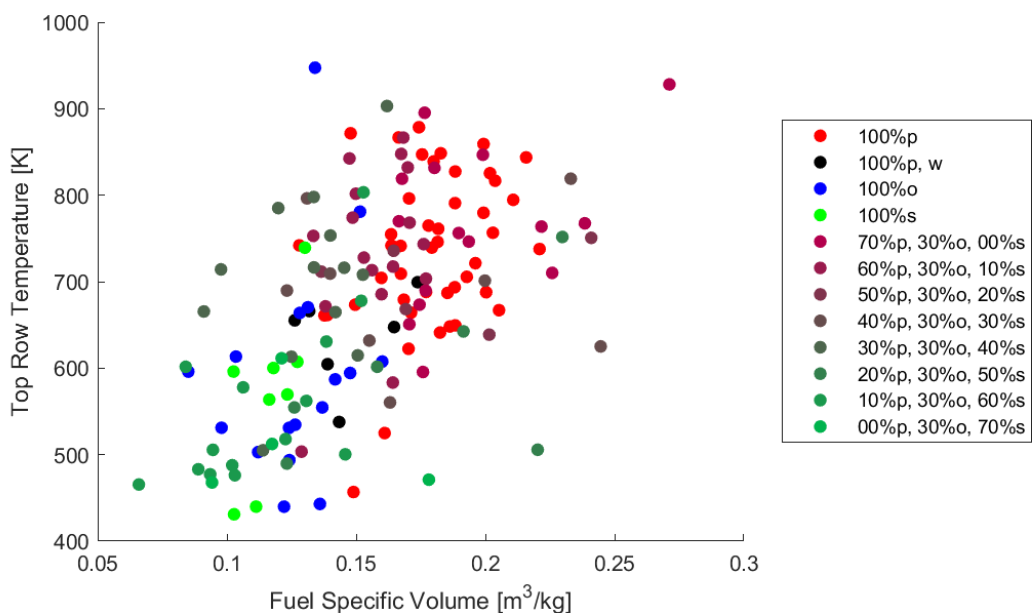

Figure 4.23: Maximum temperature along the top row compared with fuel specific volume.

The results of the temperature measurements show that the temperatures within the fuel bed differ slightly between each species, and these differences are reflected in mixed tests. The flame height was likely determined by the concentration of mass loss at any given point. This is supported by the fuel specific volume having a greater impact on the temperature as the distance from the fuel bed increased. As the concentration of mass loss is directly correlated with the combustion rate, the rate increases near stoichiometric conditions.

The mass and temperature measurements suggest that multiple interactions occur between the species tested. The pine and oak mixtures resulted in higher mass loss rates and likely higher flame heights. As sweetgum increased, the pine-oak interaction was disrupted, slowing the mass loss rate and initially producing higher combustion temperatures. As the sweetgum content of the mixture further increased, the combustion fraction and the probable height of the flame decreased to values below that of the sweetgum itself. To gain further insight into these possible interactions, optical diagnostics were used to capture the propagation rate measurements and produce a more complete picture of the impact of sweetgum content on the combustion characteristics of fuel mixtures.

4.3   Flame Front Measurements

The measurements for the location and propagation rate of the flame front are presented in this section. Flame front propagation is an import factor in flame behavior, as it has a significant impact on the mass loss rate and, therefore, the heat release rate of the fuel bed. Flame height, length, surface area, and intensity were also originally investigated; however, these measurements were ultimately excluded due to technical limitations. During tests, sweetgum and pine were found to produce significantly different flame intensities, which did not allow for a camera exposure that could consistently capture the reduced intensity of mixtures with a high sweetgum content without inaccurate results for the increased intensity of pine. These variations in intensity produced by each mixture caused difficulties in accurately measuring the geometry of the flame; however, the flame front was able to be tracked with some accuracy and is shown in Figure 4.24.

The flame front was found for each test by recording the forward most point at a given time. If the forward most point ever regressed, the previous forward most point was used instead. This was done to prevent the flame front from momentarily producing negative propagation rates during low intensity tests; however, this resulted in regions where the flame front was measured to be stationary and then jump forward. It should also be noted that the steady-state region used for optical measurements differs slightly from those used in previous sections. This is because the optical measurements were taken independently of the other measurements and began to record immediately after initial non-zero intensity measurements. This caused fuel groups to begin at positive flame front locations as initial non-zero intensity measurements occurred after ignition.
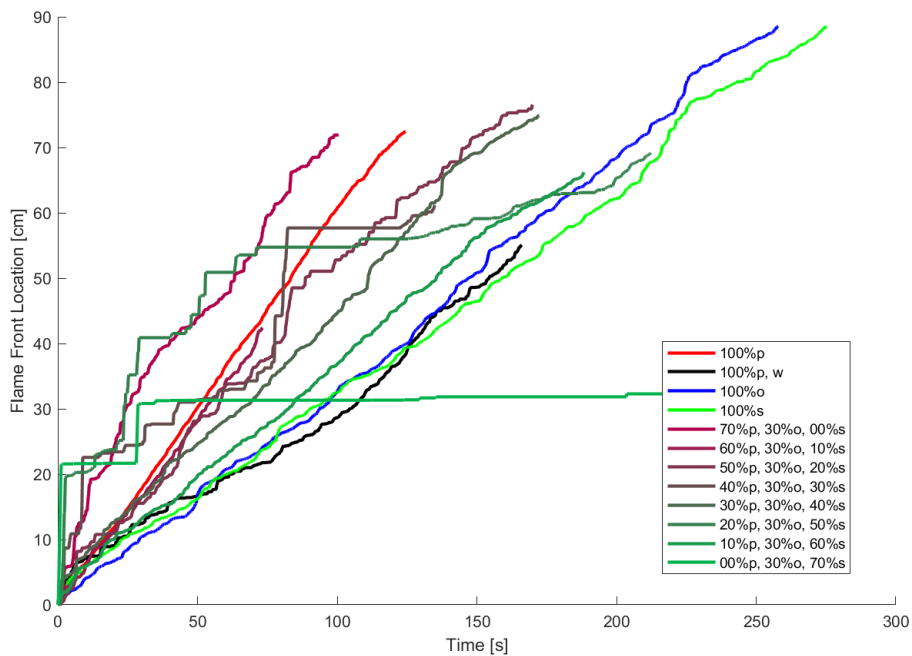
Figure 4.24: Average flame front time history.

The total propagated distance is generally shorter for the fuel mixtures with higher propagation rates, and this is most likely due to how the results were truncated. Similarly to the average mass fraction, shown in Figure 4.1, the measurements are only presented over the shortest test duration, so tests with any positive propagation rate outliers would result in shorter measurement durations. Unlike in Figure 4.1, oak was not significantly truncated. This supports the probability that moisture suppressed oak propagation, as none of the low humidity

59

oak tests were included in the tests with the Ximea optical measurements. As a result, only oak tests with low mass loss rates and propagation rates were included in Figure 4.24.

Pine and mixtures with less sweetgum produced the steepest slopes, which correlates to higher propagation rates. This suggests that the increased mass loss rates seen in these fuel groups are, at least in part, due to the increased propagation rates. As the sweetgum content increased in the mixed fuel groups, the tests were more likely to result in regions of flame intensity below the threshold to be recorded; however, this was not present in the sweetgum tests. This supports the possibility that high sweetgum mixtures produce broader flame fronts, as broad flame fronts would be less likely to produce one region of high flame intensity.

The flame front measurements were also divided into single fuel groups and clumped fuel groups to simplify the presentation of the results. The 95% confidence intervals were also included again. The flame front locations of the single fuel group are shown in Figure 4.25. Similarly to previous time figures, pine had a thin 95% confidence interval, while wet pine had a broader 95% confidence interval. Both should be expected given the previous results in which pine has been consistent and wet pine has varied due to inconsistent moisture content. The 95% confidence interval for sweetgum also mirrored previous results, being between dry and wet pine in terms of width. In contrast, oak had a much tighter 95% confidence interval than in its average mass fraction, shown in Figure 4.3. Again, this supports the possibility that humidity suppresses the propagation of the oak flame front, as there was significantly less variation in the oak results.
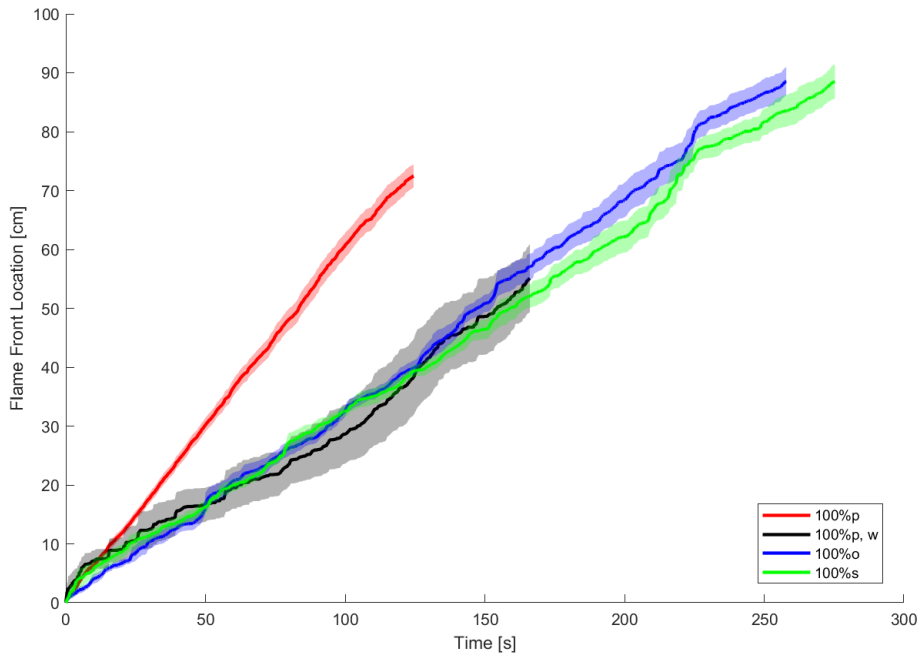
Figure 4.25: Average flame front time history for each single fuel group.

Figure 4.26 displays the average 95% confidence interval of the clumped fuel group flame front locations. As the sweetgum content increased, the 95% confidence interval widened, with the low sweetgum tests having less variation than the moderate sweetgum tests despite having a wider range of sweetgum content. This is likely caused by high sweetgum tests being prone to producing inaccurate results due to low intensities, which is also reflected in the nonlinear flame front location profile.
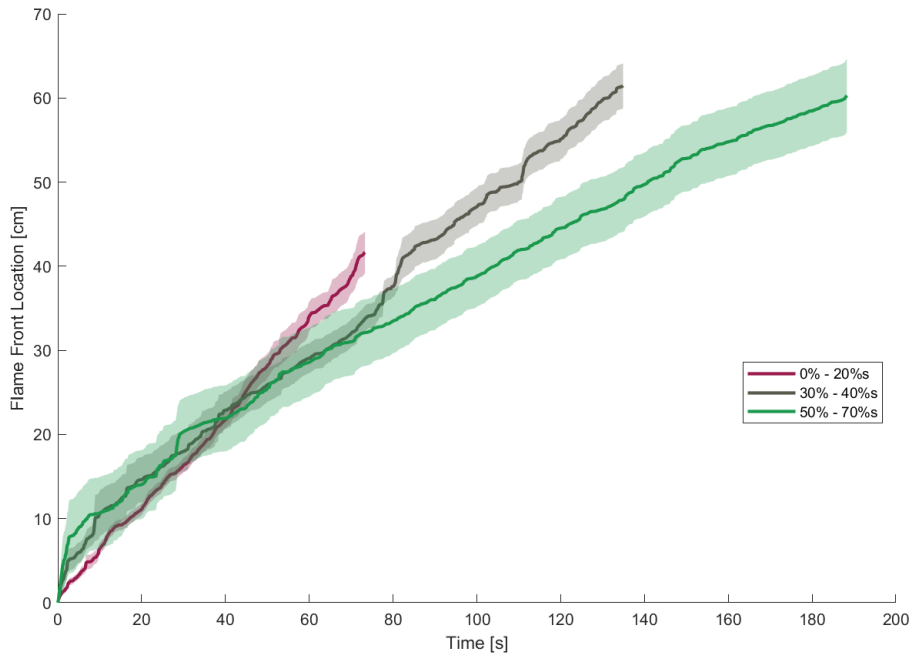
Figure 4.26: Average flame front time history for each mixed fuel group.

4.3.1 Propagation Rate

The propagation rate was found using the slope of the linear fit of the location of the flame front within the optical steady-state region for each test and is shown in Figure 4.27. Single fuel test beds and low sweetgum mixtures displayed resulted near the expected values. However, as the sweetgum content increased in mixed tests, the values decreased below reasonable expectations. This is also reflected in Figure 4.24, where multiple tests had inconsistent measurements. Although the propagation rate calculated from CH* chemiluminescence measurements is generally accurate for high intensity tests; low intensity tests likely have inaccurately low propagation rates. To correct for this and include tests without CH* chemiluminescence measurements, the propagation rate was estimated from the non-optical steady-state burn time, (t_{ss}), and propagation distance, (L_{ss}), and is shown in Figure 4.28.
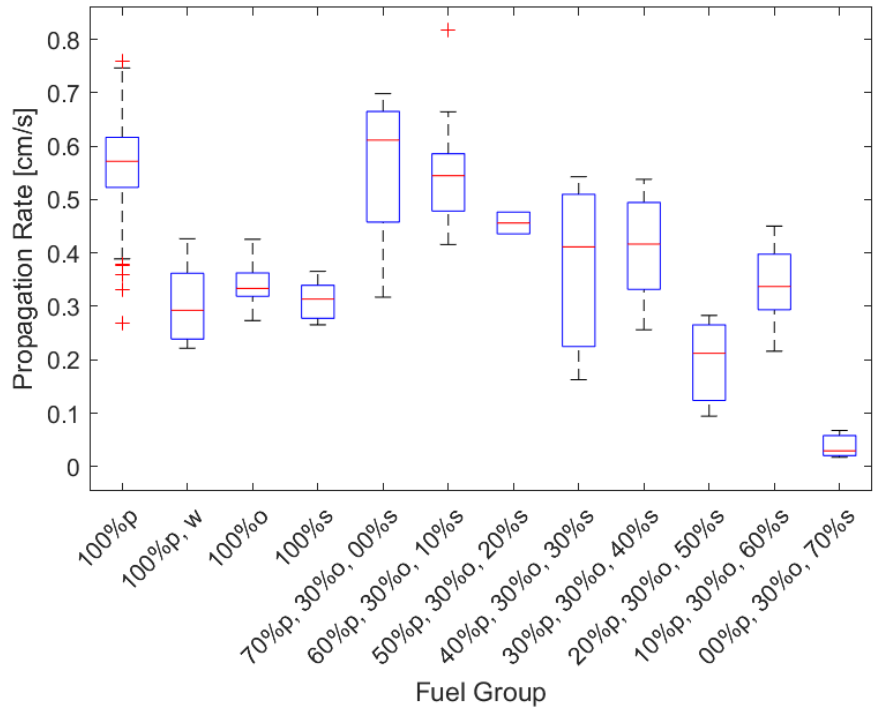
Figure 4.27: Propagation rate measurements for each fuel group.

Figure 4.28 displays the estimated propagation rate calculated from Equation 3.3. Overall, these results are clearer and likely provide better insight into how the propagation rate was impacted by fuel composition. Notably, most mixtures display a wider range of propagation rates, which is due to the inclusion of additional tests. This is most prevalent in oak litter tests and low sweetgum content mixtures, reflecting the deviations found in their mass loss rates. The median values for the single fuel tests and the tests with a low sweetgum content had only marginal changes from Figure 4.27. This indicates that these tests generally had at least some region of increased combustion intensity, resulting in consistent optical measurements. As sweetgum increased within mixed fuel tests, the median propagation rate measurements generally decreased. This suggests that high sweetgum content mixtures do not have any region of increased combustion, despite the fact that their constituent fuels do. This may be caused by either a wide enough and evenly distributed flame front or simply suppressed combustion.
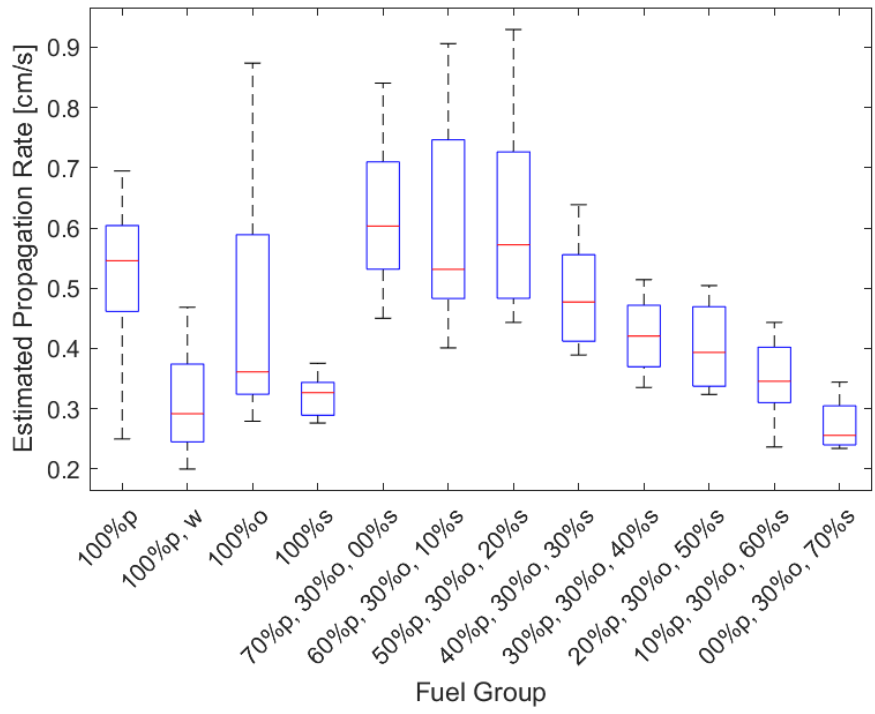
Figure 4.28: Estimated propagation rate measurements for each fuel group.

Similarly to the previous measurements, the dry pine tests were found to have the highest median propagation rate among the single fuel groups. The median propagation rate decreased significantly for wet pine (53%). This drastic decrease in propagation rate reflects the decrease found in the mass loss rate and is likely the primary cause of that decrease. The propagation rate is expected to depend on the ratio between the heat release rate near the flame front and the heat required to dry and ignite the fuel ahead of the flame front. The moisture content increases the preheating required for combustion, and this is reflected in the propagation rate of the wet pine. Like the oak (66%) mass loss rate, its propagation rate was found to be bimodal. Given the relationship between mass loss and propagation rates, this should be expected. The median propagation rate of sweetgum (60%) was also found to be close to that of the lower quartiles of oak. The propagation rates found for mixed tests also mirror their mass loss rate measurements.

The low sweetgum tests had high median values, with 0% (111%) sweetgum tests having the highest median propagation rate by a wide margin. Both the 10% (97%) and 20% (105%) sweetgum tests also had high values. The median propagation rate observed for 0% sweetgum tests mirror its median mass loss rate, although the relative propagation rates for the 10% and

20% sweetgum tests were approximately 10% higher than their relative median mass loss rates. This indicates that the 10% and 20% sweetgum tests had somewhat lower mass loss rates when factoring in their propagation rates. This supports previous observations regarding the mass loss and heat release concentrations of these mixtures. An increased concentration of heat release near the leading edge of the flame front wound increases the propagation rate without necessarily increasing the mass loss rate proportionally. In contrast, proportionally increasing mass loss rates would lead to increased mass loss concentrations.

Once the sweetgum content reached 30% (87%), the propagation rate and spread decreased immediately. This probably reflects the prevention of the presumed pine-oak interaction. As the sweetgum content increased from 40% (77%) to 60% (63%), the propagation rate decreased consistently, but dropped significantly in 70% (47%) sweetgum mixtures. Mixtures with 30%, 40%, and 70% sweetgum content have propagation rates approximately proportional to their mass loss rates. In contrast, mixtures with 50% and 60% sweetgum experienced a drop in mass loss rate that was not reflected in their propagation rate. This suggests that the changes in the mass loss rate seen in 30% and 40% sweetgum tests are caused by their changes in propagation rate, since their changes are proportional. However, once the sweetgum content reaches 50%, an additional factor is causing the mass loss rate to decrease. Then once the sweetgum content reaches 70%, another factor causes a drop in the propagation rate, without affecting the mass loss rate. This can probably be explained by the changes in the combustion fraction seen in these mixtures. The combustion fraction drops precipitously between mixtures with 40% and 50% sweetgum content, which also corresponds to the observed decrease in the mass loss rate. As the sweetgum content increases to 70%, the combustion fraction increased, thus changes in the mass loss rate were again reflected in changes in the propagation rate.

The estimated propagation rate of each test was compared with its fuel specific volume in Figure 4.29. The fuel specific volume was found to have a strong linear relationship ($m = 2.29 \; cm \; kg/m^3s$, $\sigma = 0.282 \; cm/s \; t_{stat} = 8.11$, $p_{val} = 1.43e\text{-}13$) with the fuel propagation rate. Again, this relationship indicates fuel-rich combustion.
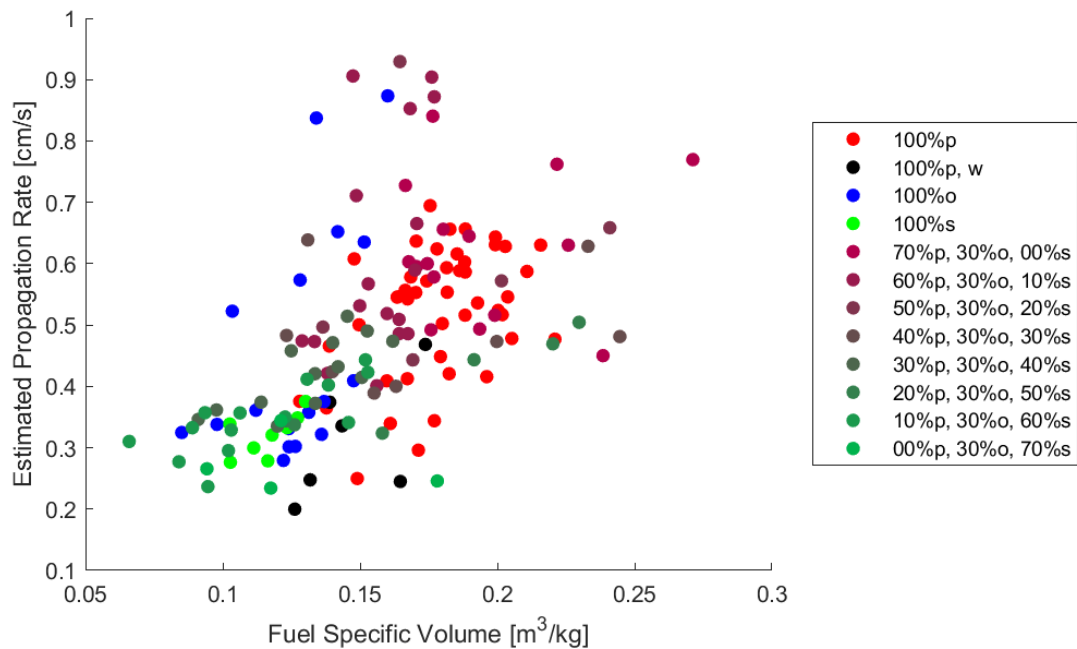
Figure 4.29: Estimated propagation rate compared with fuel specific volume.

Figure 4.30 compares the estimated propagation rate with the ambient humidity of each test. Ambient humidity did not have a statistically significant relationship with the propagation rate, but again shows that low humidity oak tests had increased propagation rates. This further supports the possibility that the propagation of the oak flame front is more dependent on ambient humidity than the pine or sweetgum.
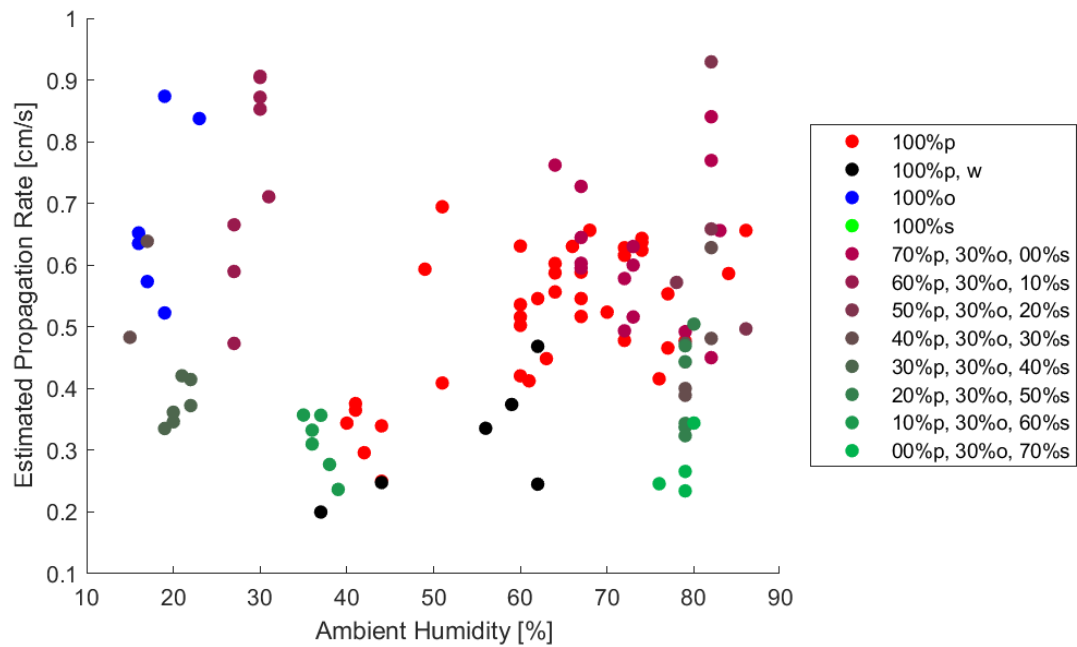
Figure 4.30: Estimated propagation rate compared with ambient humidity.

4.4 Fuel Temperature Measurements

This section aims to compare the overall temperature of the fuel bed with the results of the previous temperature section. Note that these measurements were not originally included in the scope of this project. As such, these results are included to offer an additional perspective and act as preliminary testing for future test methods. Additionally, tests were conducted with either the Ximea or the FLIR camera, and since fuel temperature measurements were not originally included in this study, there are limited data points for the fuel temperature and not all fuel groups were used with the FLIR camera. The average fuel temperature was calculated by measuring the infrared emission throughout the fuel bed as described in Section 3.3.4. Fuel temperature measurements were recorded for the entire test independently of both the optical and non-optical steady-state regions. Figure 4.31 shows the average fuel temperature at each point in time for each fuel group included in the FLIR tests using the same method as used for the previous time-averaged figures.
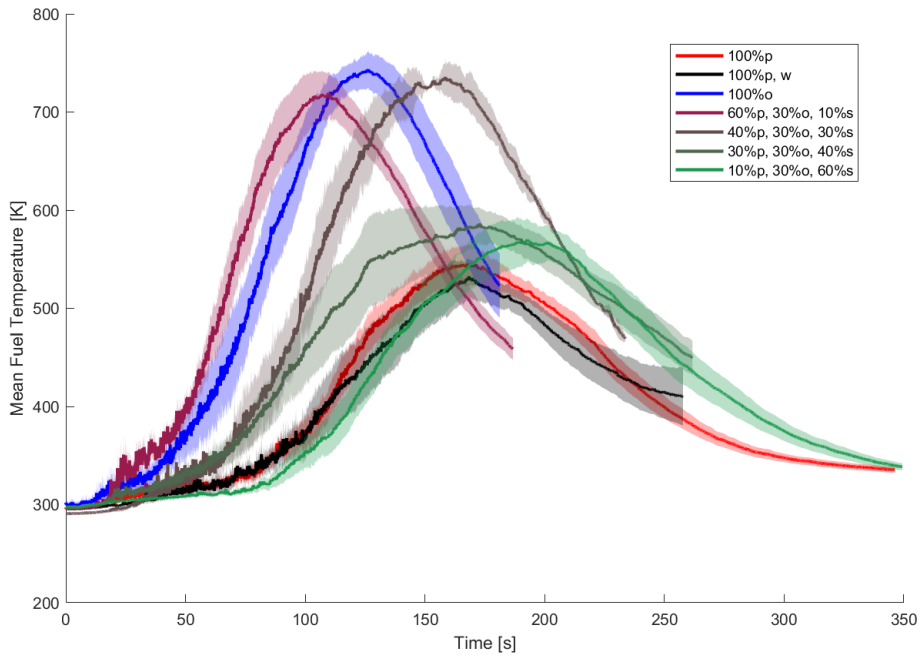
Figure 4.31: Average fuel temperature across the fuel bed.

The time when the temperatures peaked for each mixture was generally slightly after the time the same mixture had completely propagated in Figure 4.24. A notable exception to this is the results for oak; however, this is likely due to Figure 4.24 excluding low humidity oak tests, while Figure 4.31 only has low humidity oak tests. Given how the propagation rate of the oak flame front changed with the ambient humidity, this should be expected. Since the flame front location was truncated to include only the optical steady-state region and the fuel temperature measurements were not, the time shown in Figure 4.31 is longer than the corresponding time shown in the flame front location figures. This indicates that the average fuel temperature peaks once the entire fuel bed has burned, which should be expected.

Dry pine produced a temperature profile with gradual, non-linear changes in temperature and a low temperature peak. In combination with the high median propagation rate of pine, this indicates a thin region of increased combustion with minimal smoldering. The increase in moisture content slightly reduced the peak of the pine, but within expectations. The moisture content also changed the way the temperature profile increased and decreased, which also re-sulted in wider confidence intervals before and after the peak. In light of how the confidence

interval flails out before and after the peak, the moisture content probably had progressive changes in the width of the flame front.

The low humidity oak tests produced the highest temperature peak. Given that the temperature peak is much higher than that of pine, this likely reflects a larger region of smoldering combustion. This is also reflected in the linear temperature decrease behind the peak, which would be caused by the progressive decline in smoldering combustion. Mixed tests with only 10% sweetgum content had a slightly lower and earlier temperature peak than dry oak. This slight decrease in the temperature peak may be caused by the reduced smoldering seen in pine. The tests with 30% sweetgum maintained a moderately delayed temperature peak, but maintained a magnitude similar to the 10% sweetgum tests. This probably reflects the reduced propagation rates found for these mixtures, as well as the increase in smoldering expected with reduced pine litter.

Increasing the sweetgum content to 40% resulted in a significant decrease in the peak temperature, with minimal change in the time it occurred. Furthermore, this mixture showed a wide confidence interval throughout the duration of the temperature profile. This may suggest that there is a threshold near 40% sweetgum content that causes a reduction in the smoldering combustion. This is also reflected in the tests with 60% sweetgum, which produced a temperature peak slightly lower and later than the average 40% sweetgum test, except with much less deviation. Although the results for mixtures with 60% sweetgum content and dry pine are somewhat similar, this is probably caused by the former having increased smoldering and the latter having increased propagation rates. In contrast, dry oak and low sweetgum mixtures exhibit both traits, leading to higher average fuel temperatures. However, because of the limited results from the fuel temperature tests, these findings provide only a general insight, and more tests will be required to produce conclusive results.

Thus far, the results have suggested that changes in fuel composition and moisture content cause distinct changes in flame behavior once certain conditions have been met. However, the previous observations are based only on apparent relationships between the different burning characteristics to support these claims. For this reason, the principle component analysis

(PCA) was performed to provide a more complete understanding of the relationship between the burning characteristic.

4.5 Principal Component Analysis

To understand how the variations of the burning characteristics were related to each other, PCA was performed using the method described in Section 3.4. The constituent variables used included the mass loss rate, combustion fraction, flame temperature at each height, and estimated propagation rate. The estimated propagation rate was used instead of the optically measured propagation rate so that more tests could be included in the analysis.

The first four principal components were found to explain 94% of the variance in the results. The first principal component explained 56% of the variance and was most strongly associated with the temperature of the top row ($r = 0.49$), the mass loss rate ($r = 0.48$), the propagation rate ($r = 0.45$) and the temperature of the middle row ($r = 0.42$). The variable r describes the correlation between the measured variable and the principal component and has a value between 1 and -1. This component also had moderately positive relationships with the temperature of the bottom row ($r = 0.29$) and the combustion fraction ($r = 0.26$). Given that this component has a positive correlation with the six original variables, it can likely be associated with overall flammability. The values of the first principal component for each fuel group are shown in Figure 4.32. Note that in the following box plot figures, the value found for pine will no longer be used as a reference point, and instead the exact values will be displayed in parentheses for each fuel group.

Pine (1.05) had the only positive median first principal component value of the single fuel groups; however, oak had positive values in its upper quartile. The median values for oak (-2.10), wet pine (-1.51) and sweetgum (-1.60) were negative. Also, while oak had the highest values in its upper quartile, it also had the lowest values in its lower quartiles. The increased value for pine should be expected, as pine displayed the highest median values for all measured variables, and the first principal component was also positively correlated with all six. Likewise, reduced values for wet pine, oak, and sweetgum should also be expected given the decreased values found in the previous sections.
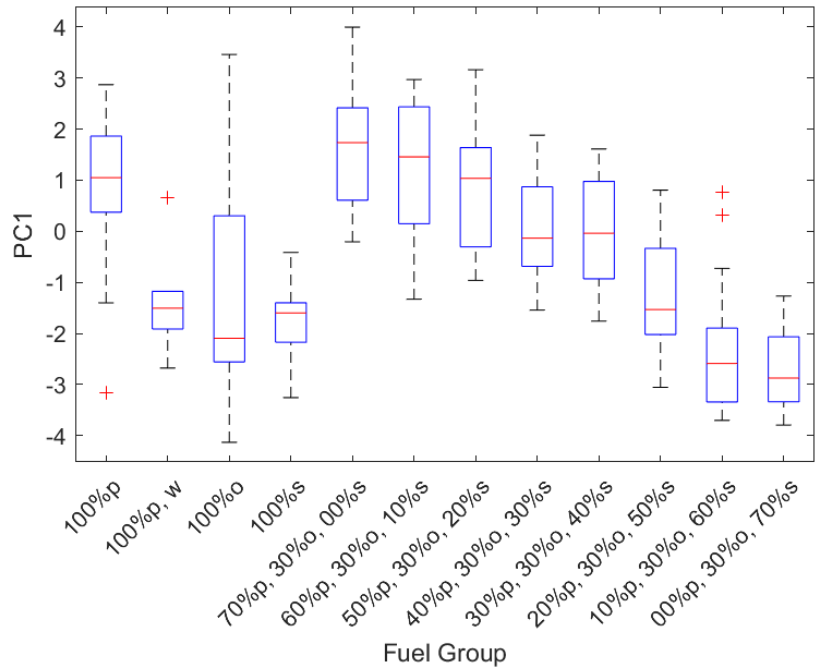
Figure 4.32: First principal component for each fuel mixture.

The tests with 0% (1.73) sweetgum had the highest median values for the first principal component. The median values of the first principal component decreased relatively moderately at 10% (1.46) and 20% (1.04) sweetgum content. Once the sweetgum content reached 30% (-0.14) the value of the first principal component decreased substantially, had little change at 40% (-0.04) sweetgum content. The median values decreased sharply again at the sweetgum content of 50% (-1.53) and 60% (-2.59) and moderately at 70% (-2.87). In particular, mixtures with sweetgum contents of 0% and 10% produce values exceeding that of pine and mixtures with 60% and 70% produce values below those of sweetgum. These results also reflect the likely pine-oak and oak-sweetgum interactions, as the low and high sweetgum mixtures exhibited more extreme values than the single fuel groups.

The second principal component had a strong positive correlation with the combustion fraction ($r = 0.86$) and a strong negative correlation with the temperature along the bottom row ($r = -0.47$) and explained 15% of the variation in the results. Positive values indicate that heat released within the flame front is applied to the combustion completion, while negative values indicate that a higher proportion of heat release is applied to the combustion temperature. The values of the second principal component for each fuel group are shown in Figure 4.33.

71
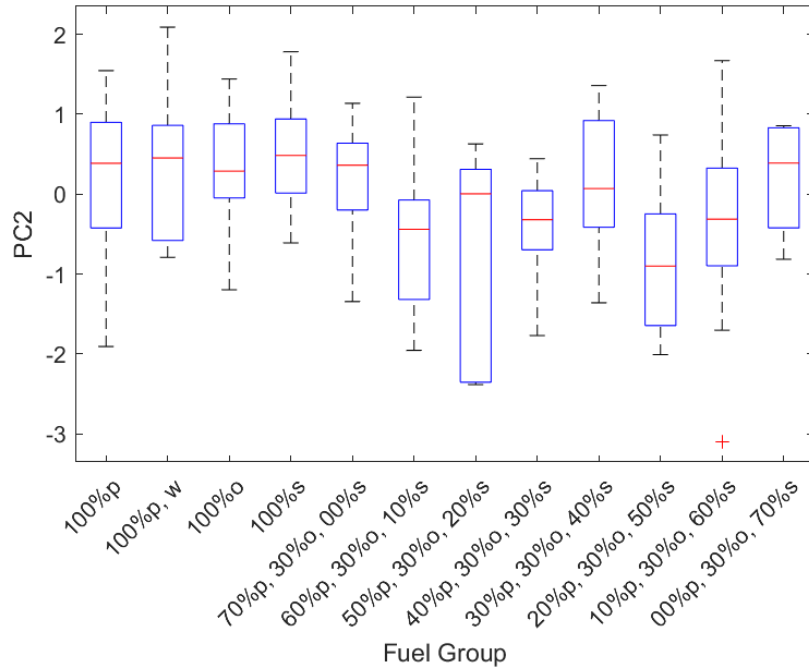
Figure 4.33: Second principal component for each fuel mixture.

Of the single fuel groups, sweetgum (0.48) had the highest median value, followed by wet pine (0.45), pine (0.39) and oak (0.29). Pine and wet had a large spread of values for the second principal component, with pine having a negative skew and wet pine having a positive skew. Of the mixed fuel groups, 0% (0.36) sweetgum content tests had the highest values, which decreased from the 10% (-0.44) to the 20% (0.00) sweetgum content. Although the median values appear to increase from 10% to 20% sweetgum content fuel group, the average value of the 20% sweetgum content tests (-0.78) is likely a better representation of the results given the reduced number of tests conducted for this fuel group. Once the sweetgum content increases further to 30% (0.07) and 40% (-0.32), the values of the second principal component increase. At 50% (-0.9) the median value drops, before increasing again at 60% (-0.31) and 70% (0.39) sweetgum content.

The third principal component explained 13% the variance in the data. This component had a positive correlation with the temperature of the bottom row ($r = 0.75$) and the combustion fraction ($r = 0.34$), and a negative correlation with the propagation rate ($r = -0.48$). This probably corresponds to the location of the heat release concentration. Tests with high values for the third principal component would have released more heat within or behind the flame

front, whereas tests with lower values would have released more heat near the leading edge of the flame front. The values of the third principal component for each fuel group are shown in Figure 4.34.
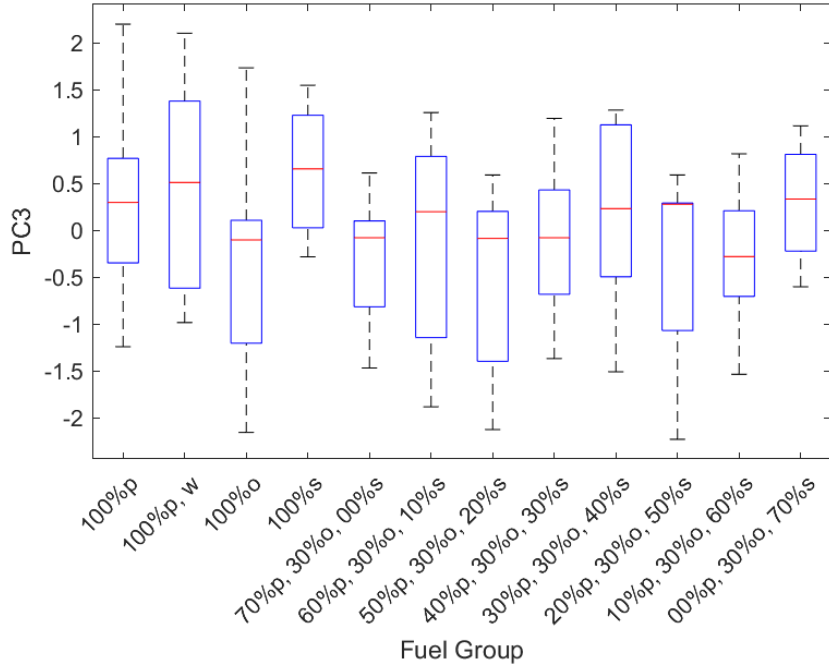
Figure 4.34: Third principal component for each fuel mixture.

Like the second principal component, sweetgum (0.66) had the highest median value, followed by wet pine (0.51), pine (0.3) and oak (-0.1). However, pine, wet pine, and oak all had large spreads, resulting in high positive and low negative values at either extreme. Tests with 0% (-0.08) sweetgum content resulted in a median value near zero, but a much lower average value (-0.32). The increase in the sweetgum content to 10% (0.2) increased the value of the principal component before again decreasing at 20% (-0.09) sweetgum content, with a much lower average value (-0.54). Although the upper quartile values increased for the 10% sweetgum content tests, the lower quartile values decreased at 10% and 20% sweetgum content. The median value continues to fluctuate between increasing and decreasing as the sweetgum content increases. The median value increases for 30% (-0.08) and 40% (0.23) sweetgum content. At 50% (0.28) sweetgum content, the median value increases slightly but has a significant negative skew, resulting in a much lower average value (-0.31). The tests with a sweetgum content of 60% (-0.28) and 70% (0.33) had a lower spread than the other mixed fuel groups.

73

The fourth principal component explained 10% of the total variation in the data. This component has a strong correlation to the temperature of the middle row (0.75) and negative correlations with the mass loss rate (-0.39) and the temperature of the bottom row (-0.35). The values of the fourth principal component for each fuel group are shown in Figure 4.35.
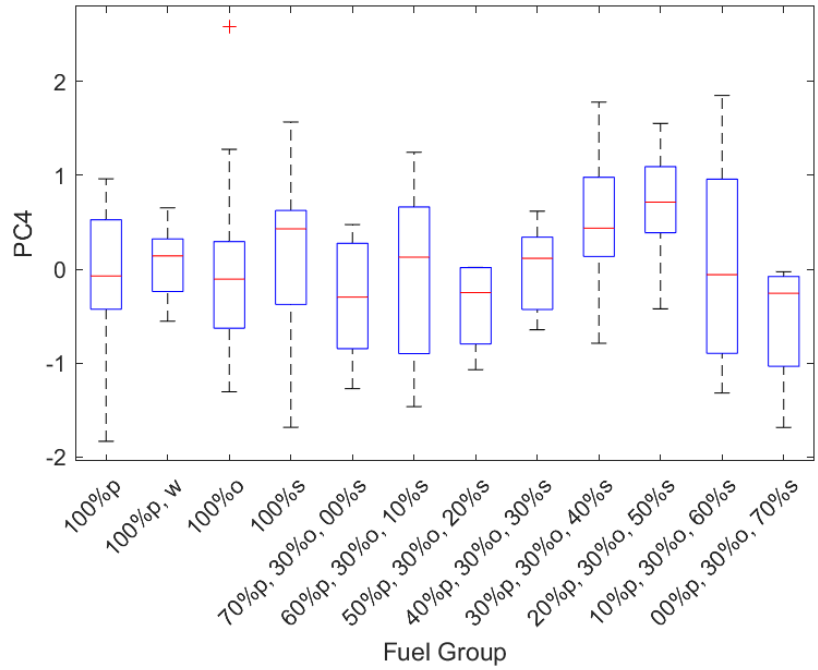
Figure 4.35: Fourth principal component for each fuel mixture.

Sweetgum (0.43) had the highest median value of the single fuel groups, followed by wet pine (0.14), pine (-0.07) and oak (-0.11). The median value for the fourth principal component fluctuated for low sweetgum content mixtures, starting low for 0% (-0.3) sweetgum tests, increased at 10% (0.13) sweetgum, and again decreased at 20% sweetgum (-0.25). The median value then steadily increased for 30% (0.12), 40% (0.44), and 50% (0.71) sweetgum content tests. At 60% (-0.06) sweetgum, the median value suddenly decreased and continued to decrease for 70% (-0.26) sweetgum content tests. The fourth principal component is likely less practically significant because the temperatures were measured at discrete heights, rather than continuously. The reason for this is that the middle row temperature has a distinct drop, despite the flame height gradually decreasing.

4.5.1 Cluster Analysis

Using the PCA results, the tests were categorized into one of five clusters. The MATLAB evalclusters function was used to calculate the optimal number of clusters, and the kmedoids function was used to assign each test to a cluster. The five clusters are ordered according to their PC1 values, from highest to lowest, which is expected to reflect overall flammability. As the sweetgum content increased, the tests typically moved into higher clusters. Pine tests were found within the first three cluster, while oak and sweetgum tests were found primarily within the fifth cluster. An exception to this was that low humidity tests appeared in the first and third clusters. The composition of each cluster is shown in Table 4.1.

Table 4.1: Cluster Compositions

Fuel Groups	Cluster 1	Cluster 2	Cluster 3	Cluster 4	Cluster 5
Pine	18	10	14	1	2
Oak	3	0	4	1	9
Sweetgum	0	0	3	1	4
Wet Pine	0	1	1	1	3
0% Sweetgum	10	2	3	0	0
10% - 20% Sweetgum	9	8	3	2	0
30% - 40% Sweetgum	3	4	10	4	0
50% - 60% Sweetgum	0	4	1	9	6
70% Sweetgum	0	0	0	1	3

Figure 4.36 shows the average mass fraction over time for each fuel group, with the addition of the 95% confidence interval. Of the five clusters, the first had the steepest slope, indicating a higher mass loss rate. The second and third clusters had similar mass loss profiles, both less steep than the first cluster. The third cluster had a slightly steeper slope than the second cluster; however, the difference is marginal. The fourth and fifth clusters were the least steep profiles, both much less steep than the previous two clusters. Although the fourth and fifth clusters had relatively similar profiles, the fourth cluster's profile was slightly steeper and ended earlier. In contrast, the fifth cluster tests took longer to complete, despite likely having similar mass loss rates. This may be due to at least one high propagation rate test being included in the fourth cluster. Another possibility is that the smoldering mass loss lasted longer

in the fifth cluster tests, which would cause the mass loss to continue longer after the flame front propagated.
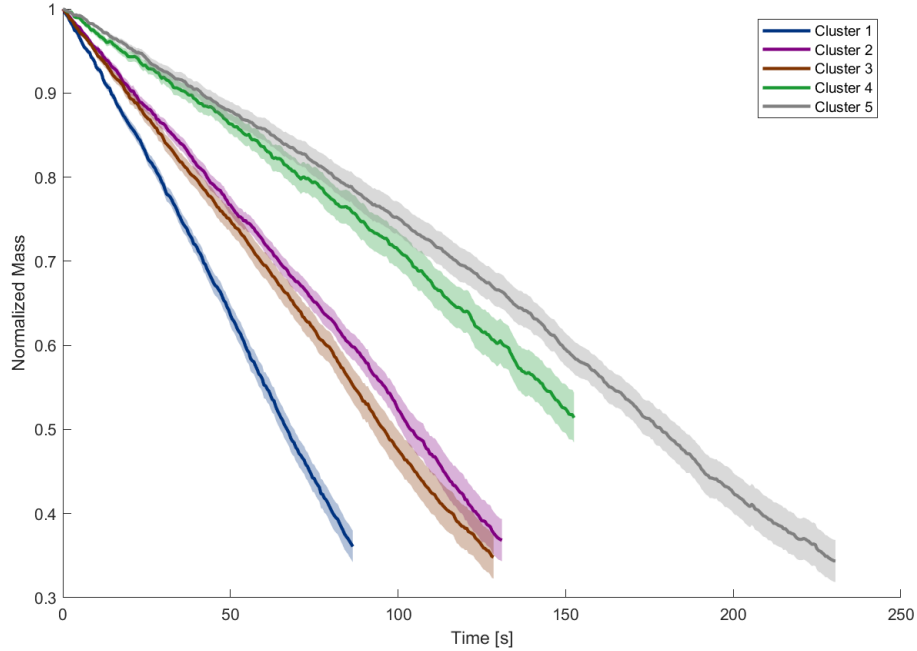
Figure 4.36: Average mass fraction of each cluster.

Figure 4.37 shows the box plots of the normalized mass loss rate for each cluster. The normalized mass loss rate was calculated and presented in the same way as the previous normalized mass loss rate results shown in Figure 4.4. Like with the previous box plot figures, the median values relative to pine are provided in parentheses. The first cluster had the highest median normalized mass loss rate (11%), which was higher than the values of its constituent species. The highest values in this cluster were much higher than those seen in the other clusters, however, the lower bound values were similar to the median values of the second and third cluster. Two sample t-tests were used to determine whether or not two clusters had statistically significant different values. The second cluster did have a statistically significant ($p < 10e-11$) lower median mass loss rate (82%). The normalized mass loss rate did not experience a statistically significant ($p = 0.44$) normalized mass loss rate (82%). This suggests that the changes in the normalized mass loss rate from the first to second cluster are caused by a distinct change in the flame front behavior, rather than gradual changes in flammability. Another statistically significant ($p < 10e-6$) and sharp drop in normalized mass loss rate (54%) from the third to fourth

cluster. Given that the magnitude of the change in the normalized mass loss rate is similar to that seen between the first and second clusters, it is likely that another distinct change in flame front behavior occurs. The decrease in the normalized mass loss rate is more gradual between the fourth and fifth (45%) clusters and not statistically significant ($p = 0.08$).
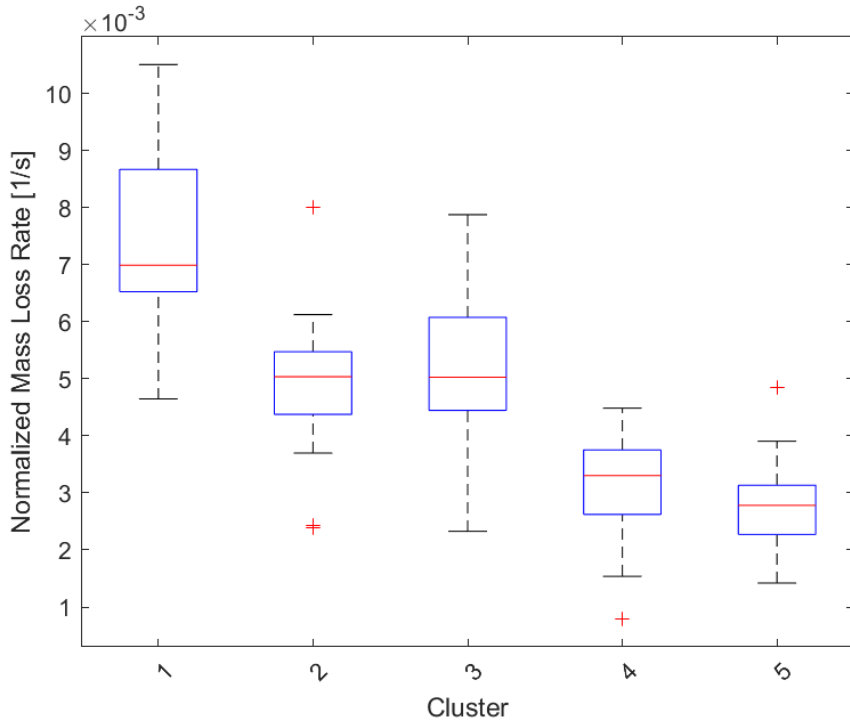
Figure 4.37: Normalized mass loss rate for each cluster.

Figure 4.38 presents the combustion fraction for each cluster. The first cluster had the highest median combustion fraction (100%), which was similar to that of pine. The decrease in the combustion fraction from the first to second cluster was moderate (95%), but statistically significant (p ¡ 10e-3). The combustion fraction actually increased slightly with the third cluster (98%), which was also statistically significant ($p = 0.01$). Although the previous changes in the combustion fraction were fairly small, the combustion fraction dropped dramatically with the fourth cluster (82%), which was much lower than any of the individual species. The drop in combustion fraction was statistically significant (p ¡ 10e-12). The combustion fraction recovered in the fifth cluster (95%), which was again statistically significant (p ¡ 10e-8). The combustion fractions found outside of the fourth cluster are likely largely caused by the combustion fractions of the individual species. The sharp drop in combustion fraction seen in the

fourth cluster further supports the idea that oak and sweetgum are interacting to prevent complete combustion in moderately high sweetgum content mixtures. As the sweetgum content increases further, this interaction is less likely to occur, and the combustion fraction returns to values similar to that of unmixed sweetgum.
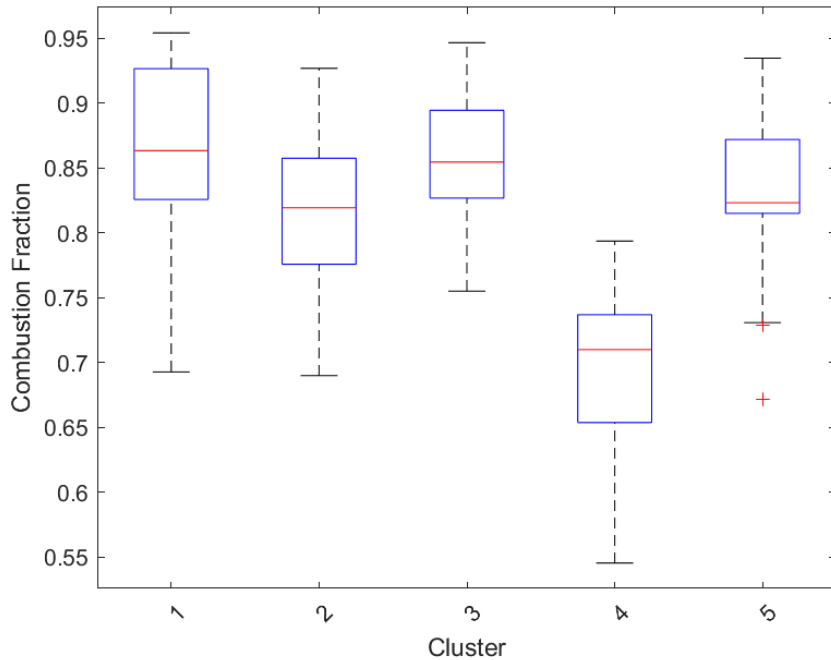
Figure 4.38: Combustion fraction for cluster.

The average temperatures across the bottom row of the thermocouples are shown in Figure 4.39. Despite the fact that the first cluster was the most flammable, the second cluster had the highest peak temperature. The profile of the second cluster had a sharp increase in temperature, with a wide peak, and a gentle decrease in temperature. These traits mirror those found in the lowest sweetgum mixture fuel groups, shown in Figure 4.9. The second cluster had a profile that was similar to that found for pine, with a high and narrow temperature peak. The temperature peak dropped sharply with the third cluster. The peak continued to gradually drop and widen with subsequent clusters. These results indicate that the interaction causing the increased mass loss rates seen in cluster one may also cause a reduction in the concentration of heat release. In contrast, the elimination of that interaction leads to an increase in the heat release concentration, producing the high peak temperatures seen in cluster two. As the pine content decreased, the concentration of heat released decreased as a result of a reduction in total heat release.
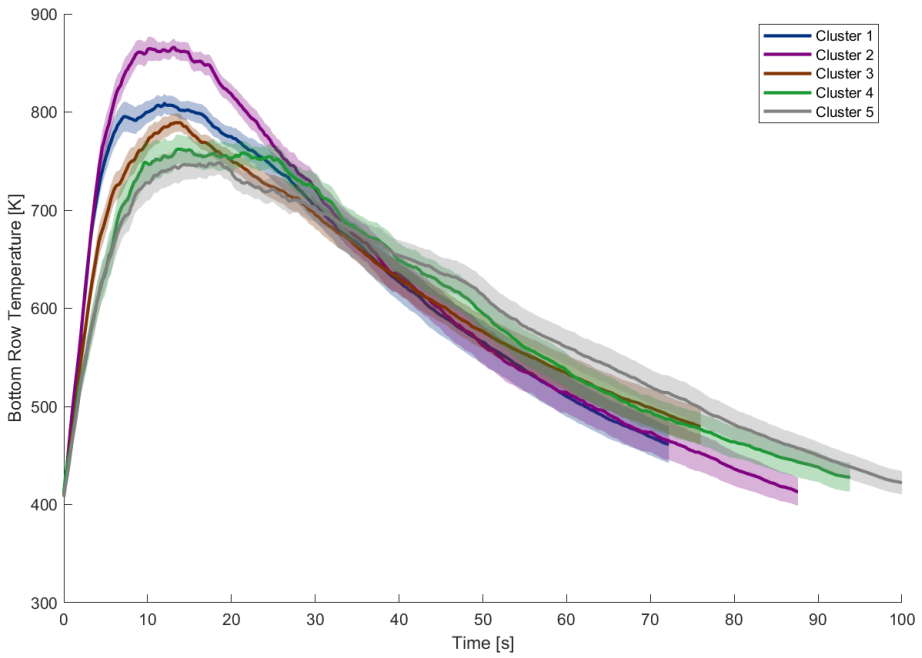
Figure 4.39: Temperature profile across the bottom row for each cluster.

Figure 4.40 shows the average temperatures in the middle row of the thermocouples for each cluster. The temperature peaks lowered and narrowed as expected, given the previous results. Unlike the bottom row, the first cluster now had the highest and narrowest temperature peak, with the second cluster's temperature peak only being slightly lower. For each subsequent cluster, the temperature peak lowered and widened, although the changes between the fourth and fifth clusters were more marginal.

The average temperatures across the top row for each cluster are shown in Figure 4.41. Again, the temperature peaks decreased as the height increased. Like with the middle row, the first cluster had the highest peak temperature; however, now, the difference between the first and second clusters was much greater. The temperature peak did lower and broaden with each cluster, with a moderate difference between the second and third clusters, a large change between the third and fourth cluster, and a marginal change between the last two. Although the first cluster had a lower peak temperature along the bottom row, its peak temperature increased relative to the other clusters as the height from the fuel bed increased. This suggests a higher flame, which would be caused by an increase in the mass loss concentration.
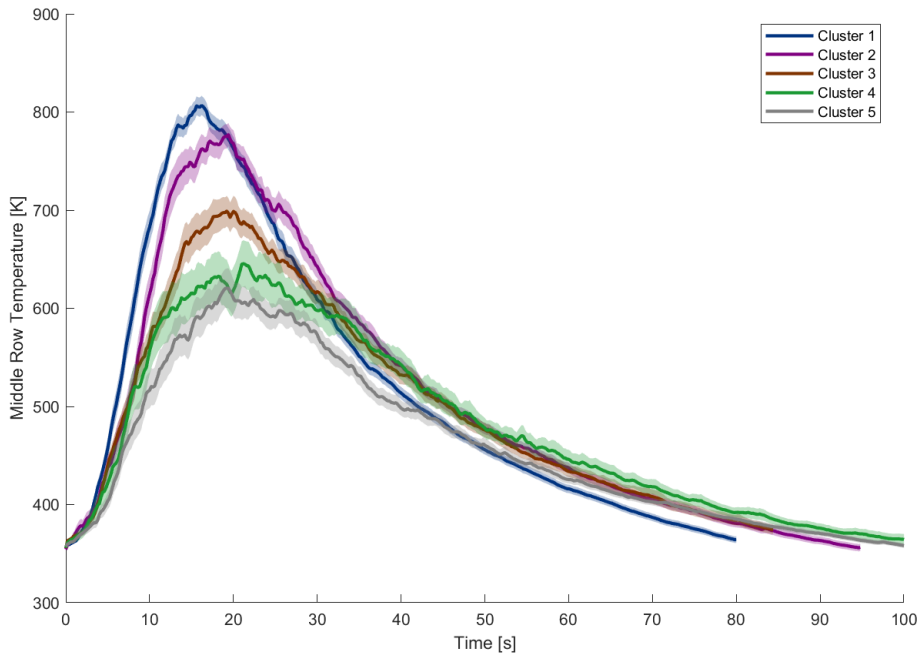
Figure 4.40: Temperature profile across the middle row for each cluster.
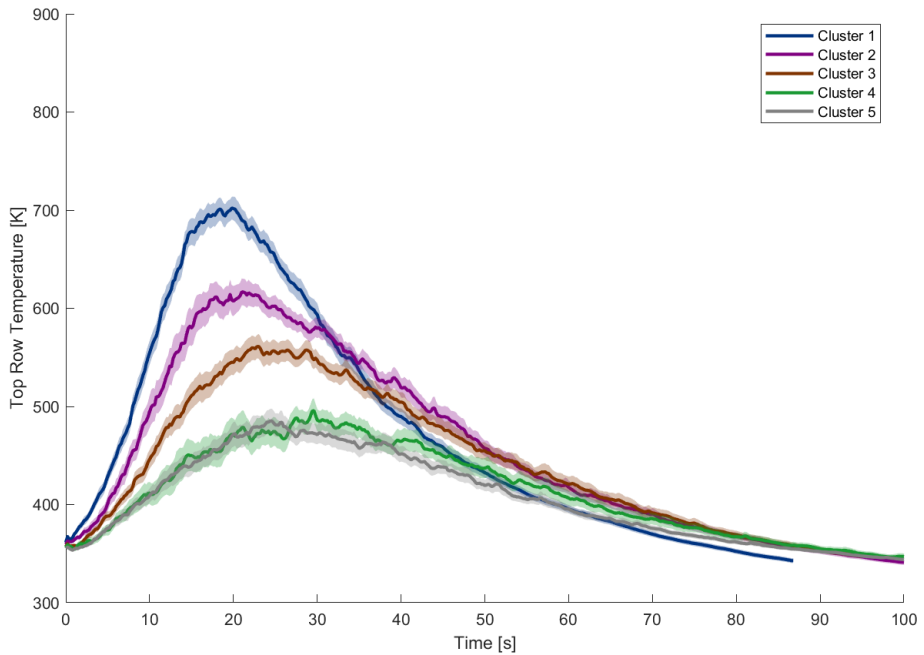
Figure 4.41: Temperature profile across the top row for each cluster.

Figure 4.42 shows the maximum temperature along the bottom row of the thermocouples for each cluster. The first cluster had a maximum temperature (99%) slightly lower than that of pine. However, the temperature in the bottom row increased significantly for the second

cluster (106%) with the change being statically significant (p ¡ 10e-5). This again reinforces the claim that the second cluster produces a region of increased heat release concentration. The maximum then drops with the third cluster (97%), which again is statically significant (p ¡ 10e-11). The maximum temperature continues to decrease with the fourth (93%) and fifth clusters (94%) however, these changes are not statically significant ($p = 0.06$, $p = 0.53$). Overall, these results indicate that a distinct aspect of the second cluster's flame front leads to a region of increased heat release concentration and therefore to the temperature.
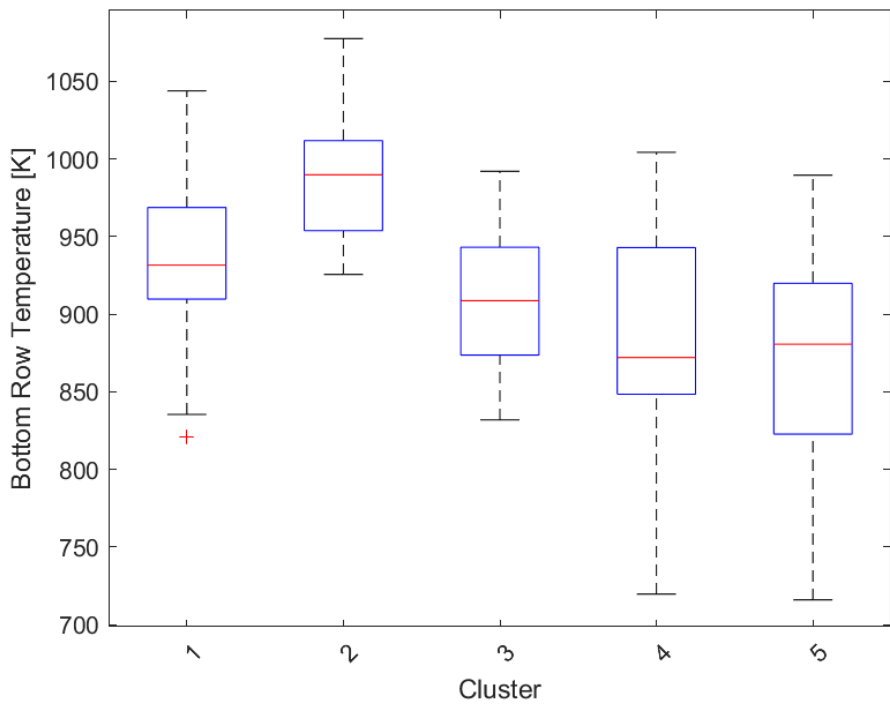
Figure 4.42: Max temperature measurements along the bottom row for each cluster.

Figure 4.43 shows the maximum temperature along the middle row of the thermocouples for each cluster. Along this row, the second cluster had the highest maximum temperature (103%); however, it was not statically different ($p = 0.76$) from the first cluster (102%). The temperature dropped moderately with the third cluster (94%), which was statically significant ($p < 10e-6$). From the third to fourth cluster (91%), the decrease in temperature was small but statically significant ($p = 0.01$). The sharpest temperature drop occurred with the fifth cluster (77%), which was also statically significant ($p < 10e-3$). The sharp decrease seen in the fifth cluster suggests that tests within this cluster did not produce flame heights that

consistently reached the middle row of thermocouples. The increasing spread of temperature values seen in the fourth and fifth clusters also suggests this, as whether or not the flame reached the thermocouples would have a large impact on the temperature readings.
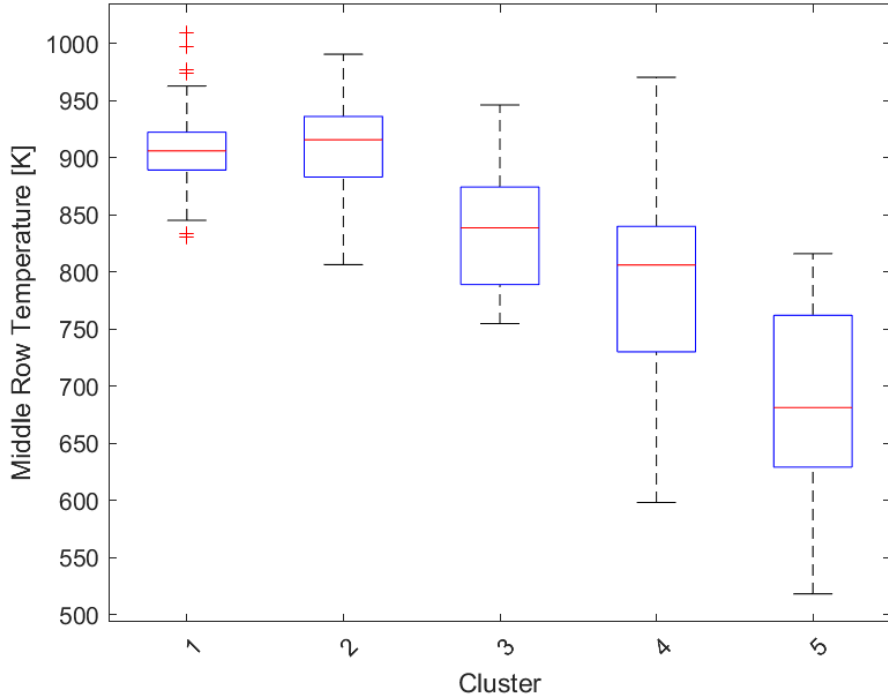
Figure 4.43: Max temperature measurements along the middle row for each cluster.

The maximum temperature measurements along the top row are shown in Figure 4.44. Like the average temperature in the top row, shown in Figure 4.41, the highest maximum temperature is now found in the first cluster (107%). The temperature drops notably for the second cluster (100%), with the change being statically significant ($p < $ 10e-3). The temperature continues to drop for each cluster. The decrease in temperature in the third (90%) and fourth cluster (76%) is relatively high, and both are statically significant ($p < $ 10e-4, $p < $ 10e-7). The temperature decreases for the fifth cluster (70%), although this change is almost, but not quite statically significant ($p = 0.06$). The sharp decrease in temperature between the third and fourth cluster is probably due to a reduced flame height, where the fourth and fifth cluster tests did not consistently reach the top row of thermocouples.
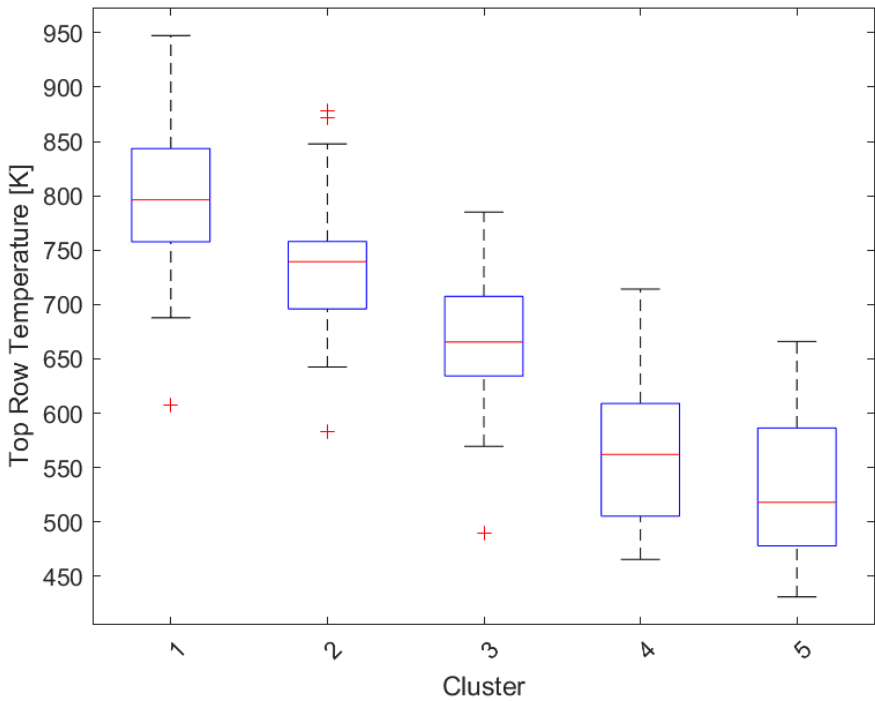
Figure 4.44: Max temperature measurements along the top row for each cluster.

Figure 4.45 shows the estimated propagation rate for each cluster. Like with the normalized mass loss rate, the first cluster had a much higher (116%) median value than the other clusters. The propagation rate decreased dramatically in the second cluster (86%) with the change, unsurprisingly, being statically significant ($p < 10e\text{-}9$). The propagation rate increased slightly in the third cluster (88%), but this change was insignificant ($p = 0.36$). The propagation rate decreased substantially again with the fourth cluster (65%), which was also statically significant ($p < 10e\text{-}2$). The difference between the fourth and fifth cluster (60%) was more gradual, but still statically significant ($p < 10e\text{-}2$). The decreases in propagation rate are likely in part due to inherit differences in the flammability of the different species. However, the sharp changes in propagation rate between the first and second, and the third and fourth clusters suggest distinct changes in the flame front behavior.

The values of the first principal component, which relates to overall flammability, for each cluster are shown in Figure 4.46. As mentioned previously, the clusters were ordered based on their PC1 values. As such, the first cluster had the highest median value (1.96). Like the first cluster, the second cluster (0.77) also had a positive value, indicating that these two
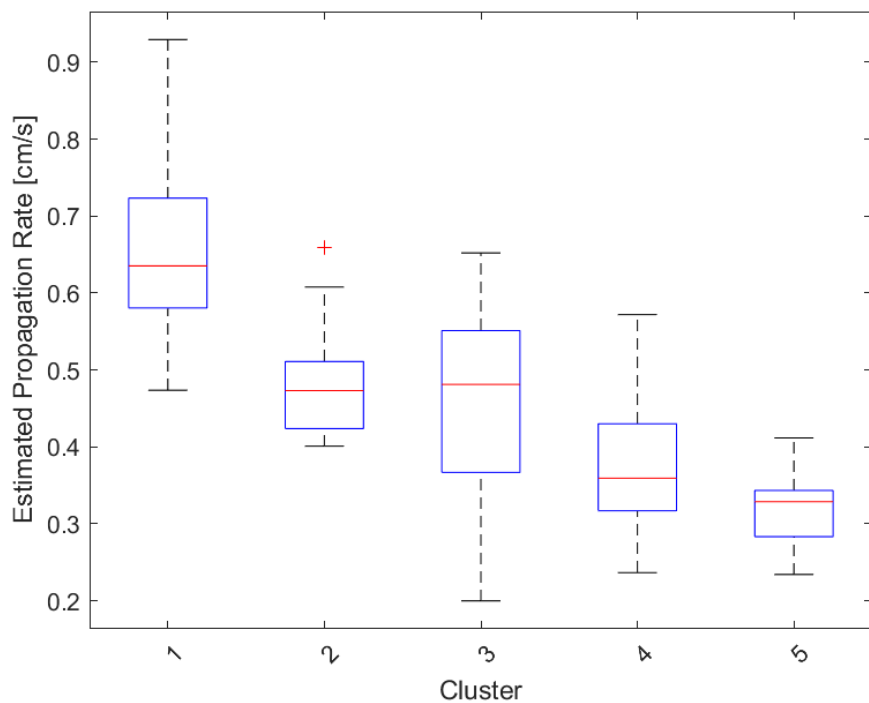
Figure 4.45: Estimated propagation rate measurements for each cluster.

clusters exhibited high flammability. The difference between these two clusters was statically significant ($p < 10e\text{-}10$). The third cluster (-0.04) had a value near zero, indicating moderate flammability, the decrease from the second to the third cluster was also statically significant ($p < 10e\text{-}4$). The fourth (-1.85) and fifth cluster (-2.54) had negative PC1 values, indicating low flammability. The difference between the third and fourth cluster was statically significant ($p < 10e\text{-}12$), but the difference between the fourth and fifth clusters was not significant, although close to it ($p = 0.052$).
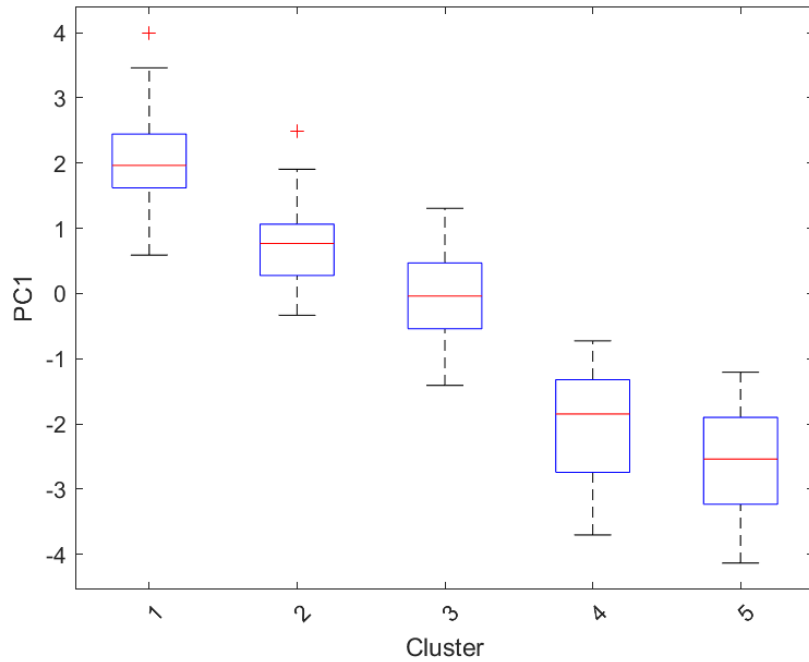
Figure 4.46: First principal component for each cluster.

Figure 4.47 displays the values of the second principal component for each cluster. Positive PC2 values indicated that relatively more heat is applied to combustion completion, while negative values indicated that more heat is used to increase temperature, flame front propagation, or is wasted. The first cluster (0.13) typically had slightly positive PC2 values. Although the first cluster had a slightly positive median value, it had high and low values in its outer quartiles. These results indicate that typically a large amount of heat release is directed toward combustion completion; however, tests with rapid propagation may produce lower PC2 values. The second cluster (-0.55) had the second lowest values for PC2, which reflects the high temperatures in the bottom row seen in this cluster. The difference between the PC2 values of the first and second clusters is statically significant ($p < 10e\text{-}3$). The third cluster (0.44) had the second highest median PC2 value, which reflects the slight increase in combustion fraction and the drop in temperature seen in this cluster compared to the second cluster. The difference between the PC2 values of the second and third clusters is also statically significant ($p < 10e\text{-}9$). The fourth cluster (-0.8) had the lowest median PC2 value, which is reasonable given the especially low combustion fractions seen in these tests. The difference between the third and

fourth PC2 values is also statically significant ($p < 10e$-9). The fifth (0.77) cluster had the high-est median PC2 values, which was a statically significant ($p < 10e$-7) change from the fourth cluster. This should be expected given the combustion fraction recovery, reduced temperature, and propagation rate seen in this cluster.
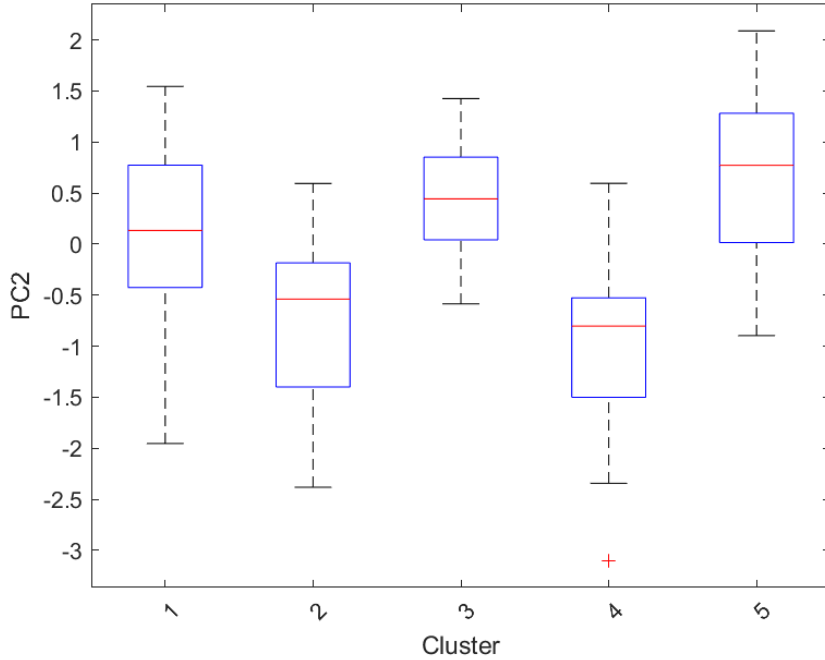
Figure 4.47: Second principal component for each cluster.

The values of the third principal component for each cluster are shown in Figure 4.48. The third principal component indicated the location of the heat release concentration, positive values suggesting a greater amount of heat release toward the center of the flame front, and negative values indicating a greater amount of heat release near the leading edge of the flame front. The first cluster (-0.27) had the second lowest median PC3 value, reflecting the increased propagation rate seen in this cluster. The second cluster (0.82) had the highest median PC3 value, which reflects the highest bottom row temperatures occurring within this cluster. The difference between the first two clusters is statistically significant ($p < 10e$-9). The third cluster (0.1) had a slightly positive median PC3 value, which was statically significant ($p < 10e$-4) from the values of the second cluster. This reflects the decrease in the bottom row temperature seen in this cluster. The fourth cluster (-0.55) had the most negative median PC3 value, which was caused by the significantly reduced combustion fractions found for the tests in this cluster.

The difference between the third and fourth cluster was statically significant ($p = 0.02$). The fifth cluster (0.04) had a neutral median value, the differences between the PC3 values of the fourth and fifth cluster were statically significant ($p = 0.05$). The median PC3 value for this cluster reflects the overall lower concentration of heat release across the entire flame front.
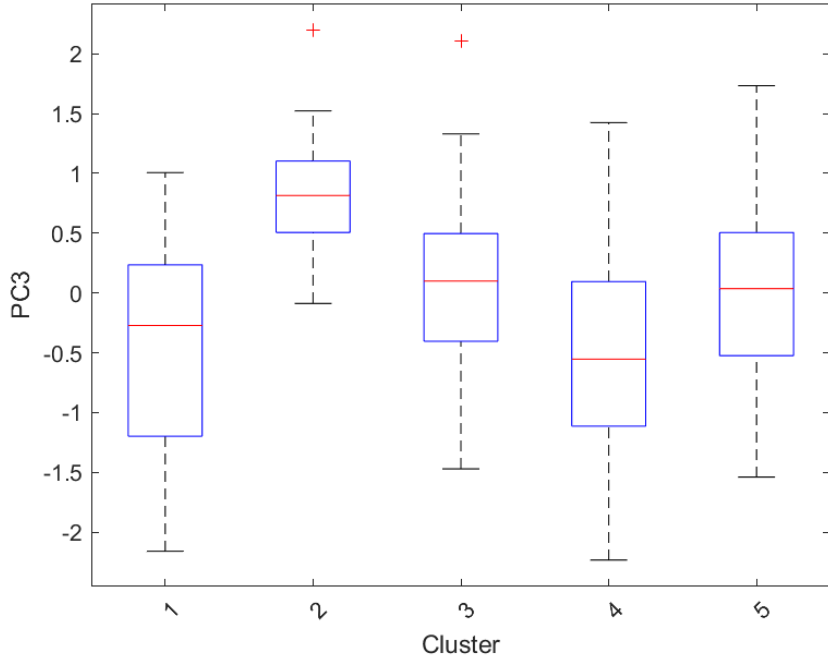
Figure 4.48: Third principal component for each cluster.

4.6 Results Comparison

The findings of this study can be compared with those of several other studies that used similar methods or fuel species. Of particular note is the study conducted by Stubbs et al. [14], which originally developed the testing facility used in this study. Stubbs et al. studied the effects of fuel loading with $Pinus\ taeda$ using loadings of 0.98, 1.31, and 1.63 kg/m^2 in contrast to 0.57 kg/m^2 used in the current study. Additionally, in the study by Stubbs et al. fuel was compressed to have a consistent fuel bulk density of 20.6 kg/m^3, where as in this study the test bed was not compressed and had bulk densities between 4 and 10 kg/m^3.

The mean normalized mass loss rate found by Stubbs et al. was 2.5e-3 in tests with fuel loadings of 0.98 kg/m^2, the load closest to those used in this study, and increased slightly with fuel loading. This is significantly lower than the 5.5e-3 found in the current study and

is probably due to differences in the bulk fuel densities. Using linear regression between the normalized mass loss rate and the bulk density of pine needles in this study, a mass loss rate of -3.6e-3 is predicted given the bulk densities used in the study by Stubbs et al. As a negative mass loss rate is impossible, the bulk densities used by Stubbs et al. likely exceed the linear region of the bulk density and mass loss relationship. The mass loss rate and fuel specific volume are shown in Figure 4.5 to have asymptotic relationships approximately above 0.2 m^3/kg and below 0.15 m^3/kg; or 5 kg/m^3 and 6.7 kg/m^3. Although this makes a direct comparison of the mass loss rate between these studies difficult, the mass loss rates found by Stubbs et al. reflect the lower bound of the mass loss rate found in other fuels tested in this study with similar fuel bulk densities.

The mean residual mass fraction found by Stubbs et al. was 0.21, compared to 0.13 found for dry pine tests in the current study. Similarly to the differences in the mass loss rate, the contrast in the residual mass fractions is probably due to differences in the bulk density of the fuel.

Stubbs et al. [14] found a median maximum flame temperature of 977 K along the bottom row of thermocouples compared to 937 K found in this study. Although fuel specific volume was shown to have a statistically significant relationship across all tests, it was insignificant when only pine litter tests were considered. Furthermore, the time-averaged temperatures found by Stubbs et al. showed some differences from those found in the current study. The 0.98 kg/m^2 fuel loading tests produced a bottom row temperature profile similar to that of this study. However, as the fuel loading increased, the temperature peak flattened and the temperature decrease after the peak was more gradual. All fuel loadings along the middle row produced similar results to those found along the bottom row in this study. Along the top row the temperature profiles of the 1.31 and 1.63 kg/m^2 fuel loading tests were similar to the pine temperature profiles in the middle row. The 0.98 kg/m^2 fuel loading tests produced temperature profiles in the top row similar to the pine temperature profiles in the top row found in the current study.

Stubbs et al. [14] found an average propagation rate of 0.44 cm/s in 0.98 kg/m^2 fuel loading tests compared to 0.52 cm/s found here. The propagation rates found by Stubbs et al. are similar to those found in pine litter tests with higher fuel bulk densities and can be seen in

Figure 4.29. This may suggest that pine litter has a higher minimum propagation rate asymptote than oak or sweetgum litter.

Some results from the current study compare fairly well with the results from Stubbs et al., however, there are a few notable differences, most of which are reasonably explained by changes in the bulk density. Differences in fuel species are expected to contribute as well, but comparisons between these two tests are insufficient to isolate these differences.

To gain further insight into the differences between the litters of individual species, the study by Varner et al. [31] was reviewed. Varner et al. used the method originally developed by Fonda et al. [27], which is also used in several studies that are discussed in the following paragraphs. For these tests, 20 by 20 cm, 15 g samples were oven dried and placed on a 35 by 35 cm grid of eight strings soaked in xylene. In addition to performing several tests, Varner et al. also reviewed and included the results of several other studies. In total, 50 species of tree litter from several southern forest communities were studied. In particular, some species from the coastal plains uplands community were included in the species tested in the current study.

Table 4.2: Comparison of the combustion fractions in the present study and in Varner et al. for shared fuel species.

Fuel Species	Present Study	Varner et al.
$P.\ palustris$	0.87	0.92
$Q.\ falcata$	0.82	0.87
$L.\ styraciflua$	0.84	0.87

Table 4.3: Flame height, smolder time and fireline intensity results in Varner et al. for shared fuel species.

Fuel Species	Flame Height	Smolder Time	Fireline Intensity
$P.\ palustris$	86.8 cm	273.7 s	415 kW/m^{-2}
$Q.\ falcata$	75.0 cm	399.8 s	302 kW/m^{-2}
$L.\ styraciflua$	54.4 cm	288.6 s	151 kW/m^{-2}

The combustion fractions found in this study and in Varner et al. are shown in Table 4.2. The results between the two studies are similar; however, those found in Varner et al. are slightly higher for each species. The difference between the combustion fractions is likely due to differences in the test methods used. In the present study, ignition was achieved using denatured alcohol along the width of one side of the test bed. This often leads to small pockets of reduced combustion as a result of variations in the flame front propagation. In contrast, Varner et al. used a grid of xylene-soaked strings that heated the entire fuel bed, preventing any regions of reduced combustion.

Varner et al. also measured the height of the flame, the time of the smolder, and the flame intensity of each species and are shown in Table 4.3. Although these measurements were not directly measured in the present study, they are related to the findings of this study. The flame heights found by Varner et al. for pine and sweetgum compare favorably with the flame heights implied by the flame temperature profiles found in Figures 4.10, 4.13, and 4.16, with pine producing significantly higher flame heights than sweetgum. However, Varner et al. found that oak resulted in flame heights between those of pine and sweetgum, while in the present study the flame height was observed to be close to that of sweetgum. Again, this is likely due to differences between the test methods, since the xylene-soaked string grid may have had a similar impact on oak as pine did in the current study.

Varner et al. found that the smolder times for $P.\ palustris$ and $L.\ styraciflua$ were close to 280 s, while $Q.\ falcata$ smolder for almost 400 s. Although the smolder time was not directly measured in the present study, it is reflected in the time-averaged temperature figures 4.9 through 4.17, and the average fuel temperature figure 4.31. Assuming that the residual temperatures displayed in these figures depend on the smoldering combustion of the test, the smolder times found by Varner et al. compare favorably with those from this study.

The flame intensities found by Varner et al. corroborate the possibility that sweetgum suppresses oak combustion. The results found in the current study suggest that the moisture content and sweetgum suppress the combustion and propagation rate of oak; however, pine can counteract these effects. Presumably, the xylene-soaked strings in the study by Varner et al. could act similarly to pine in the current study, so the presence of moisture had less impact

on oak combustion. In contrast, sweetgum produced significantly reduced flame intensities, reinforcing the suggestion that it suppresses the propagation of oak combustion as a result of reduced heat release along the leading edge of the flame front.

Despite direct comparisons between Varner et al. [31] and the current study being restricted to the combustion fraction, several indirect comparisons can be made. In general, the combustion fractions found in this study compare favorably with the combustion fractions found by Varner et al. Additionally, several findings from this study show trends that would be expected given the results found by Varner et al. [31]. Although the results of individual species are indicative of potential relationships, tests including mixtures will also need to be evaluated.

A particular study focusing on the mixtures of pyrophyte-mesophyte fuels was the study by Kreye et al. [30]. Kreye et al. studied the burning characteristics and moisture retention of fuel mixtures using the same method developed by Fonda et al. [27]. The mixtures used by Kreye et al. used several species to represent both pyrophytes and mesophytes and included tests with litter of 0%, 33%, 66% and 100% mesophyte litter. Kreye et al. tested dry, moderate moisture, and high moisture tests by saturating tests and allowing them to dry for either 12 or 24 hours, respectively. The fuel mixtures used by Kreye et al. [30] compare favorably with those used in the present study. The 100% mixed pyrophyte and 100% mixed mesophyte tests of Kreye et al. can be compared to the oak and sweetgum tests of the current study, and the 66% mesophyte, 33% pyrophyte tests can be compared to the 70% sweetgum, 30% oak tests in the present study.

Unlike the current study, Kreye et al. [30] was able to achieve consistent combustion for increased moisture tests. Moisture retention was found to increase with the mesophyte content, and the combustion fraction was found to decrease with the moisture content. The ability of these tests to achieve combustion further suggests that the ignition method used reduces the impact of the moisture content compared to a propagating flame front.

The comparison between the combustion fractions found by Kreye et al. and those of the current study is shown in Table 4.4. The combustion fractions for oak / 0% mesophytes compare favorably, as well as reflecting the combustion fraction found by Varner et al. [31].

Table 4.4: Combustion fractions in the present study and in Kreye et al. for similar fuel mixtures.

Fuel Mixture	Present Study	Kreye et al.
Oak / 0% Mesophyte	0.82	0.88
70% Sweetgum / 66% Mesophyte	0.80	0.81
Sweetgum / 100% Mesophyte	0.84	0.76

However, as the mesophyte content increased, the differences between the combustion fraction results also increased. The mesophyte mixture used by Kreye et al. consisted of 30% sweetgum and differences in the combustion fraction may be due to the other constituent species of the mesophyte mixture.

Table 4.5: Smolder time results in Kreye et al. for shared fuel species.

Fuel Mixture	Smolder Time
0% Mesophyte	229 s
33% Mesophyte	276 s
66% Mesophyte	246 s
100% Mesophyte	217 s

The smolder time was also measured by Kreye et al. and was found to increase in the tests with pyrophyte and mesophyte fuels present. In the current study, a similar trend can be seen in the time-averaged temperature profile, particularly along the bottom row. Figure 4.11 displays the "clumped" temperatures along the bottom row and shows how the final measured temperatures were highest in the moderate sweetgum content tests.

Although the results from thermogravimetric analysis cannot be directly compared with the results of the current study, reviewing their findings can provide applicable information. Two studies of interest that focused on the chemical kinetics of wildland fuel were those by Bach et al. [23] and Yang et al. [18].

Bach et al. [23] studied the impacts of wet torrefaction on the combustion kinetics of Norway spruce ($Picea\ abies$) and an unspecified birch wood using thermogravimetric analysis. Thermogravimetric analysis was carried out with 0.5 mg fuel samples that were ground into fine powder and filtered through a 90 μm sieve. Before each test, the samples were heated to 105 °C for 1 hour to dry. During the tests, the samples were heated to 700 °C with a constant heating rate of 10 °C per minute and supplied with 80 ml/min of air flow.
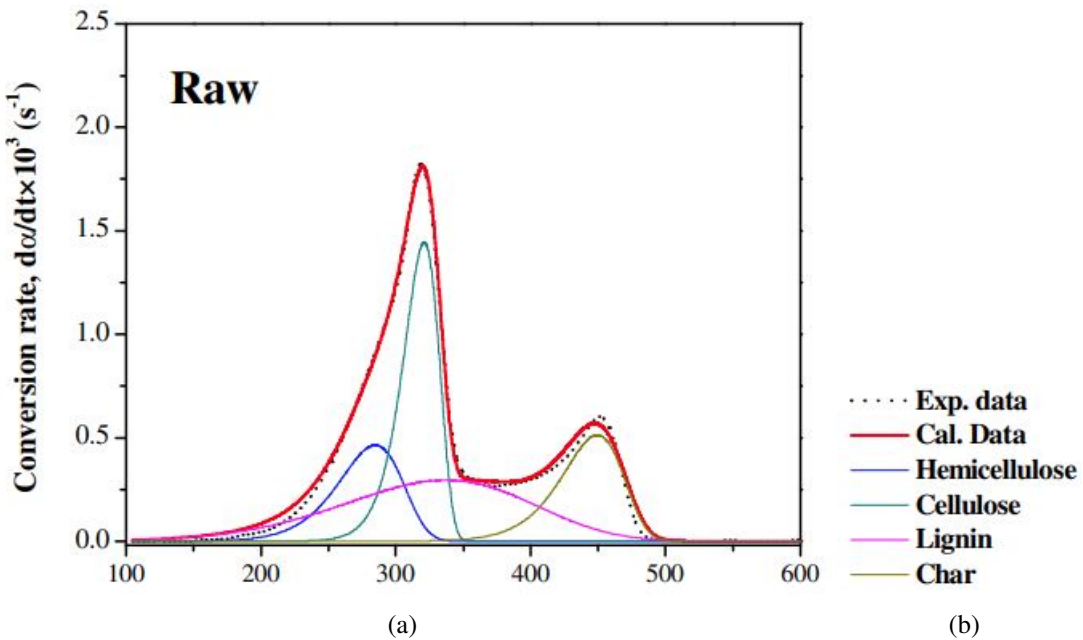
Figure 4.49: The modeled conversion rate of each of the three lignocellulosic components over a temperature range found by Bach et al.

Although the focus of this study is not particularly relevant to the current study; it does provide a good example of the combustion process through which forest fuels are burned. Bach et al. states that the combustion of lignocellulosic biomass, such as leaf litter, undergoes three stages; drying, devolatilization, and char production. Lignocelluosic biomass consists of hemicellulose, cellulose, and lignin, each of which demonstrate different behaviors during pyrolysis. Using thermogravimetric analysis, Bach et al. identified the degradation ranges for each of these components and showed their respective mass loss profiles. Hemicellulose was shown to be the most reactive of the three components and was degraded between 200 and 300 °C. Cellulose degraded from 325 to 375 °C. The degradation of lignin occurred over the widest temperature range, specifically 250 to 500 °C. The mass loss due to char was found to begin near 350 °C and complete near 500 °C. Although these ranges were shown as typical ranges, the exact properties of each of the three lignocellulosic components are slightly different within each species. The modeled conversion rate of each of the three lignocellulosic components over a temperature range (in Celsius) is shown in Figure 4.49.

In Yang et al. [18]. the pyrolysis characteristics of powdered hemicellulose, cellulose, and lignin were studied using thermogravimetric analysis and differential scanning calorimetry.

The fuel samples were approximately 10 mg, with particle sizes of approximately 50 μm for cellulose and lignin and approximately 100 μm for hemicellulose. During the tests, the samples were heated to 900 °C at a constant rate of 10 ° C/min and then kept at 900 °C for 3 minutes. Pure nitrogen supplied at 120 ml/min was used for the atmosphere in these tests. The heat release profile for each lignocellulosic component over a temperature range found by Yang et al. is shown in Figure 4.50.
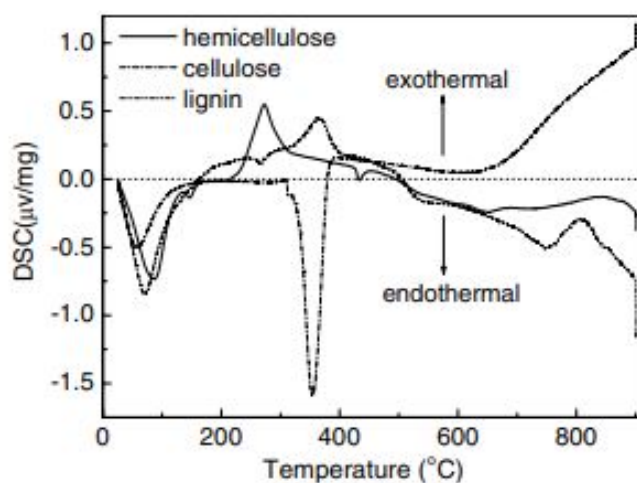
Figure 4.50: The heat release profile for each lignocellulosic component over a temperature range.

Hemicellulose was found to rapidly start decomposition, with weight loss occurring primarily between 220 and 315 °C. The maximum hemicellulose mass loss rate was 0.95 wt.% / °C and occurred at 268 °C. After testing, approximately 20% of the hemicellulose mass remained as solid residue. Cellulose pyrolysis occurred between 315 and 400 ° C, with a maximum mass loss rate of 2.84 wt.% / °C at 355 °C. After 400 °C most cellulose pyrolysis had occurred with only 6.5% of the mass remaining. Lignin slowly decomposed over the entire temperature range with a mass loss rate less than 0.14 wt.% / °C. Furthermore, lignin had the highest residual mass after testing, with approximately 45.7% remaining.

When temperatures were below 200 °C, all three components were endothermic, although to a lesser extent for cellulose. Lignin became exothermic at approximately 175 °C and remained exothermic until 500 °C, with a peak at 365 °C. Hemicellulose became exothermic at

approximately 200 °C and continued to be exothermic until 500 °C, with a peak at approximately 275 °C. Cellulose was extremely endothermic in a short range centered around 355 °C. Yang et al. attributed the peaks of the three lignocellulosic components to their pyrolysis. Once the temperature exceeded 500 °C, hemicellulose and lignin became endothermic. In contrast, cellulose became increasingly exothermic at temperatures above 400 °C.

Table 4.6: Component composition for each fuel

Fuel	Lignin	Cellulose	Hemicellulose	Carbon	Nitrogen
Pine	20.3%	29.1%	10.9 %	50%	0.4%
Oak	16%	15.7%	10.3%	49.4%	0.7%
Sweetgum	11.1%	12.5%	5.8%	45.1%	0.8%

So that the findings of Bach et al. [23] and Yang et al. [18] can be applied to the current study, the hemicellulose, cellulose, lignin, nitrogen and carbon for each of the fuels used in the current study are shown in Table 4.6. These values were found as part of another ongoing study at sites in north Florida (H. Alexander, unpublished data). The percentage of lignin, cellulose and hemicellulose was determined after digestion in 72% sulfuric acid for 3 hours at ambient temperature in an ANKOM Daisy Incubator (ANKOM Technology, Macedon, NY). Percent carbon and nitrogen was determined by combustion using a CN928 Macro Determinator (LECO Corporation, Saint Joseph, MI). All chemical analyzes were performed at the Dairy One Forage Testing Laboratory (Ithaca, NY). Also, it should be noted that in Table 4.6 the sum of the pine components exceeds 100%, this is because some of the carbon content exists within the lignocellulosic components. In contrast, the components for oak and sweetgum do not add up to 100%; this is because other trace components exist but are not included in Table 4.6.

Other studies focused directly on how the chemical composition and morphology of the fuel impact the burning characteristics of leaf litter. Grootemaat et al. (2015) and Grootemaat et al. (2017) focused on how the morphology and chemical composition of the fuel impacted both the flammability and the decomposability of different species [34, 41]. Although decomposability is not relevant to the current study, the findings related to flammability are. The specific leaf area, which is the one-sided leaf area dived by its mass, was found to decrease the time to ignition and the maximum flame temperature, while increasing the spread rate [34, 41].

In Grootemaat et al. (2015) lignin was found to have little impact on measured flammability traits, but Grootemaat et al. (2017) found that lignin increased fuel consumption [34, 41].

Willis et al. conducted field tests using leaf litter, fruits and cones [45]. In addition to measuring the effects of fruits and cones within the fuel bed, Willis et al. measured the nitrogen, carbon, and lignin content of the fuel species. Both lignin and carbon were found to increase fuel consumption and flame height, while nitrogen had inverse effects.

In general, the burning characteristics seen in the current study reflect many of the observed properties attributed to the chemical composition and morphology of the fuel. Pine had high amounts of hemicellulose and lignin, which would correspond to higher heat requirements for combustion, but also higher quantities of early heat release. This reflects the findings of the current study, as this would cause humidity and moisture to have a reduced impact on the propagation of the flame front. Unlike pine, reduced concentrations of lignocellulosic components in oak and sweetgum would lead to reduced heat release during combustion, especially in sweetgum. Also, while not measured, the specific surface areas of the oak and sweetgum leaves are clearly higher than those of the pine needles. Given that the specific surface area was found to decrease the time to ignition, it is likely that oak and sweetgum are able to achieve higher propagation rates than pine under ideal circumstances [34]. This was seen in some oak tests, specifically during low humidity tests. Overall, heat release probably peaked during the early stages of hemicellulose pyrolysis and combustion, whereas the peak mass loss likely occurred during cellulose pyrolysis.

Lignin was also shown to ignite first but progress through combustion slowly. Slow lignin combustion and reduced lignin content within oak supports the possibility that oak propagation is suppressed by moisture content. In the presence of low humidity, oak is able to be heated quickly enough so that hemicellulose combustion is near the flame front and has a greater contribution to propagation. However, humidity may increase the heat required to achieve ignition to the point that hemicellulose combustion is delayed and lignin combustion drives propagation. Sweetgum had the lowest lignin and hemicellulose content, which limited its overall flammability. Although oak propagation was conditionally driven by lignin combustion,

sweetgum propagation may always be driven by it. This reflects the consistent propagation rates found for sweetgum litter in the current study.

The results of the current study generally compare well with the results of previous studies for results that can be directly compared. The differences found between the results of the present study and previous studies are within expectations given the variations in experimental methods and fuel species. Although several fuel species can be categorized as mesophytes or pyrophytes, there are still significant differences between species within each group and are shown in the results of Varner et al. [31]. This variance between groups indicates that the interactions between mesophytes and pyrophytes will also vary with the constituent species. This variance is likely to be reflected in the differences in the distribution of the lignocellulosic components, although additional tests will be needed to confirm this. Furthermore, the findings of the current study are supported by the results of Bach et al. [23] and Yang et al. [18]. Although direct comparisons can not be made between these studies and the present one, the burning characteristics found are within expectations given the attributes of the lignocellulosic components found by Bach et al. and Yang et al.

Chapter 5

Discussion

The aim of this study is to investigate the relationship between sweetgum content and combustion characteristics within mixed litter fuel beds. This chapter expands on the observations and discussions from the previous chapter.

Of the three fuel species tested, pine had the highest median values for both the mass loss rate and the propagation rate. This is probably due to early combustion of lignin and hemicellulose in quick succession. This allows the heat released from the combustion of the hemicellulose to contribute to the propagation of the flame front. Additionally, the high concentration of heat release near the leading edge of the flame front allows pine to overcome the higher heat requirements for propagation caused by factors such as increased moisture content.

Pine also had the highest median combustion fraction of the single fuel groups. This was probably due to its increased heat release that allowed for a more consistent combustion completion. This is also reflected in the wet pine tests, as increased heat release would be necessary to overcome moisture, which had little impact on the combustion fraction.

Again, pine had the highest maximum temperature along the bottom row for the single species tests. The temperature was reduced in the presence of increased moisture, but was still above the values for oak and sweetgum. This was probably caused by a thin flame front, which would lead to a high concentration of heat release and therefore to a high temperature. This is also reflected in the bottom row temperature profile, where the pine had a narrower temperature peak than the other species. Moisture did cause the temperature profile to broaden, but this was likely caused by variations in the moisture content that affected the propagation rate.

As the height above the fuel bed increased, the maximum temperature of the pine remained the highest of the single fuel groups. Furthermore, the margin by which the temperature of pine was greater than oak and sweetgum also increased. This indicates that pine produced a higher flame front than those species, as the flame height has a greater effect on the temperature measurements as the thermocouple height increases. The temperature profile also became sharper as the height increased, reflecting this trend. This supports the claim that pine had a thin flame front, as a higher concentration of heat release and mass loss would increase the flame height. Moisture decreased the temperature along the middle and top rows more than it did along the bottom row, suggesting that the region of mass loss concentration was widened by moisture, while the heat release region was less affected.

Oak was found to have bimodal values for both the mass loss rate and the propagation rate. This was probably caused by ambient humidity, since all rapid burning oak tests occurred during periods of low humidity. This suggests that oak has a lower heat requirement for propagation, as small increases in moisture would have a proportionally greater impact on the propagation rate. This is also supported by the fact that the specific surface area of oak is higher than that of pine, which would allow for potentially higher propagation rates. During low humidity, the combustion of oak hemicellulose would rapidly ignite lignin and hemicellulose ahead of the flame front. During high humidity, the increase in heat required to warm the fuel ahead of the flame front would cause the distance between the combustion of lignin and hemicellulose to increase. This in turn caused hemicellulose combustion to have a reduced impact on the propagation rate.

The median combustion fraction found for oak was 95% that found for pine and was the lowest of the three fuel species. However, unlike the mass loss rate and propagation rate, the combustion fraction was not found to be bimodal. Like wet pine, this shows that while moisture reduces the propagation rate of the fuel, it does not inherently reduce its ability to complete combustion. In general, the reduced combustion fraction seen in oak litter is probably caused by inconsistencies in combustion as a result of reduced net heat release.

Oak also had the lowest bottom row temperature of the single fuel groups, at 93% that of pine. Like its combustion fraction, the bottom row temperature was not bimodal. The temperature profile along the bottom row had a much lower peak temperature with a gradual increase in temperature. This suggests that oak has a relatively broad flame front, as a wider flame front would reduce the concentration of heat release. This is also reflected by the gradual increase in temperature, as the region of peak combustion would be slightly further from the leading edge of the flame front. Behind the temperature peak, the temperature slowly decreased with an extended region of increased residual temperatures. This indicates extended char combustion, which produces continuous heat release. Given the increase in the amount of cellulose in oak, this is within reasonable expectations.

Along the middle row of thermocouples, oak produced temperatures above that of wet pine. In addition, the temperature peak for the oak was sharp along the middle row. Both suggest that the region of increased mass loss concentration was smaller than the overall width of the flame front. This is because a thin region of increased mass loss would result in a thin region of increased flame height within a broad region of combustion. However, along the middle row, the temperature of the oak was again below that of the wet pine. Despite this, some low humidity oak tests did produce top row temperatures near those oak produced along the middle row. Along the top row, the temperature peak became much lower and rounded, but had an increased 95% confidence interval with a positive skew near the peak. These results suggest that, while the region of increased mass loss is thin, the flame height was only high enough to reach the top row when the mass loss rate was sufficiently high. The broad region of combustion seen along the bottom row is probably caused by the moderate lignin found in oak. In contrast, the thin region of increased flame height probably corresponds to hemicellulose and cellulose pyrolysis.

Sweetgum had the lowest median mass loss rate of the single fuel groups. In addition, within the single fuel groups, the sweetgum propagation rate was only higher than that of wet pine. In high humidity oak tests, it was suggested that hemicellulose combustion had a reduced impact on the propagation of the flame front. The propagation of sweetgum probably behaved similarly; however, the low hemicellulose content within the sweetgum would cause this to

occur consistently. This is reflected in the lower median mass loss and propagation rates found for sweetgum, as well as the sweetgum not having high modes for these measurements. This behavior would also be made more consistent by the high heat requirement for propagation as a result of the lignin content in sweetgum.

Sweetgum had a higher median combustion fraction value than oak, but less than dry and wet pine. Like oak, this was likely a result of the reduction net heat release.

Like with the combustion fraction, the bottom row temperature of sweetgum was above that found for oak, but below those found for dry and wet pine. The temperature rise was gradual, leading to a broad and flat peak. The temperature profile likely resulted from the lignin content within the sweetgum. The slow propagation rate would cause the temperature to gradually increase. Lignin combustion begins before hemicellulose but peaks after hemicellulose does. Given that hemicellulose typically produces a higher mass loss and heat release rate at its peak, the flat temperature profile likely reflects the transition from hemicellulose to lignin, producing an even distribution of combustion.

The relative temperature along the middle row dropped moderately for sweetgum. Although the peak temperature profile became thinner, it remained flat, in contrast to the sharp temperature peaks seen in pine and oak. This supports the broadened flame front and evenly distributed combustion proposed from the bottom row temperature results. An even distribution of combustion would cause both the flame front and the region of increased flame height to broaden, rather than just the flame front. Like oak, the temperature of the top row fell further for sweetgum. The temperature profile at this height was also similar to that found for oak, except that the temperature was slightly lower as it rose and higher as it fell. This was most likely caused by the hemicellulose peak occurring earlier in the flame front than that of the lignin. Given the increased hemicellulose content in oak and the relatively increased lignin content in sweetgum, their temperature profiles mirror this.

In mixed fuel groups, the results indicated several categories of behavior caused by moisture and sweetgum content. The results within each mixed fuel group were often less consistent than those found in the single fuel groups. Principal component analysis was conducted to reduce the relevant variables to better distinguish how the burning characteristics change within

each mixed fuel group. During principal component analysis, four significant principal components were identified. The first principal component described most of the variance within the results and was associated with the overall flammability. The second principal component was associated with the heat release used for combustion completion as opposed to combustion temperature. Positive values of the second component indicate that a greater proportion of the heat released is used to drive combustion, whereas negative values indicate that more heat is used for temperature. The third principal component was attributed to the distribution of heat release across the flame front. Positive values reflected heat released behind the leading edge of the flame front, increasing the combustion fraction and temperature. Negative values corresponded to more heat being released near the leading edge of the flame front. The fourth principal component was indicative of the height of the flame. However, since temperature measurements were taken at distinct intervals, as opposed to continuously with height, this component is likely flawed.

From the results of this and previous studies, it is suspected that the variations within each mixed fuel group are primarily determined by the cellulose, hemicellulose, lignin, and moisture content of the species. In addition, fuel combustion can be described in seven phases, with each component showing different behaviors in each phase.

The first phase of combustion is the drying and preheating phase. During this phase, all three lignocellulosic components are endothermic. Although all three components are endothermic, cellulose is the least endothermic, while lignin is slightly more endothermic than hemicellulose. This phase directly impacts the propagation rate of the fuel, as it determines the heat required for combustion. This is also the phase in which moisture has the greatest impact as it also increases the heat requirement for combustion. For example, pine likely has a high heat requirement for propagation, which is reflected in its high hemicellulose and lignin content.

The second phase is characterized by early combustion of lignin with little impact from cellulose and hemicellulose. This phase occurs immediately after the fuel is preheated and concludes when hemicellulose combustion begins. This phase directly impacts propagation, as this phase occurs along the leading edge of the flame front. Although oak still has a moderate

102

lignin content, its content is lower than that of pine. The reduced lignin content in oak would also reduce the heat release along the leading edge of the flame front, which contributes to oak's sensitivity to moisture content. Pine, on the other hand, has the highest lignin content of the three species, which also contributes to the proportionally reduced impact of moisture on pine propagation.

In the third phase, hemicellulose ignites rapidly and the combustion of lignin gradually increases. In slow burning fires, propagation is driven by initial lignin combustion, while in rapid fires, phases two and three occur almost simultaneously and both drive propagation. Whether or not the third phase of combustion contributes to propagation is likely a large factor in the value of the first principal component. Pine has the highest hemicellulose content of the species tested, and in conjunction with its lignin content, the third phase of pine combustion consistently impacts the propagation rate. Since sweetgum has a low hemicellulose and lignin content, its third phase of combustion does not affect propagation. The bimodal results displayed by oak probably reflect whether or not the third phase contributed to the flame front propagation.

The fourth phase is distinguished by endothermic cellulose pyrolysis, whereas hemicellulose combustion decreases rapidly and lignin combustion peaks slightly after cellulose pyrolysis. When cellulose has a decreased presence, this phase is overall exothermic and is used to further complete combustion. However, an increase in the cellulose content can cause this phase to serve as a potential barrier to further combustion if there is not sufficient heat release during previous phases.

Phase five occurs once the cellulose pyrolysis has been completed, and here all three components are mildly exothermic. This phase has a relatively small impact on the combustion behavior and serves primarily as the final phase of flaming combustion.

During the sixth phase, hemicellulose and lignin become endothermic as they approach complete combustion, and cellulose combustion is negligible. This phase can also serve as a barrier to cellulose charring if there is insufficient heat to adequately raise the temperature. For oak and sweetgum, this phase can often serve as a barrier to cellulose charring, leading

to reduced combustion fractions. This phase is more endothermic for pine than for oak and sweetgum, but less impactful since pine has greater net heat release.

The final phase is characterized by char combustion, where cellulose becomes increasingly exothermic while hemicellulose and lignin become increasingly endothermic. Although this phase is generally exothermic, the temperatures required to complete combustion are relatively high, so complete combustion is not always achieved. When oak and sweetgum complete phase six, the temperature reached during this phase dictates the combustion fraction achieved due to charring.

In mixed fuel beds, the results indicate that the species interact through their emission and absorption of heat; however, each species progresses through its combustion phases separately from the other species. The order in which the phases of each species are initiated determines the overall burning characteristics. To better identify changes in the flame front behavior, cluster analysis was used.
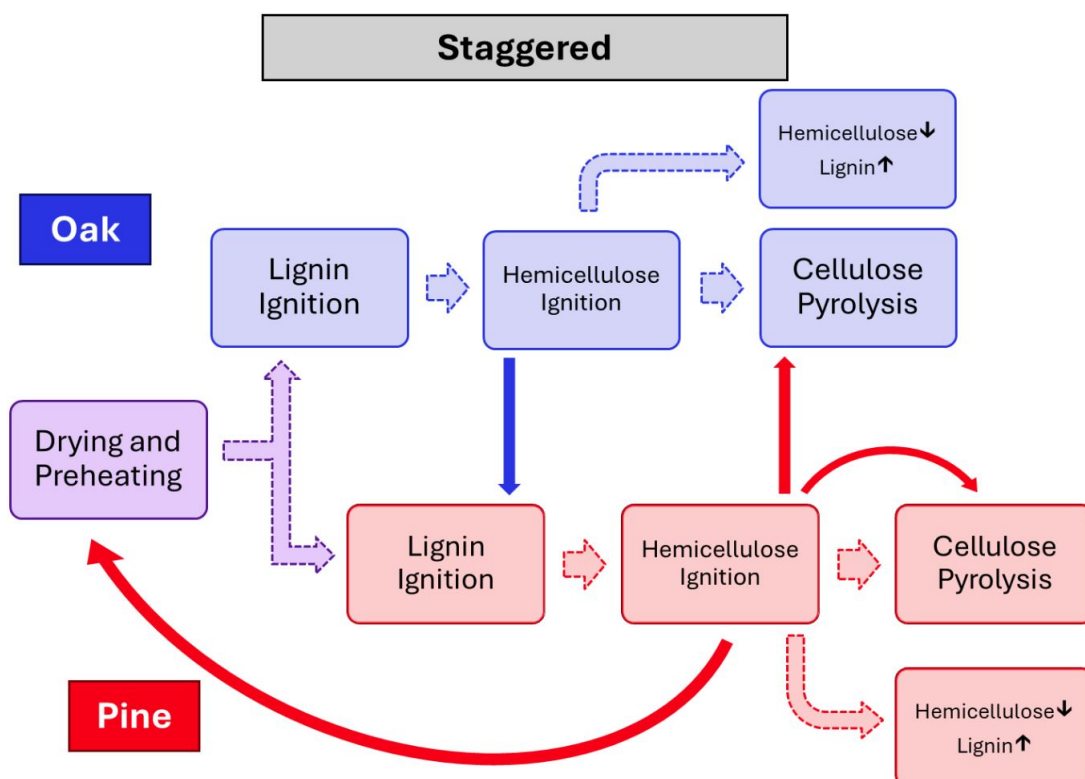

Figure 5.1: Progression of a staggered flame front. Dashed arrows denote order of phase progression. Solid arrows denote primary source of heat for endothermic phase completion.

104

Mixed tests with little or no sweetgum and low humidity potentially created "staggered" flame fronts. In these tests, oak achieves ignition before pine due to its higher specific surface area. Once the oak has ignited, it ignites the surrounding pine sooner than the pine would otherwise burn. Because pine has high values of lignin and hemicellulose content, it produces enough heat to dry, preheat, and ignite oak ahead of the flame front, even in the presence of moderate humidity. This corresponds to oak completing phases one through three before pine, with the second phase of pine occurring near to the third phase of oak, leading to a staggered flame front. This behavior is also shown in Figure 5.1. As a result, this cluster was the most flammable, which is reflected in its increased PC1 values. This also causes low values for the third principal component, as the staggered flame front causes more heat release to occur "ahead" of the flame front. Several pine tests with fuel specific volumes above average were also included in this cluster. These tests likely did not display a staggered flame front, but displayed increased flammability as a result of their fuel specific volume.

Another characteristic of staggered flame fronts is that oak phase four, which includes its cellulose pyrolysis and peak mass loss concentration, occurs during pine phase three, which is the pine's phase of peak heat release. This causes oak cellulose pyrolysis to occur much more rapidly than it typically would, which is reflected in the increased flame heights indicated by the results. The overall combustion fraction and temperature are similar to those of pine, so the values of the second principal component are similar to those found in pine.
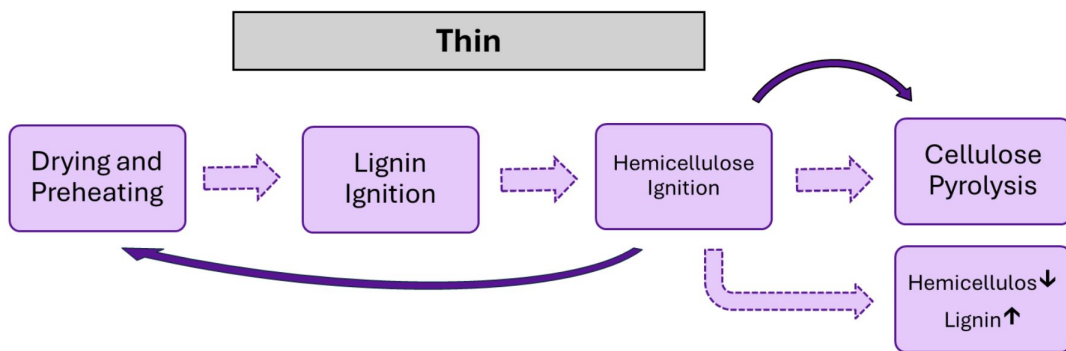

Figure 5.2: Progression of a thin flame front. Dashed arrows denote order of phase progression. Solid arrows denote primary source of heat for endothermic phase completion.

Once the sweetgum or moisture content has increased to the point that pine can no longer ignite oak early, the burn transitions to a "thin" flame front. This begins to occur with the

presence of any sweetgum, but becomes consistent near 30% sweetgum content. Here, the combustion phases for pine and oak begin to occur simultaneously. Although this leads to a reduction in flammability, the first three phases still occur rapidly, such that early combustion of lignin and hemicellulose contributes to flame front propagation. This leads to a reduction in the values of the first principal components, but they are still relatively high. Figure 5.2 displays the phase progression of a thin flame front.

The changes in the flame front geometry from a staggered to a thin flame front also prevent oak cellulose pyrolysis from occurring during peak pine hemicellulose combustion. This leads to the drop in flame height implied by the results. However, this also means that the peak heat release phases of oak and pine align, leading to the increase in combustion temperature found. This causes a drop in the values of the second principal component. Once the flame front is no longer staggered, the heat release concentration near the center of the flame front increases, leading to the increased PC3 values seen in this cluster.
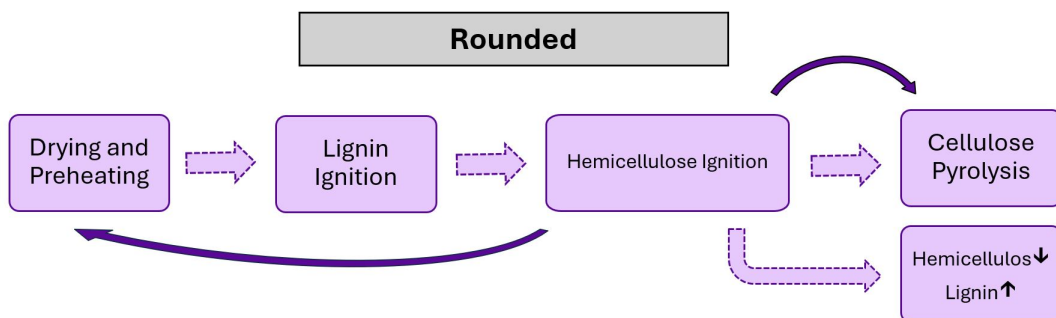
Figure 5.3: Progression of a rounded flame front. Dashed arrows denote order of phase progression. Solid arrows denote primary source of heat for endothermic phase completion.

Increasing the sweetgum content further, typically around 30% to 50% sweetgum content, the flame front transitions to a "rounded" profile. Here, hemicellulose ignition still contributes to propagation; however, progression through phase three is slower than that in a thin flame front. This reduces the concentration of heat release within the center of the flame front. Figure 5.3 depicts the phase progression of a rounded flame front. Although this decreases the height and temperature of the flame, it allows heat to be applied more efficiently to the completion of

the combustion. Although the propagation rate is not significantly different from those seen in thin flame fronts, the overall flammability is reduced because of sharp drops in the temperature measurements. The values for the second principal component also increase as heat is applied more efficiently to combustion completion. In contrast, the third principal components decrease as a result of the reduced concentration of heat release.
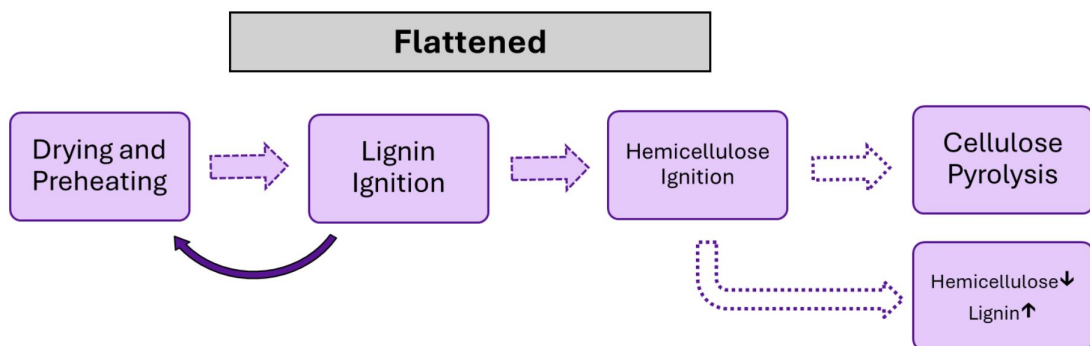

Figure 5.4: Progression of a flattened flame front. Dashed arrows denote order of phase progression. Solid arrows denote primary source of heat for endothermic phase completion. Empty arrows denote inconsistent phase progression.

Once the sweetgum content exceeds 40%, the flame front profile begins to become "flattened". The distribution of heat release becomes more evenly distributed across the flame front. The flame front also continues to broaden, causing hemicellulose to no longer contribute to the flame front propagation and, as a result, to a sharp decrease in the propagation rate. Furthermore, the flame front becomes broad enough that the hemicellulose combustion has a reduced impact on the cellulose pyrolysis. This also causes a sharp decrease in the combustion fraction and values of the second and third principal components. Figure 5.4 shows the phase progression of a skewed flame front.

Typically around 50% to 70% sweetgum content, the flame front takes on a "skewed" profile. Here, the cellulose content decreases and enough cellulose pyrolysis is again somewhat consistent despite low levels of lignin and hemicellulose. While phase three hemicellulose ignition has reduced impact on cellulose pyrolysis, hemicellulose and lignin pyrolysis during phase four can complete cellulose pyrolysis. This interaction is shown in Figure **??**. Although it has a higher sweetgum content than flattened flame front tests, the first principal component
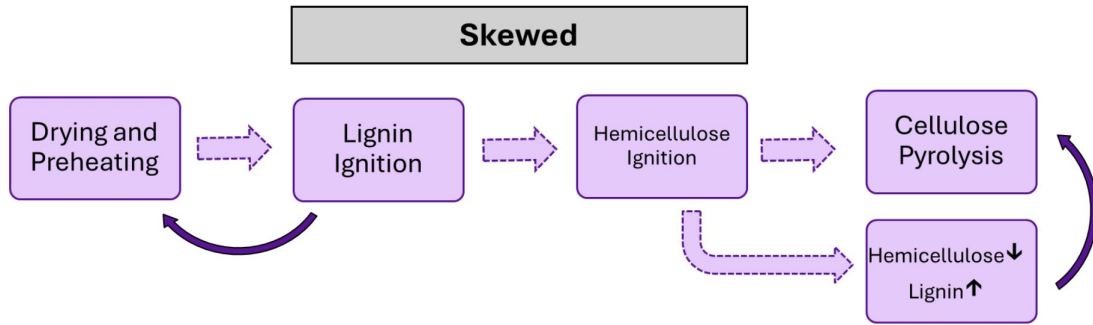
Figure 5.5: Progression of a skewed flame front. Dashed arrows denote order of phase progression. Solid arrows denote primary source of heat for endothermic phase completion. Empty arrows denote inconsistent phase progression.

is not significantly lower, due to the recovery of the combustion fraction. For the same reason, the second principal component also increases.

The results show that the fuel species interact with each other to produce different flame front profiles. In particular, pine and sweetgum were shown to have competing effects on oak. Specifically, oak showed an increased sensitivity to moisture that was counteracted by pine and exacerbated by sweetgum. The following conclusion sections summarize the findings of this study.

Chapter 6

Conclusion

This study presents valuable data on the burning characteristics of mixed fuels associated with mesophication in the southern United States. The species used in this study included longleaf pine, southern red oak, and sweetgum in both single-species fuel beds and mixed fuel beds. The mixtures used consistently contained 30% oak litter by mass, while the pine and sweetgum litter varied from 0% & 70% to 70% & 0% respectively in increments of 10%. These fuel species and mixtures were selected because of the presence of these species in upland oak forests, and during mesophication sweetgum typically supplants pine trees first. In addition, a small number of tests included an increase in moisture content. The burning characteristics measured in this study included the fuel mass loss rate, combustion fraction, flame temperature, and propagation rate, and direct measurements were used in conjunction with principal component analysis and cluster analysis. The fuel bed temperature was also explored in a select number of tests.

The measured burning characteristics are theorized to be described by seven phases of combustion, with each of the three lignocellulosic components showing different characteristics in each phase. In mixed fuel beds, species are theorized to interact through their emission and absorption of heat; however, each species progresses through its combustion phases separately from the other species. The order in which the phases of each species are initiated determines the overall burning characteristics, which are reflected in the five flame front profiles seen in this study.

The first phase of combustion is the drying and preheating of the fuel. Here, hemicellulose and lignin are fairly endothermic, while cellulose is less endothermic. This phase directly

impacts the propagation of the flame front, as it determines the heat required to achieve combustion. The second phase is characterized by early combustion of lignin with little impact of cellulose and hemicellulose. This phase occurs immediately after the fuel is preheated and concludes when hemicellulose combustion begins. In the third phase, hemicellulose ignites rapidly and the combustion of lignin gradually increases. The second and third phases drive the propagation of the flame front, as their heat release is used to dry and preheat the fuel ahead of the flame front. In slow burning fires, propagation is driven by initial lignin combustion, while in rapid fires, phases two and three occur almost simultaneously and both drive propagation.

In the fourth phase, cellulose pyrolysis is exceedingly endothermic, while hemicellulose combustion decreases, and peak lignin combustion occurs. This phase can be either exothermic or endothermic depending on the cellulose content and can potentially serve as a barrier to complete combustion. Once the cellulose pyrolysis has been completed, phase five begins and all three components are mildly exothermic. Phase six can also serve as a barrier to complete combustion as hemicellulose and lignin become endothermic and cellulose combustion is negligible. In the final phase, cellulose becomes exothermic and becomes increasingly exothermic as it chars, whereas hemicellulose and lignin become increasingly endothermic. Although this phase is generally exothermic, the temperatures required to complete combustion are relatively high, so complete combustion is not always achieved.

Mixed fuel tests with little sweetgum and or little humidity were theorized to create staggered flame fronts. First, the heat released during the combustion of pine hemicellulose would dry and heat the fuel ahead of the flame front. The preceding oak litter would then achieve combustion before the pine litter because of its reduced heat requirement. Finally, early oak combustion would ignite the surrounding pine litter earlier than it otherwise would. This caused staggered flame fronts to be more flammable than pine. In addition, a staggered flame front would cause oak cellulose pyrolysis to occur near the peak of pine hemicellulose combustion, leading to greater flame heights.

Thin flame fronts were typically as flammable as pine. Like the staggered flame fronts, enough heat was released during hemicellulose combustion to dry and preheat the preceding

fuel; however, increased humidity or sweetgum content delayed oak combustion. This resulted in the combustion phases of each fuel occurring near simultaneously. The flame height decreased, while the combustion temperature increased. This is because during staggered combustion, the peak mass loss of oak occurs with the peak mass loss and heat release of pine. Within a thin flame front, the peak heat release of oak instead occurs with the peak mass loss and heat release of pine.

As the sweetgum content increased to moderate mass fractions, the flame front became rounded. Hemicellulose combustion peaked significantly behind the leading edge of the flame front. Early hemicellulose combustion was still the primary heat source for propagation and cellulose pyrolysis; however, it progressed slower, leading to lower temperatures and flame heights. This caused a slower increase in temperature and wider regions of each combustion phase. These flame front profiles were typically between pine and sweetgum in terms of flammability.

Mixtures with moderately high sweetgum content began to flatten as the lignin and hemicellulose content decreased. Hemicellulose now had a reduced impact on the propagation rate. However, hemicellulose was also further from cellulose pyrolysis and had less contribution to combustion completion. This led to tests with flat flame front profiles that sometimes did not complete cellulose pyrolysis and, therefore, char. Tests with flat flame front profiles were slightly less flammable than sweetgum and had much lower combustion fractions.

Finally, tests with the highest sweetgum content displayed skewed flame fronts, where there was a great heat concentration toward the rear of the flame front. These tests were about as flammable as flattened flame fronts but had higher combustion fractions. These mixtures had the highest ratio of hemicellulose plus lignin to cellulose, which allowed for more consistent completion of the cellulose pyrolysis.

The results found in this study provide insight into how mesophication alters the characteristics of wildland fires. This can be used to help preserve oak landscapes in the southeastern United States. Furthermore, these results highlight the possibility that the distribution of lignocellulosic components within forest fuel beds acts as an underlying mechanism in mesophication. This study can also be used to guide future studies on this topic. In particular, tests that

include a wider range of fuel species and moisture content would serve to expand on the flame front profiles found within the current study. Although the current study experienced technical limitations, optical diagnostics would also serve to further explore changes within flame front geometry caused by variations in the distribution of lignocellulosic components.

References

[1] Hanberry, B. B., and Nowacki, G. J., "Oaks were the historical foundation genus of the east-central United States," *Quaternary Science Reviews*, Vol. 145, 2016, pp. 94–103. https://doi.org/10.1016/j.quascirev.2016.05.037.

[2] Nowacki, G. J., and Abrams, M. D., "The Demise of fire and "Mesophication" of Forests in the Eastern United States," *BioScience*, Vol. 58, 2008, pp. 123–138. https://doi.org/10.1641/B580207.

[3] Alexander, H. D., Siegert, C., Brewer, S., Kreye, J., Lashley, M. A., McDaniel, J. K., Paulson, A. K., Renninger, H. J., and Varner, J. M., "Mesophication of Oak Landscapes: Evidence, Knowledge Gaps, and Future Research," *BioScience*, Vol. 71, No. 5, 2021, pp. 531–542. URL https://doi.org/10.1093/biosci/biaa169.

[4] Bable-Plauche, E. K., Alexander, H. D., Siegert, C. M., Willis, J. L., and Berry, A. I., "Mesophication of upland oak forests: Implications of species-specific differences in leaf litter decomposition rates and fuelbed composition," *Forest Ecology and Management*, Vol. 512, 2022. https://doi.org/10.1016/j.foreco.2022.120141.

[5] Allen, D., Dick, C. W., Strayer, E., Perfecto, I., and Vandermeer, J., "Scale and strength oak-mesophyte interactions in a transitional oak-hickory forest," *National Library of Medicine*, Vol. 48, No. 11, 2018, pp. 1366–1372. https://doi.org/10.1139/cjfr-2018-0131.

[6] McShea, W. J., "The Influence of Acorn Crops on Annual Variation in Rodent and Bird Populations," *Ecological Society of America*, Vol. 81, No. 1, 2000, pp. 228–238. https://doi.org/10.2307/177146.

[7] McShea, W. J., Healy, W. M., Devers, P., Fearer, T., Koch, F. H., Stauffer, D., and Waldon, J., "Forestry Matters: Decline of Oaks Will Impact Wildlife in Hardwood Forests," *Journal of Wildlife Management*, Vol. 71, No. 5, 2007, pp. 1717–1728. https://doi.org/10.2193/2006-169.

[8] Agbeshie, A. A., Abugre, S., Atta-Darkwa, T., and Awuah, R., "A review of the efects of forest fre on soil properties," *Journal of Forestry Research*, Vol. 33, 2022, pp. 1419–1441. https://doi.org/10.1007/s11676-022-01475-4.

[9] Brewer, J. S., Abbott, M. J., and Moyer, S. A., "Effects of Oak-hickory Woodland Restoration Treatments on Native Groundcover Vegetation and the Invasive Grass, Microstegium vimineum," *Ecological Restoration*, Vol. 33, No. 3, 2015, pp. 135–146. https://doi.org/10.3368/er.33.2.135.

[10] Tallamy, D. W., and Shropshire, K. J., "Ranking lepidopteran use of native versus introduced plants," *Conservation Biology*, Vol. 23, No. 2, 2009, pp. 941–947. https://doi.org/10.1111/j.1523-1739.2009.01202.x.

[11] Alexander, H. D., and Arthur, M. A., "Implications of a predicted shift from upland oaks to red maple on forest hydrology and nutrient availability," *Canadian Journal of Forest Research*, Vol. 40, 2010, pp. 716–726. https://doi.org/10.1139/X10-029.

[12] Alexander, H. D., and Arthur, M. A., "Increasing Red Maple Leaf Litter Alters Decomposition Rates and Nitrogen Cycling in Historically Oak-Dominated Forests of the Eastern U.S." *Ecosystems*, Vol. 17, 2014, p. 1371–1383. https://doi.org/10.1007/s10021-014-9802-4.

[13] Luppold, W. G., "The Oak Timber Base and Market: Past, Present, and Future," *NC: US Department of Agriculture Forest Service*, Vol. 237, 2019, pp. 25–31.

[14] Stubbs, D. C., Humphreys, L. H., Goldman, A., Childree, M. A., Kush, J. S., and Scarborough, D. E., "An experimental investigation into the wildland fire burning characteristics of loblolly pine needles," *Fire Safety Journal*, Vol. 126, 2021. URL https://doi.org/10.1016/j.firesaf.2021.103471.

[15] Cabrera, S., Alexander, H. D., Willis, J. L., and Anderson, C. J., "Midstory removal of encroaching species has minimal impacts on fuels and fire behavior regardless of burn season in a degraded pine-oak mixture," *Forest Ecology and Management*, Vol. 544, 2023. https://doi.org/10.1016/j.foreco.2023.121157.

[16] Diez, D., Uruena, A., Pinero, R., Barrio, A., and Tamminen, T., "Determination of Hemicellulose, Cellulose, and Lignin Content in Different Types of Biomasses by Thermogravimetric Analysis and Pseudocomponent Kinetic Model (TGA-PKM Method)," *Processes*, Vol. 8, 2020, p. 1048. https://doi.org/10.3390/pr8091048.

[17] Elder, T., Kush, J. S., and Hermann, S. M., "Thermogravimetric analysis of forest understory grasses," *Thermochimic Acta*, Vol. 512, No. 1, 2011, pp. 170–177. https://doi.org/10.1016/j.tca.2010.10.001.

[18] Yang, H., Yan, R., Chen, H., Lee, D. H., and Zheng, C., "Characteristics of hemicellulose, cellulose and lignin pyrolysis," *Fuel*, Vol. 86, 2007, pp. 1781–1788. https://doi.org/10.1016/j.fuel.2006.12.013.

[19] Pasangulapati, V., Ramachandriya, K. D., Kumar, A., and Wilkins, M. R., "Effects of cellulose, hemicellulose and lignin on thermochemical conversion characteristics of the selected biomass," *Bioresource Technology*, Vol. 114, 2012, pp. 663–669. https://doi.org/10.1016/j.biortech.2012.03.036.

[20] Amini, E., Safdari, M., Weise, D. R., and Fletcher, T. H., "Pyrolysis kinetics of live and dead wildland vegetation from the Southern United States," *Journal of Analytical and Applied Pyrolysis*, Vol. 142, No. 1, 2008, pp. 172–185. https://doi.org/10.1016/j.jaap.2019.05.002.

[21] Amini, E., Safdari, M. S., Johnson, N., and Weise, D. R., "Pyrolysis kinetics of wildland vegetation using model-ftting methods," *Journal of Analytical and Applied Pyrolysis*, Vol. 157, 2012. https://doi.org/10.1016/j.jaap.2021.105167.

[22] Rovira, P., Kurz-Besson, C., Couteaux, M. M., and Vallejo, V. R., "Changes in litter properties during decomposition: A study by differential thermogravimetry and scanning calorimetry," *Soil Biology and Biochemistry*, Vol. 40, No. 1, 2007, pp. 172–185. https://doi.org/10.1016/j.soilbio.2007.07.021.

[23] Bach, Q. V., Tran, K. Q., and Skreiberg, S., "Combustion kinetics of wet-torrefied forest residues using the distributed activation energy model (DAEM)," *Applied Energy*, Vol. 185, 2017, pp. 1059–1066. https://doi.org/10.1016/j.apenergy.2016.02.056.

[24] Polka, M., "Analysis of the heat and smoke release rate of selected undergrowth types," *Infraeko*, Vol. 45, 2018. https://doi.org/10.1051/e3sconf/20184500068.

[25] White, R. H., Weise, D. R., Mackes, K., and Dibble, A. C., "Cone Calorimeter Testing of Vegetation: An Update," *International conference on fire safety*, Vol. 35, 2002, pp. 1–13. URL https://www.fs.usda.gov/treesearch/pubs/8596.

[26] Dickinson, M. B., Hutchinson, T. F., Dietenberger, M., Matt, F., and Peters, M. P., "Litter Species Composition and Topographic Effects on Fuels and Modeled Fire Behavior in an Oak-Hickory Forest in the Eastern USA," *PLoS ONE*, Vol. 11, No. 8, 2016. https://doi.org/10.1371/journal.pone.0159997.

[27] Fonda, R. W., Belander, L. A., and Burley, L. L., "Burning characteristics of western conifer needles," *Northwest Sci*, Vol. 72, 1998, pp. 1–9.

[28] Fonda, R. W., "Burning Characteristics of Needles from Eight Pine Species," *Forest Science*, Vol. 47, No. 3, 2001, pp. 390–396. URL https://academic.oup.com/forestscience/article/47/3/390/4617403.

[29] Kane, J. M., Varner, J. M., and Hiers, J. K., "The burning characteristics of southeastern oaks: Discriminating fire facilitators from fire impeders," *Forest Ecology and Management*, Vol. 256, 2008, p. 2039–2045. https://doi.org/10.1016/j.foreco.2008.07.039.

[30] Kreye, J. K., Varner, J. M., Hamby, G. W., and Kane, J. M., "Mesophytic litter dampens flammability in fire-excluded pyrophytic oak–hickory woodlands," *Ecosphere*, Vol. 9, No. 1, 2018, pp. 1–10. URL https://doi.org/10.1002/ecs2.2078.

[31] Varner, J. M., Kane, J. M., Kreye, J. K., and Shearman, T. M., "Litter Flammability of 50 Southeastern North American Tree Species: Evidence for Mesophication Gradients Across Multiple Ecosystems," *Frontier for Global Change*, Vol. 4, 2021. https://doi.org/10.3389/ffgc.2021.727042.

[32] Kane, J. M., Kreye, J. K., Barajas-Ramirez, R., and Varner, J. M., "Litter trait driven dampening of flammability following deciduous forest community shifts in eastern North America," *Forest Ecology and Management*, Vol. 489, 2021. https://doi.org/10.1016/j.foreco.2021.119100.

[33] Kreye, J. K., Kane, J. M., and Varner, J. M., "Multivariate roles of litter traits on moisture and flammability of temperate northeastern North American tree species," *Fire Ecology*, Vol. 19, 2023. https://doi.org/10.1186/s42408-023-00176-5.

[34] Grootemaat, S., Wright, I. J., van Bodegom, P. M., Cornelissen, J. H. C., and Cornwell, W. K., "Burn or rot: leaf traits explain why flammability and decomposability are decoupled across species," *Functional Ecology*, Vol. 29, 2015, pp. 1486–1497. https://doi.org/10.1111/1365-2435.12449.

[35] Santoni, P. A., Morandini, F., and T, B., "Determination of fireline intensity by oxygen consumption calorimetry," *Journal of Thermal Analysis and Calorimetry*, Vol. 104, No. 3, 2011, pp. 1005–1015. https://doi.org/10.1007/s10973-010-1256-0.

[36] Barboni, T., Morandini, F., Rossi, L., Molinier, T., and Santoni, P. A., "Relationship Between Flame Length and Fireline Intensity Obtained by Calorimetry at Laboratory

Scale," *Combustion Science and Technology*, Vol. 184, No. 2, 2012, pp. 186–204. https://doi.org/10.1080/00102202.2011.625373.

[37] Morandini, F., Simeoni, A., Santoni, P. A., and Balbi, J. H., "A Model for the Spread of Fire Across A Fuel Bed Incorporating the Effects of Wind and Slope," *Combustion Science and Technology*, Vol. 177, No. 7, 2005, pp. 1381–1418. https://doi.org/10.1080/00102200590950520.

[38] Tihay, V., Morandini, F., Santoni, P. A., Perez-Ramirez, Y., and Barboni, T., "Combustion of forest litters under slope conditions: Burning rate, heat release rate, convective and radiant fractions for different loads," *Combustion and Flame*, Vol. 161, No. 12, 2014, pp. 3237–3248. https://doi.org/10.1016/j.combustflame.2014.06.003.

[39] Awad, C., Morvan, D., Rossi, J. L., Marcelli, T., Chatelon, F. J., Morandini, F., and Balbi, J. H., "Fuel moisture content threshold leading to fire extinction under marginal conditions," *Fire Safety Journal*, Vol. 118, 2020. https://doi.org/10.1016/j.firesaf.2020.103226.

[40] Magalhaes, R. M. Q., and Schwilk, D. W., "Leaf traits and litter flammability: evidence for non-additive mixture effects in a temperate forest," *Journal of Ecology*, Vol. 100, 2012, pp. 1153–1163. https://doi.org/10.1111/j.1365-2745.2012.01987.x.

[41] Grootemaat, S., Wright, I. J., van Bodegom, P. M., and Cornelissen, J. H. C., "Scaling up flammability from individual leaves to fuel beds," *Oikos*, Vol. 126, 2017, pp. 1428–1438. https://doi.org/10.1111/oik.03886.

[42] Davies, G. M., and Legg, C. J., "Fuel Moisture Thresholds in the Flammability of Calluna vulgaris," *Fire Technology*, Vol. 47, No. 2, 2011, pp. 421–436. https://doi.org/doi.org/10.1007/s10694-010-0162-0.

[43] Arthur, B. A., M A an Blankenship, Schorgendorfer, A., Loftis, D. L., and Alexander, H. D., "Changes in stand structure and tree vigor with repeated prescribed fire in an Appalachian hardwood forest," *Forest Ecology and Management*, Vol. 340, 2015, pp. 46–61. https://doi.org/10.1016/j.foreco.2014.12.025.

[44] McDaniel, J. K., Alexander, H. D., Siegert, C. M., and Lashley, M. A., "Shifting tree species composition of upland oak forests alters leaf litter structure, moisture, and flammability," *Forest Ecology and Management*, Vol. 482, 2021. https://doi.org/10.1016/j.foreco.2020.118860.

[45] Willis, J. L., Milton, T. F., and Alexander, H. D., "Cone and fruit impacts on understory fammability depend on traits and forest foor coverage," *Fire Ecology*, Vol. 20, No. 52, 2024. https://doi.org/10.1186/s42408-024-00281-z.

[46] Babrauskas, V., and Peacock, R. D., "Heat release rate: The single most important variable in fire hazard," *Fire Safety Journal*, Vol. 18, 1992, pp. 255–272. https://doi.org/10.1016/0379-7112(92)90019-9.

[47] Turns, S., *An Introduction to Combustion: Concepts and Applications*, McGraw-Hill series in mechanical engineering, McGraw-Hill, 2012.